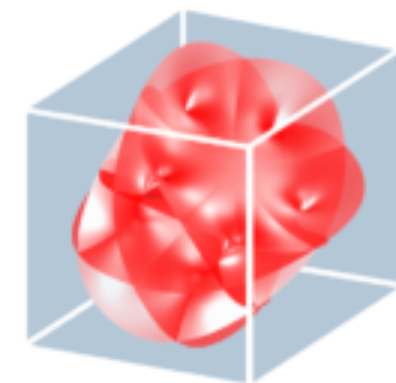


Metal-to-metal quantum phase transitions not described by symmetry breaking orders

Strongly Correlated Quantum Materials
and High Temperature Superconductors



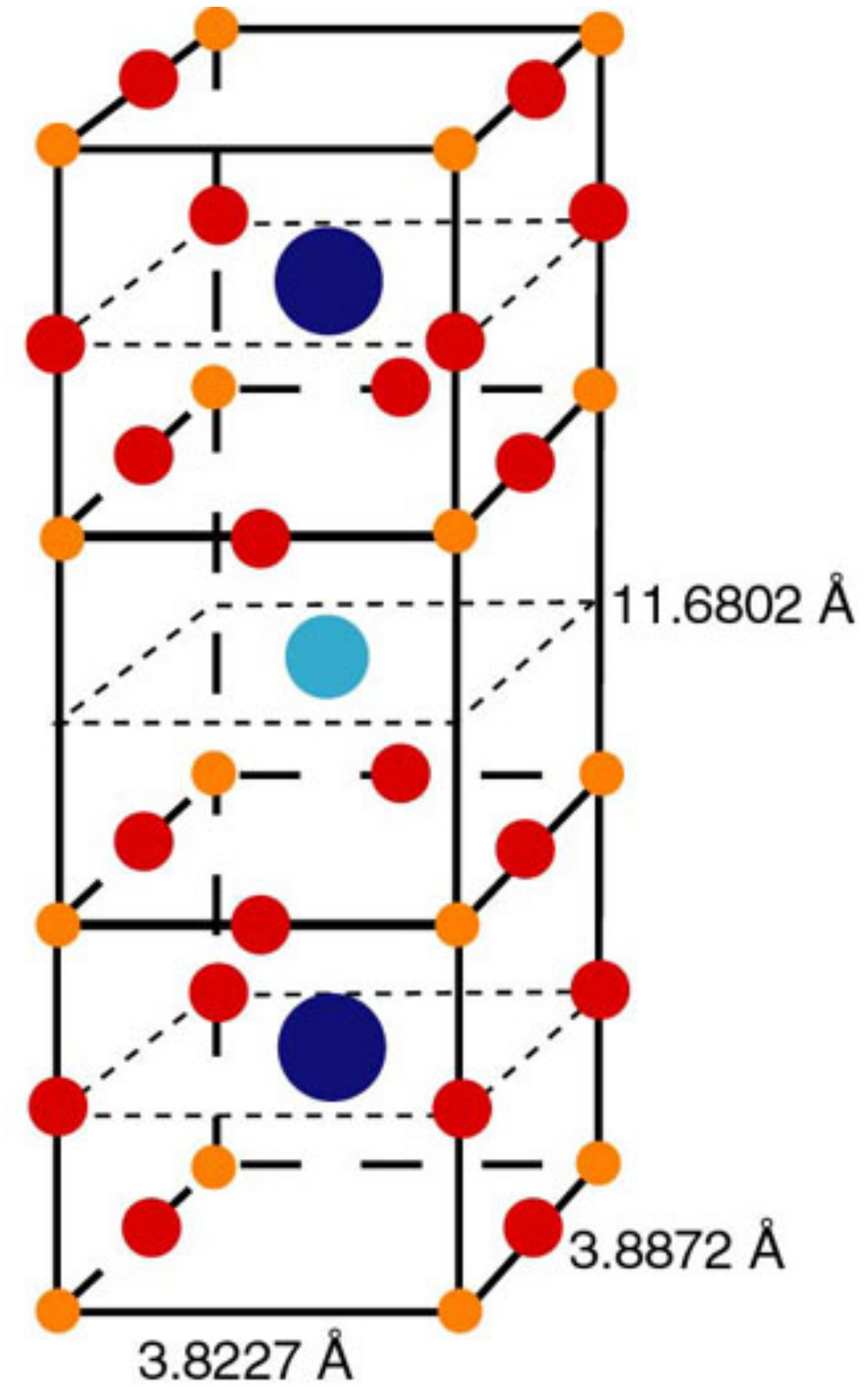
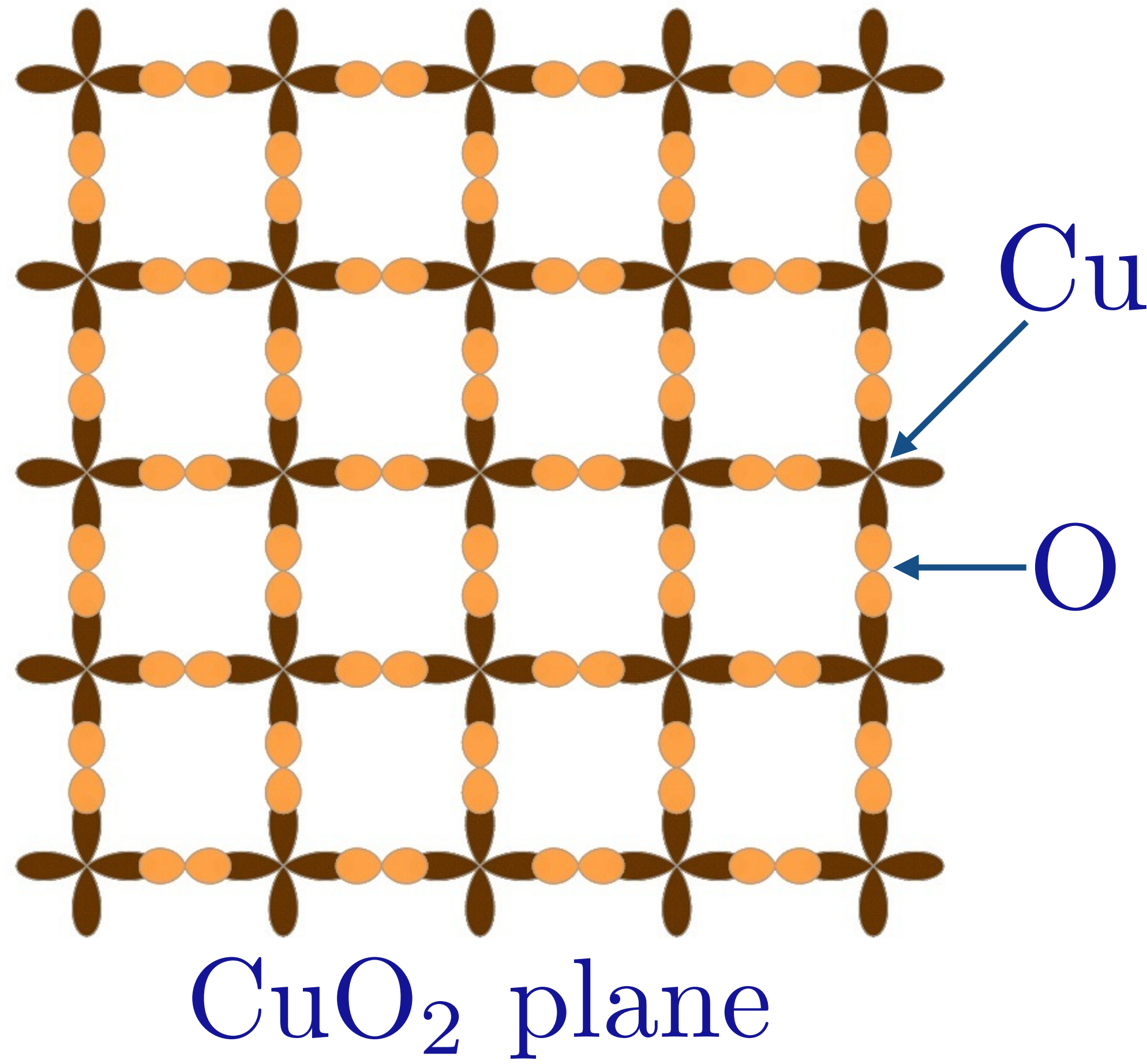
HARVARD UNIVERSITY
CENTER OF MATHEMATICAL
SCIENCES AND APPLICATIONS

September 2, 2020
Subir Sachdev

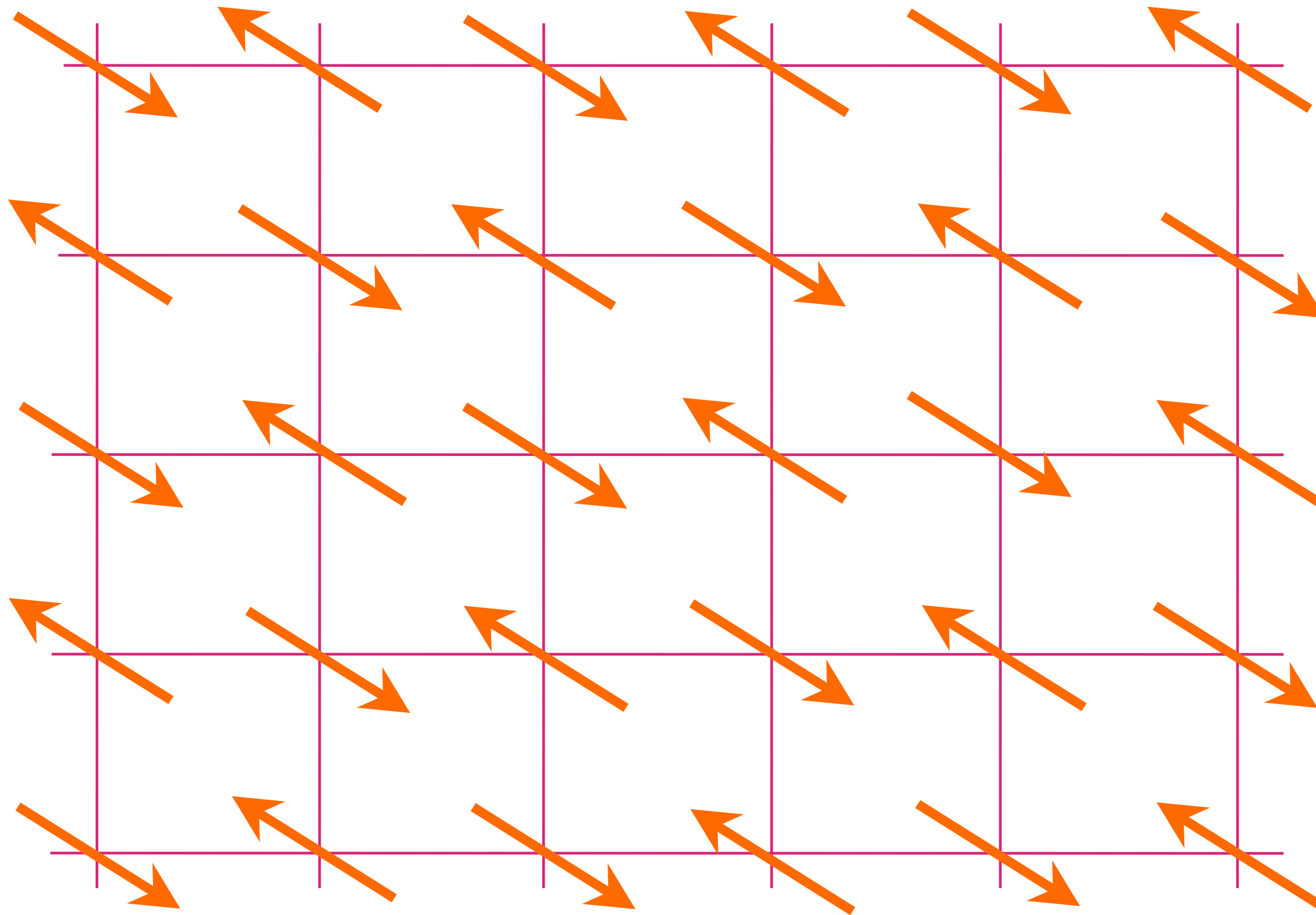


Talk online: sachdev.physics.harvard.edu

High temperature superconductors

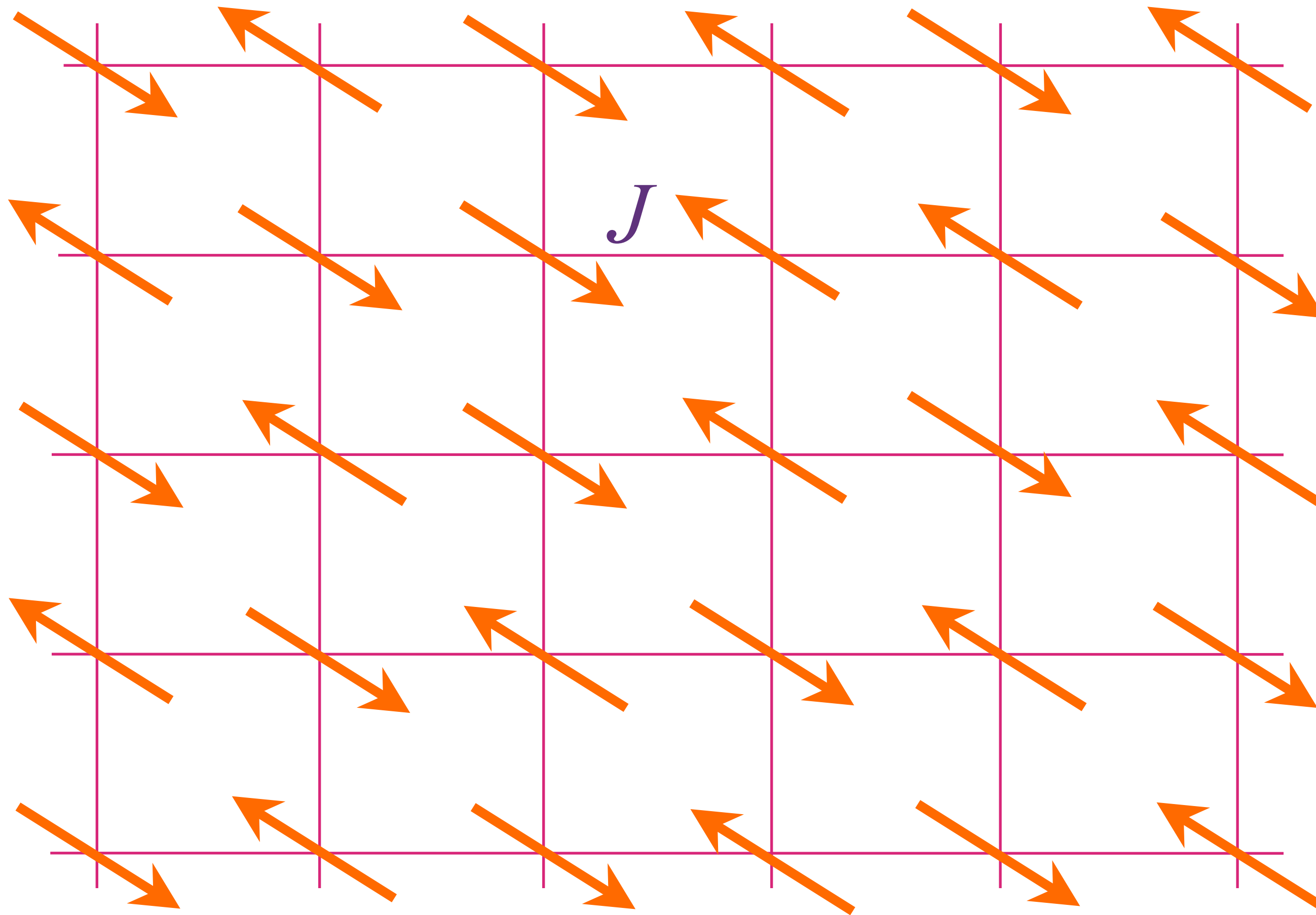


Insulating antiferromagnet



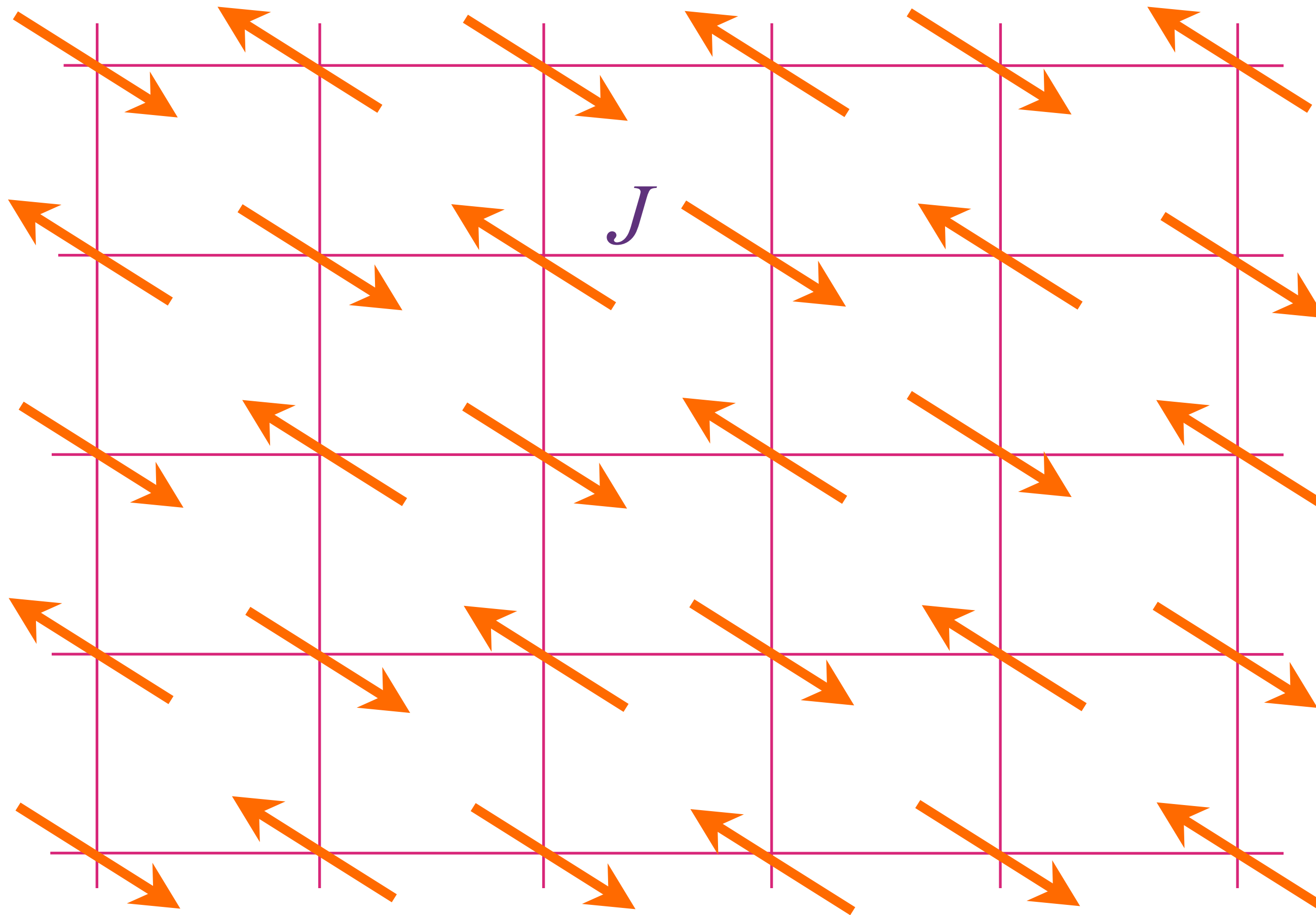
$$H = J \sum_{\langle ij \rangle} \left[X_i X_j + Y_i Y_j + Z_i Z_j \right]$$

Insulating antiferromagnet



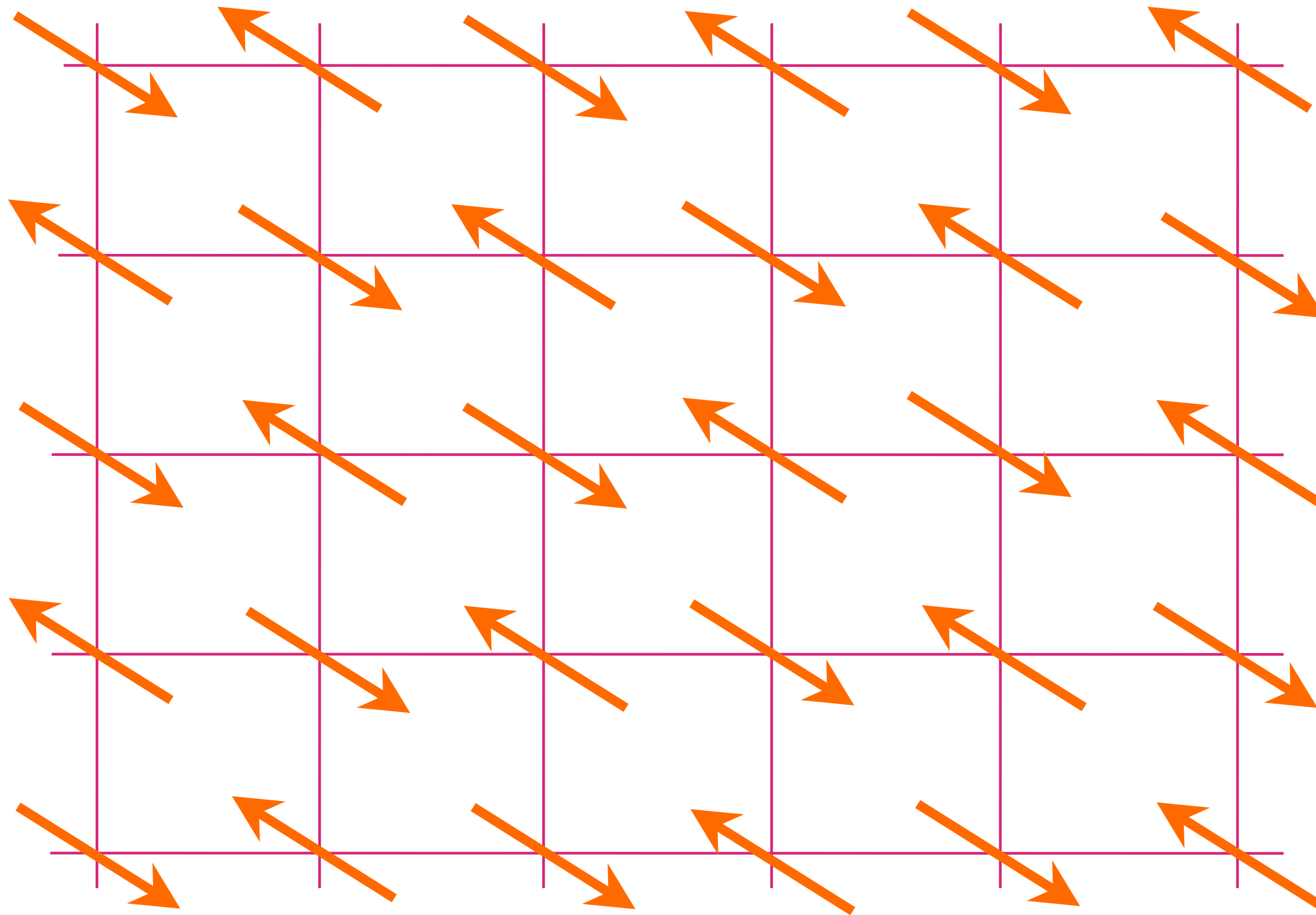
$$H = J \sum_{\langle ij \rangle} \left[X_i X_j + Y_i Y_j + Z_i Z_j \right]$$

Insulating antiferromagnet



$$H = J \sum_{\langle ij \rangle} \left[X_i X_j + Y_i Y_j + Z_i Z_j \right]$$

Insulating antiferromagnet



$$H = J \sum_{\langle ij \rangle} \vec{S}_i \cdot \vec{S}_j$$

$$\alpha = \uparrow, \downarrow$$

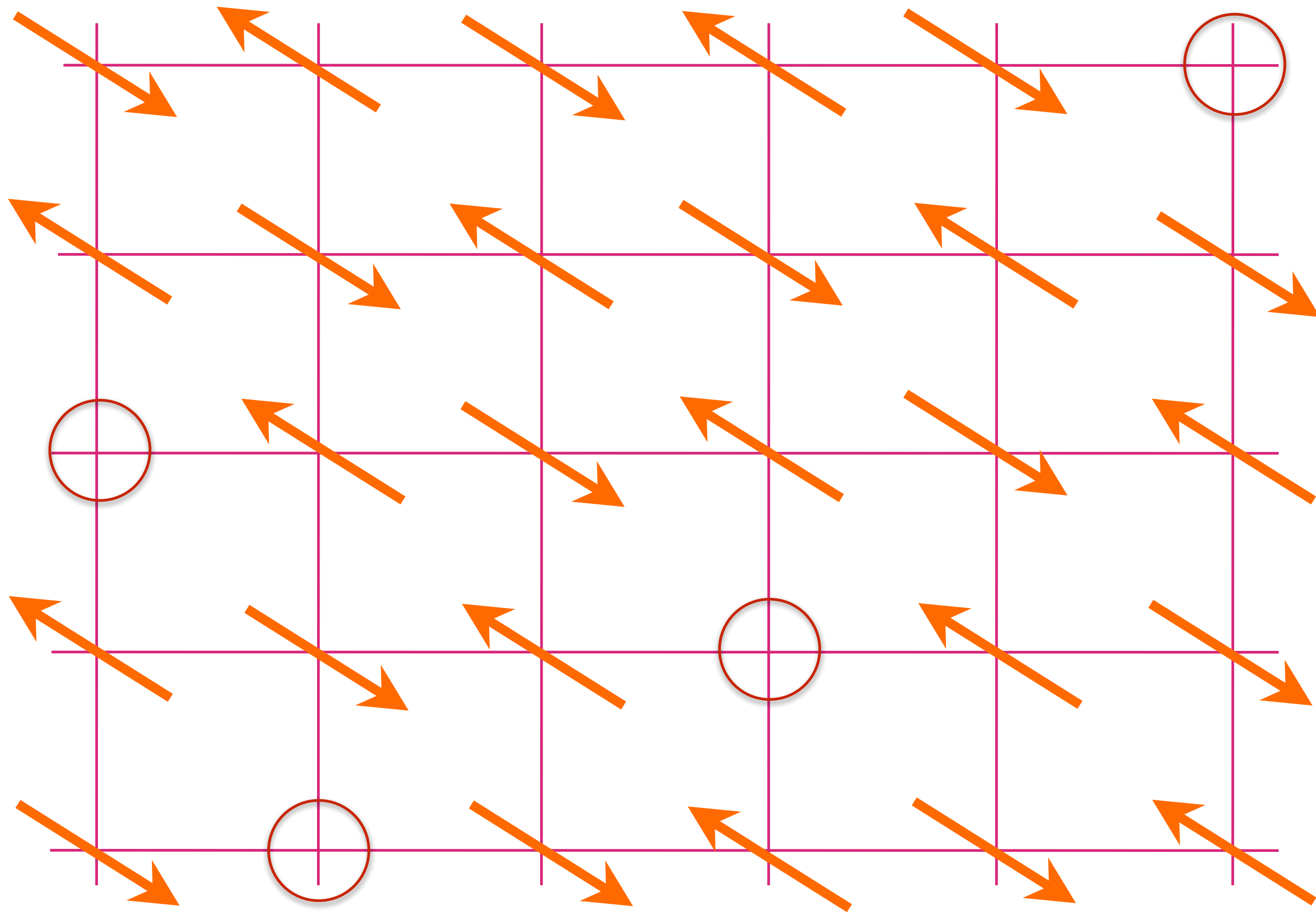
$$\{c_{i\alpha}, c_{j\beta}^\dagger\} = \delta_{ij} \delta_{\alpha\beta},$$

$$\{c_{i\alpha}, c_{j\beta}\} = 0$$

$$\sum_{\alpha} c_{i\alpha}^\dagger c_{i\alpha} = 1$$

$$\vec{S}_i = \frac{1}{2} c_{i\alpha}^\dagger \vec{\sigma}_{\alpha\beta} c_{i\beta}$$

Antiferromagnet doped with hole density p



$$H = J \sum_{\langle ij \rangle} \vec{S}_i \cdot \vec{S}_j$$

$$-t \sum_{\langle ij \rangle} c_{i\alpha}^\dagger c_{j\alpha} + \text{H.c.}$$

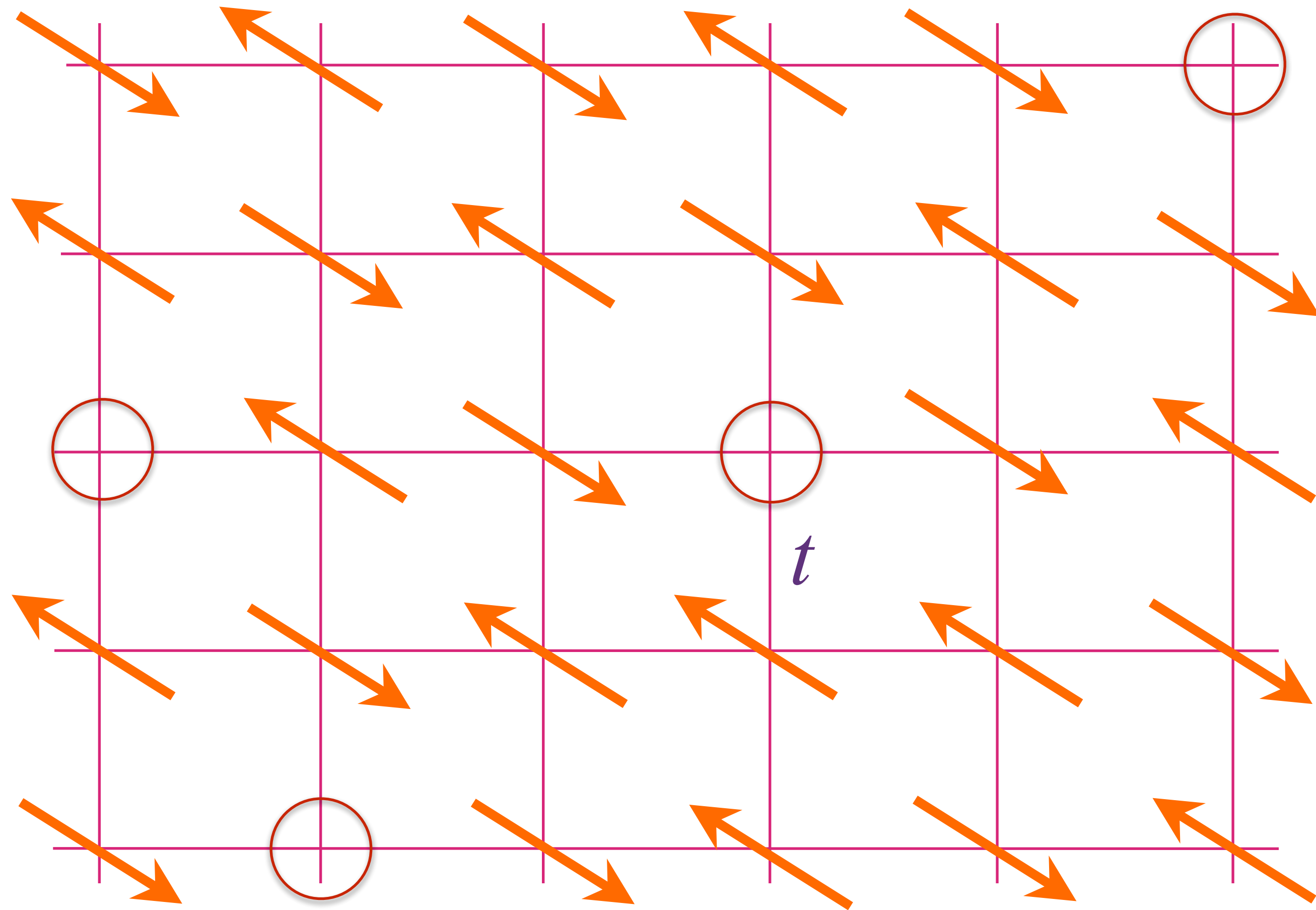
$$\sum_{\alpha} c_{i\alpha}^\dagger c_{i\alpha} \leq 1$$

$$\frac{1}{N} \sum_{i\alpha} c_{i\alpha}^\dagger c_{i\alpha} = 1 - p$$

$$\alpha = \uparrow, \downarrow, \quad \{c_{i\alpha}, c_{j\beta}^\dagger\} = \delta_{ij} \delta_{\alpha\beta},$$

$$\{c_{i\alpha}, c_{j\beta}\} = 0, \quad \vec{S}_i = \frac{1}{2} c_{i\alpha}^\dagger \vec{\sigma}_{\alpha\beta} c_{i\beta}$$

Antiferromagnet doped with hole density p



$$H = J \sum_{\langle ij \rangle} \vec{S}_i \cdot \vec{S}_j$$

$$-t \sum_{\langle ij \rangle} c_{i\alpha}^\dagger c_{j\alpha} + \text{H.c.}$$

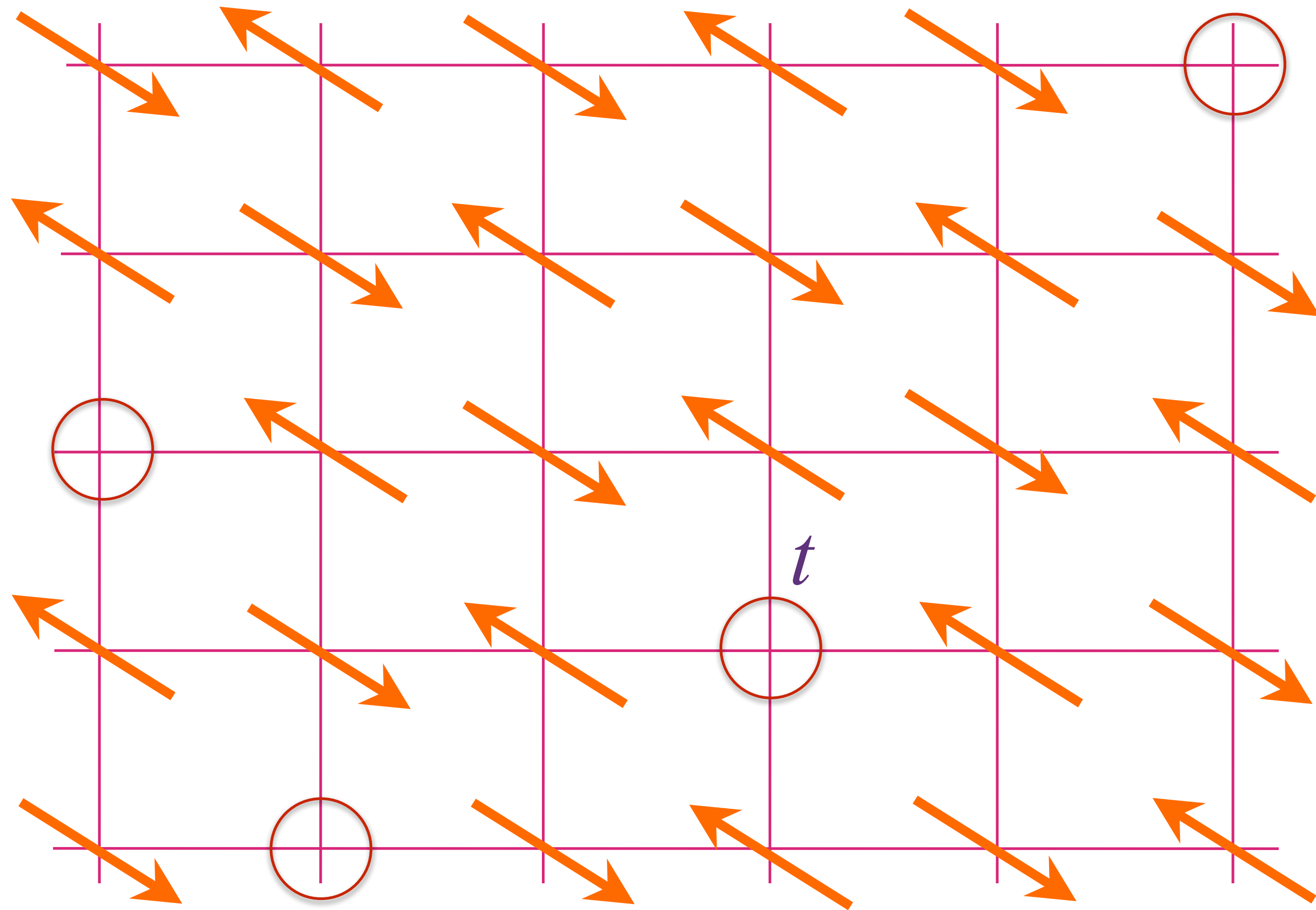
$$\sum_{\alpha} c_{i\alpha}^\dagger c_{i\alpha} \leq 1$$

$$\frac{1}{N} \sum_{i\alpha} c_{i\alpha}^\dagger c_{i\alpha} = 1 - p$$

$$\alpha = \uparrow, \downarrow, \quad \{c_{i\alpha}, c_{j\beta}^\dagger\} = \delta_{ij} \delta_{\alpha\beta},$$

$$\{c_{i\alpha}, c_{j\beta}\} = 0, \quad \vec{S}_i = \frac{1}{2} c_{i\alpha}^\dagger \vec{\sigma}_{\alpha\beta} c_{i\beta}$$

Antiferromagnet doped with hole density p



$$H = J \sum_{\langle ij \rangle} \vec{S}_i \cdot \vec{S}_j$$

$$-t \sum_{\langle ij \rangle} c_{i\alpha}^\dagger c_{j\alpha} + \text{H.c.}$$

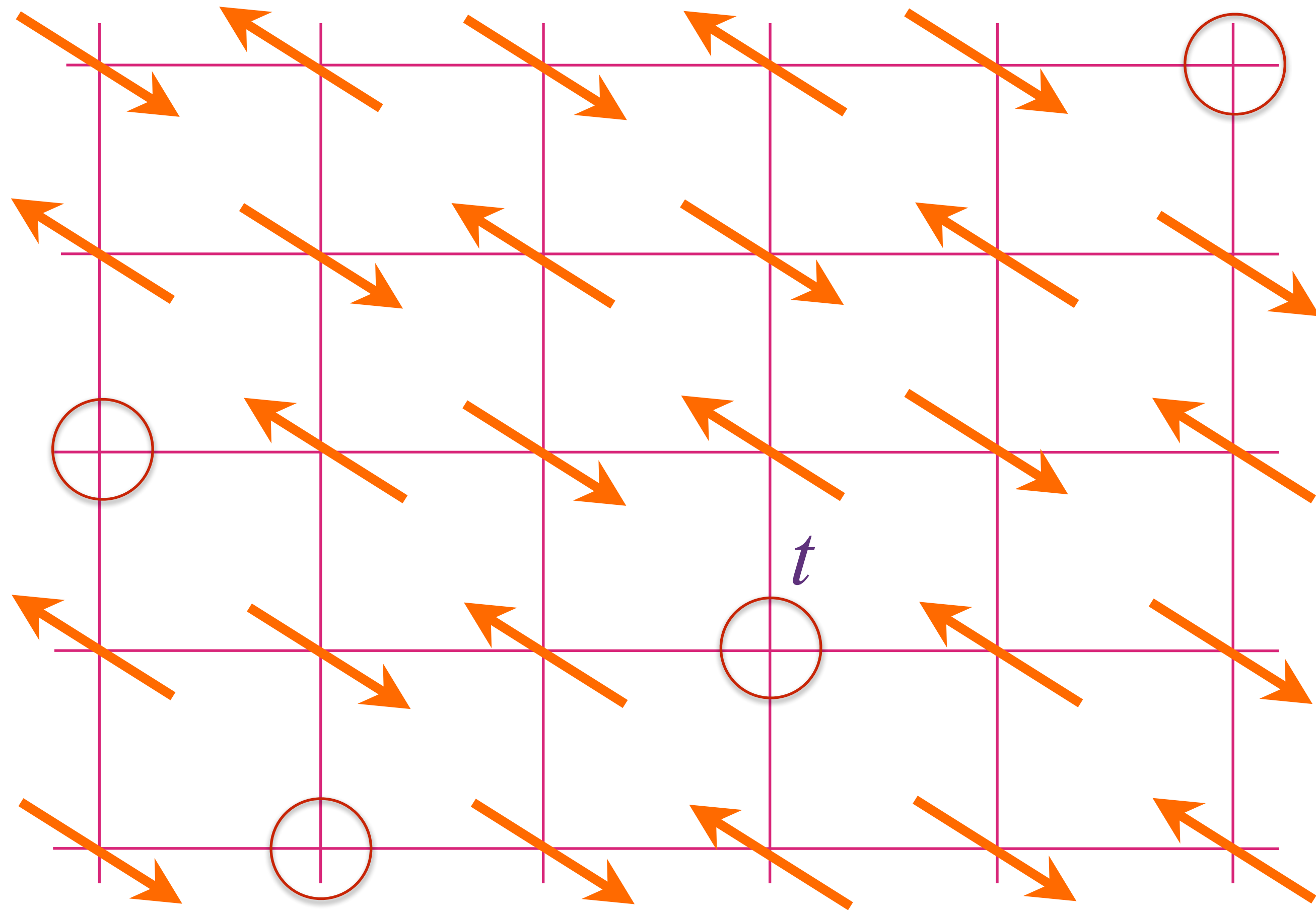
$$\sum_{\alpha} c_{i\alpha}^\dagger c_{i\alpha} \leq 1$$

$$\frac{1}{N} \sum_{i\alpha} c_{i\alpha}^\dagger c_{i\alpha} = 1 - p$$

$$\alpha = \uparrow, \downarrow, \quad \{c_{i\alpha}, c_{j\beta}^\dagger\} = \delta_{ij} \delta_{\alpha\beta},$$

$$\{c_{i\alpha}, c_{j\beta}\} = 0, \quad \vec{S}_i = \frac{1}{2} c_{i\alpha}^\dagger \vec{\sigma}_{\alpha\beta} c_{i\beta}$$

Antiferromagnet doped with hole density p



Complete mathematical definition
of the high- T_c problem !

$$H = J \sum_{\langle ij \rangle} \vec{S}_i \cdot \vec{S}_j$$

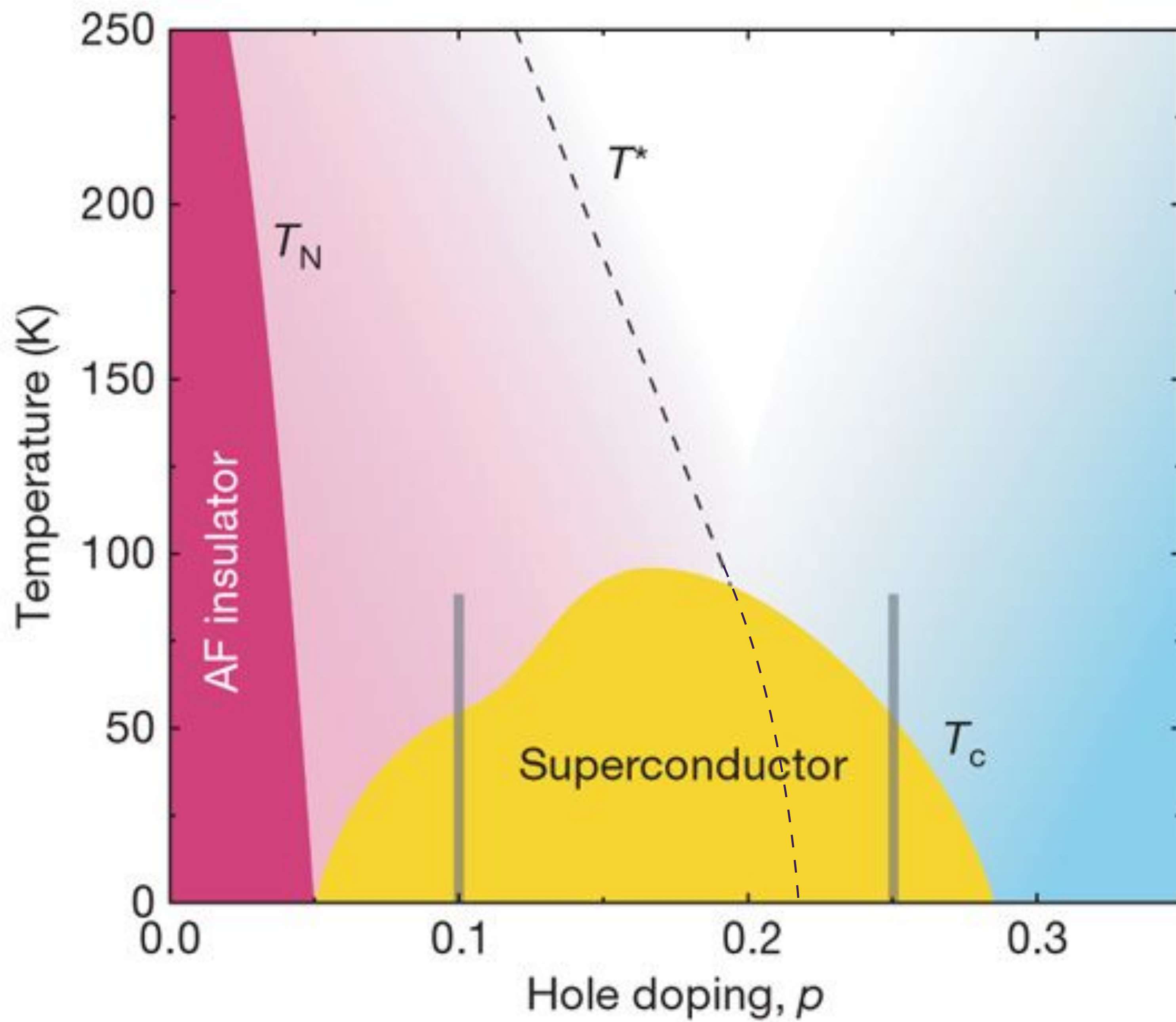
$$-t \sum_{\langle ij \rangle} c_{i\alpha}^\dagger c_{j\alpha} + \text{H.c.}$$

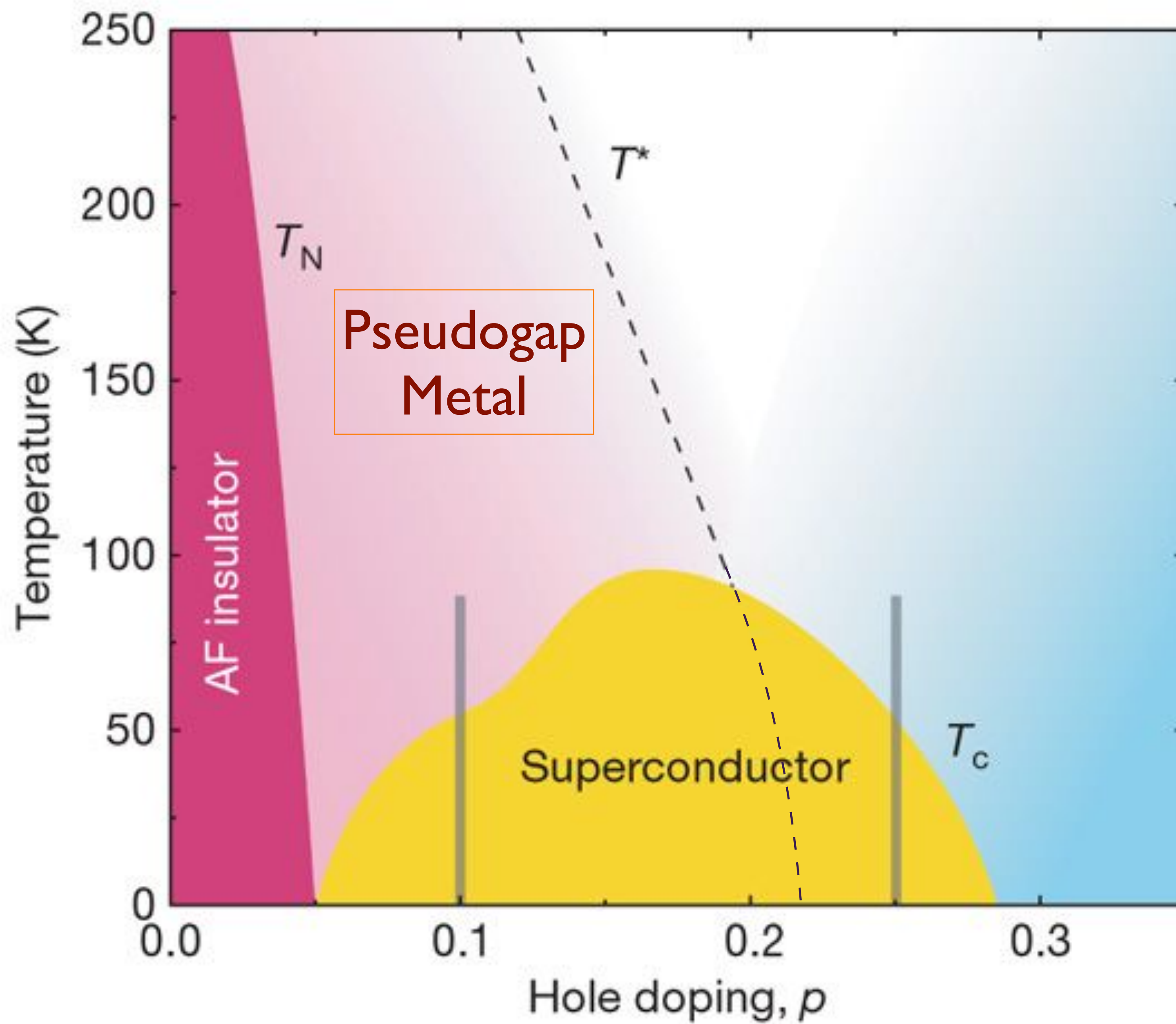
$$\sum_{\alpha} c_{i\alpha}^\dagger c_{i\alpha} \leq 1$$

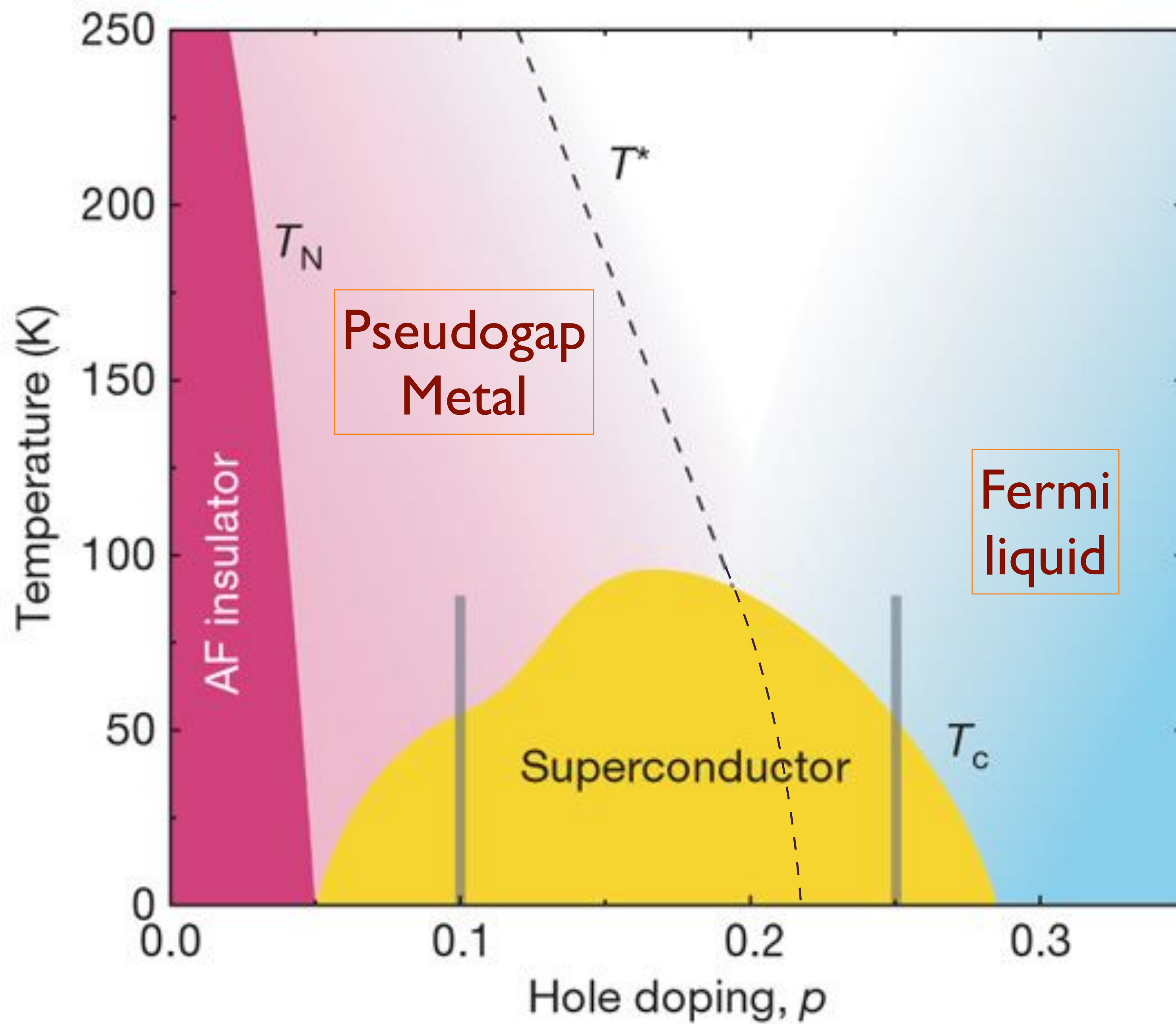
$$\frac{1}{N} \sum_{i\alpha} c_{i\alpha}^\dagger c_{i\alpha} = 1 - p$$

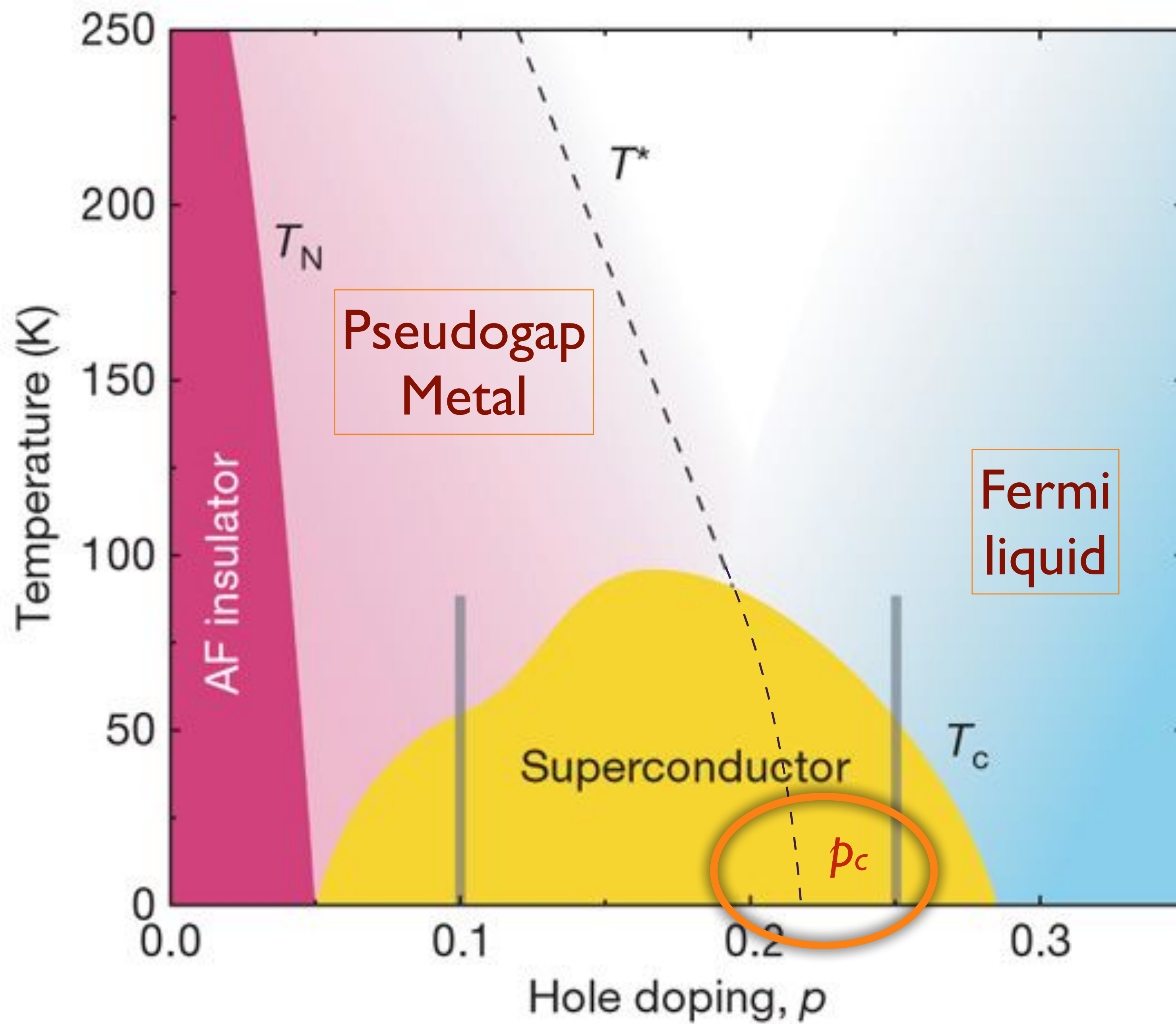
$$\alpha = \uparrow, \downarrow, \quad \{c_{i\alpha}, c_{j\beta}^\dagger\} = \delta_{ij} \delta_{\alpha\beta},$$

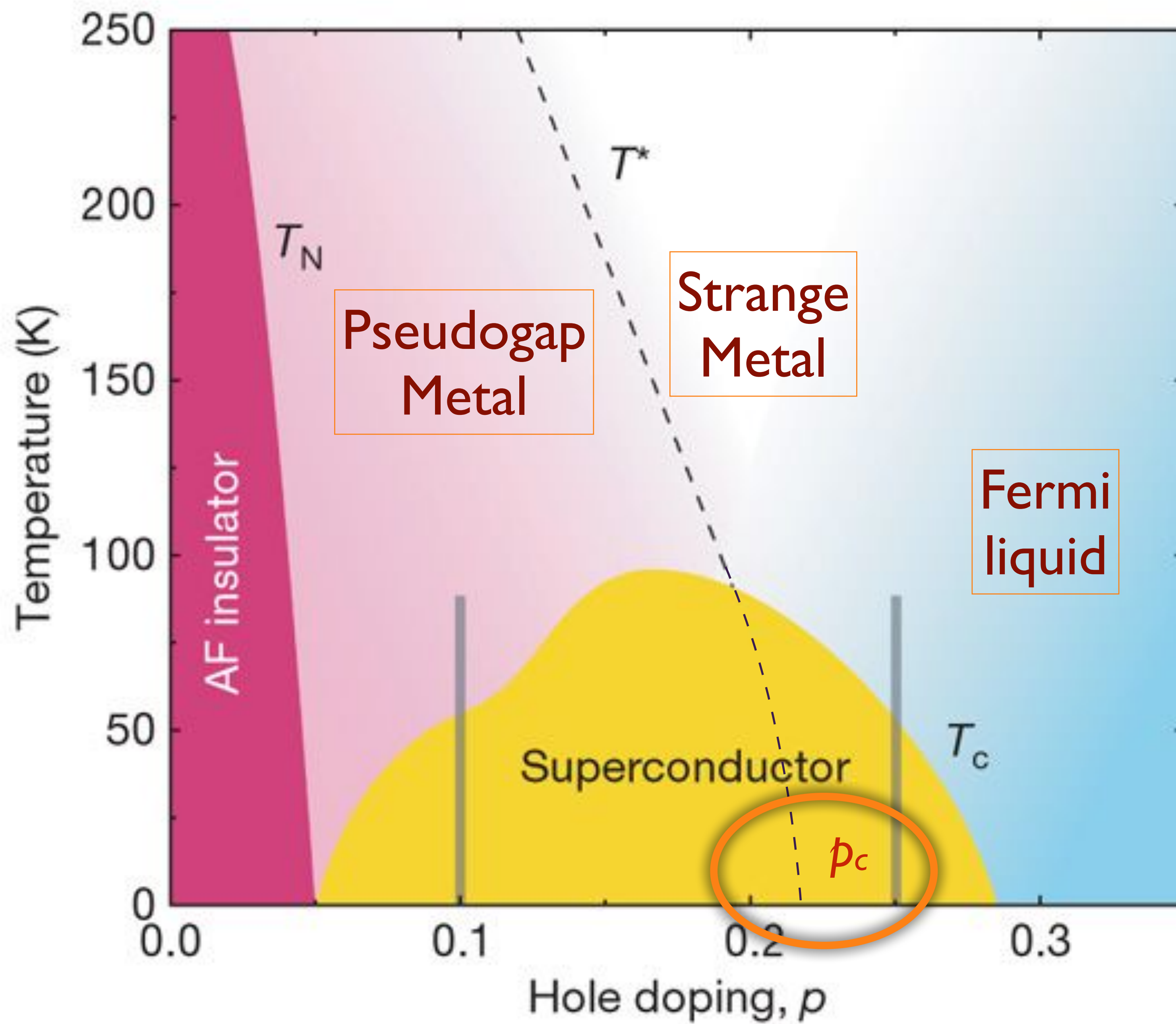
$$\{c_{i\alpha}, c_{j\beta}\} = 0, \quad \vec{S}_i = \frac{1}{2} c_{i\alpha}^\dagger \vec{\sigma}_{\alpha\beta} c_{i\beta}$$



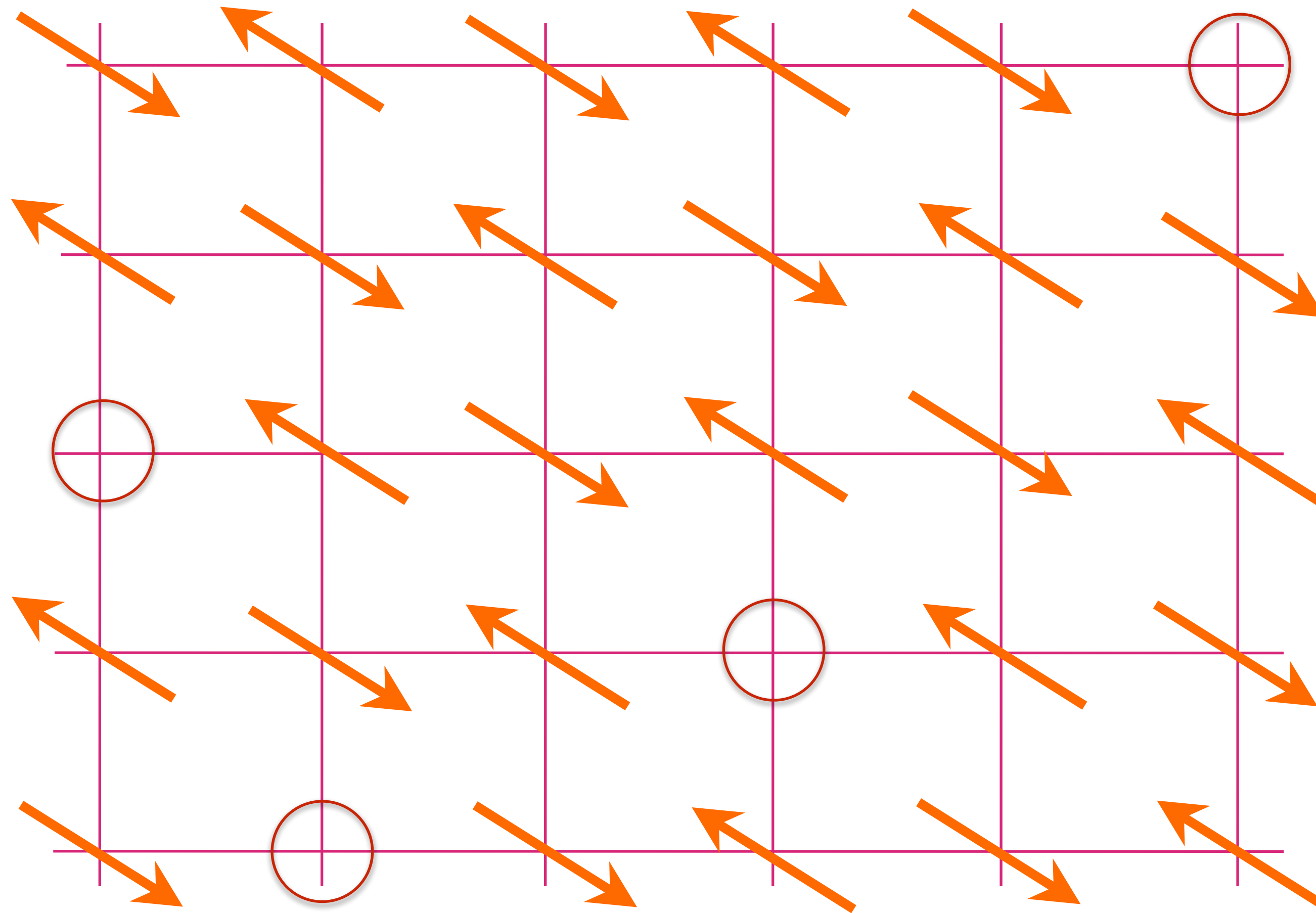






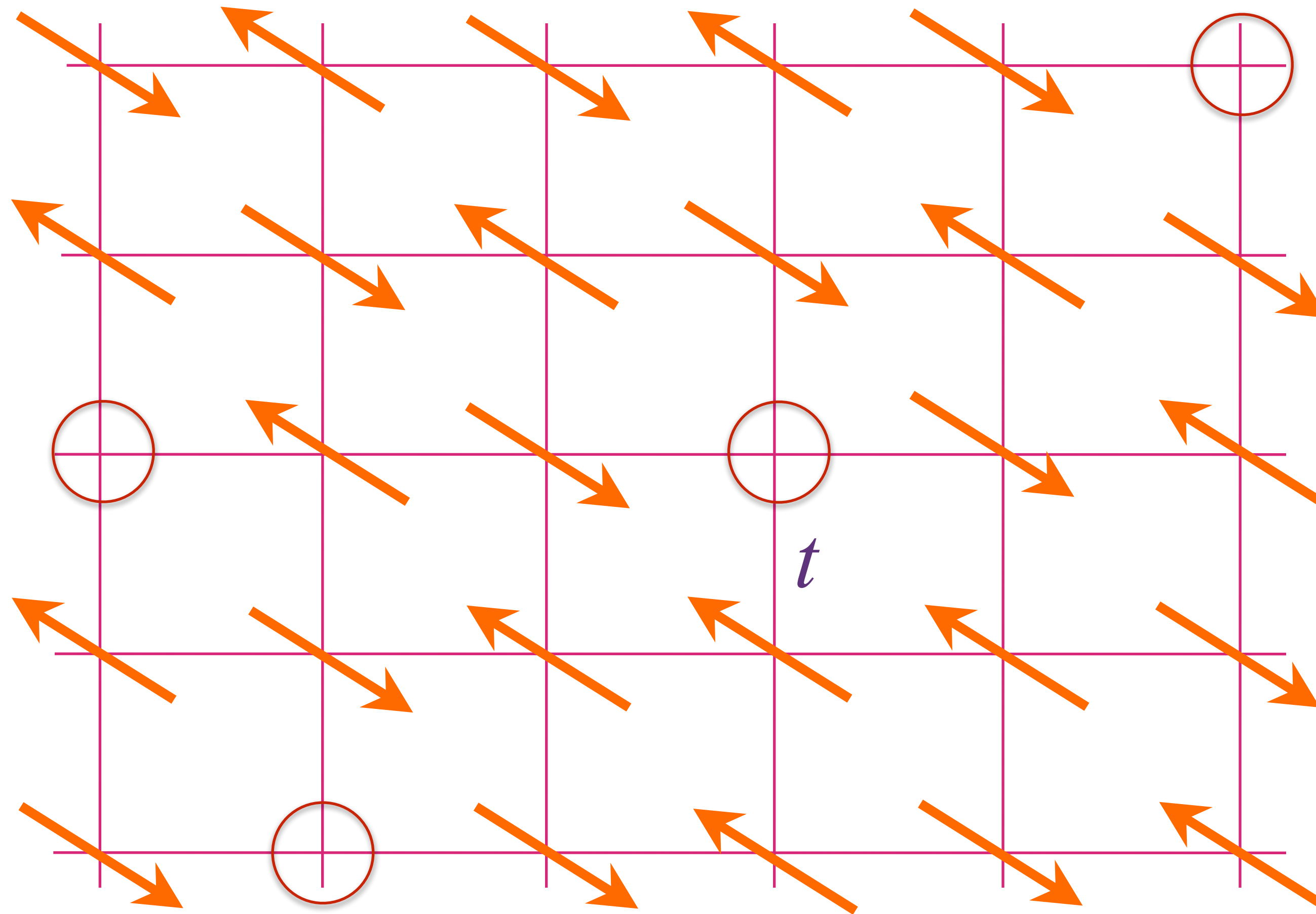


Real-space view at small p



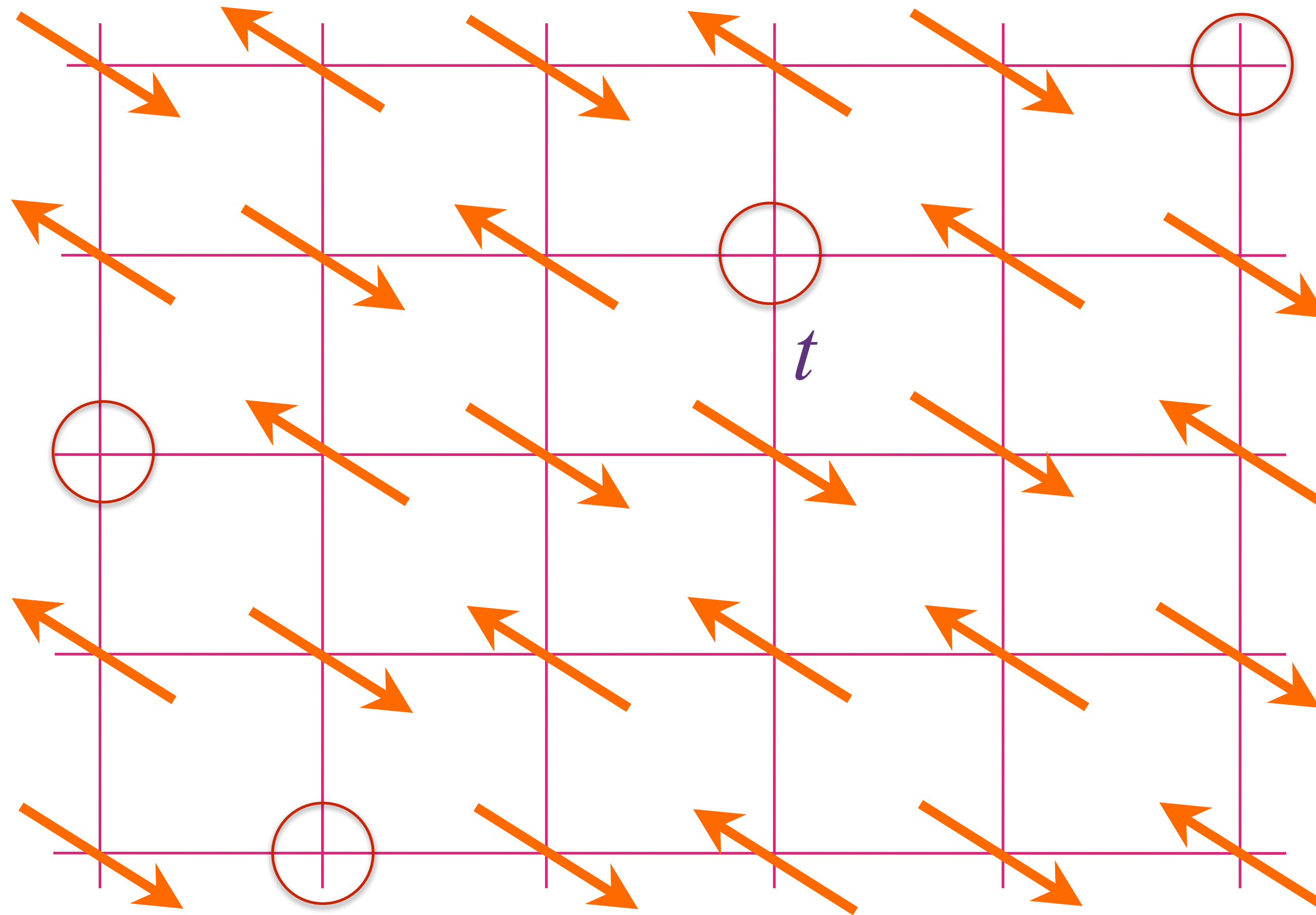
p mobile holes in a background of
fluctuating spins

Real-space view at small p



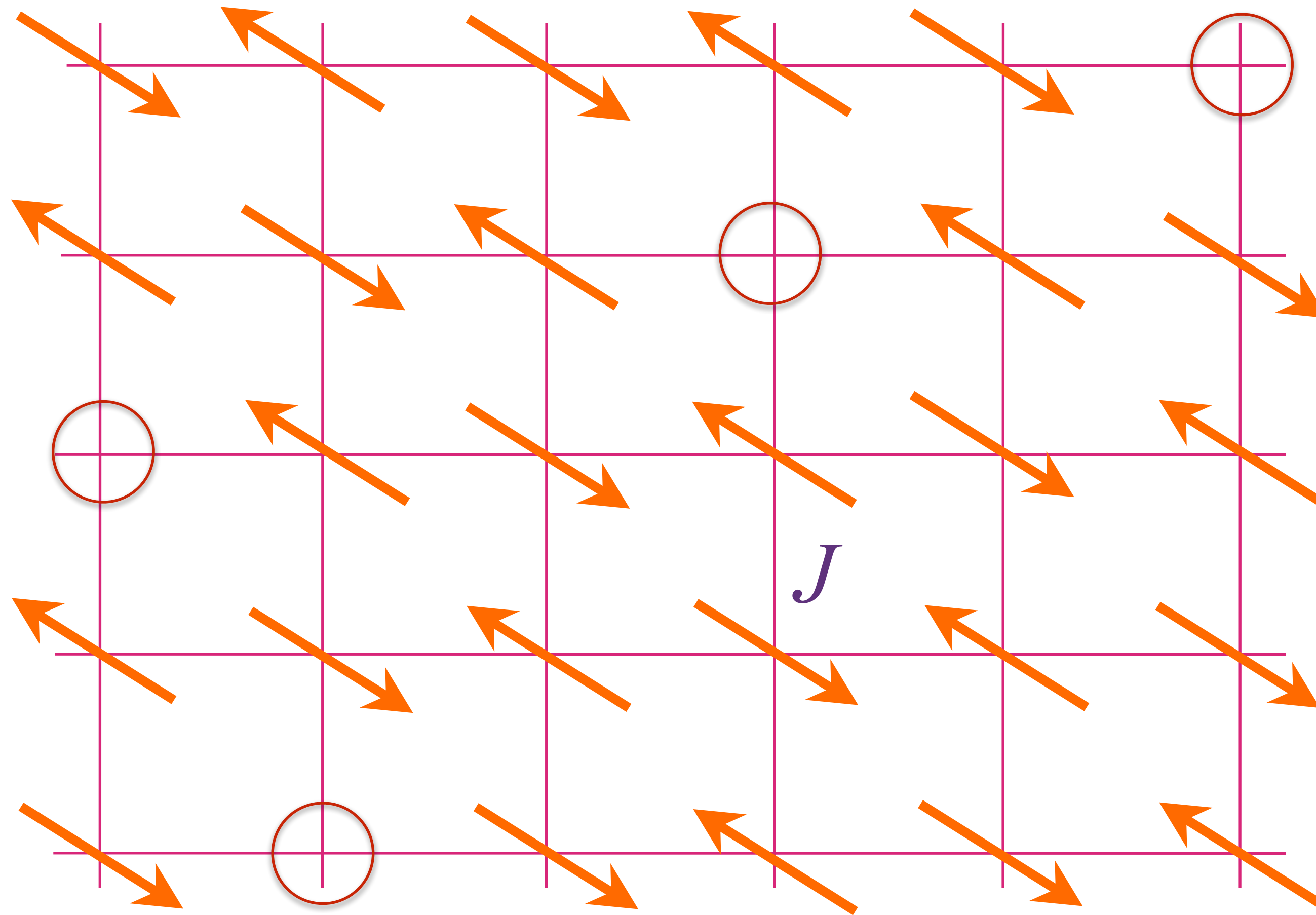
p mobile holes in a background of
fluctuating spins

Real-space view at small p



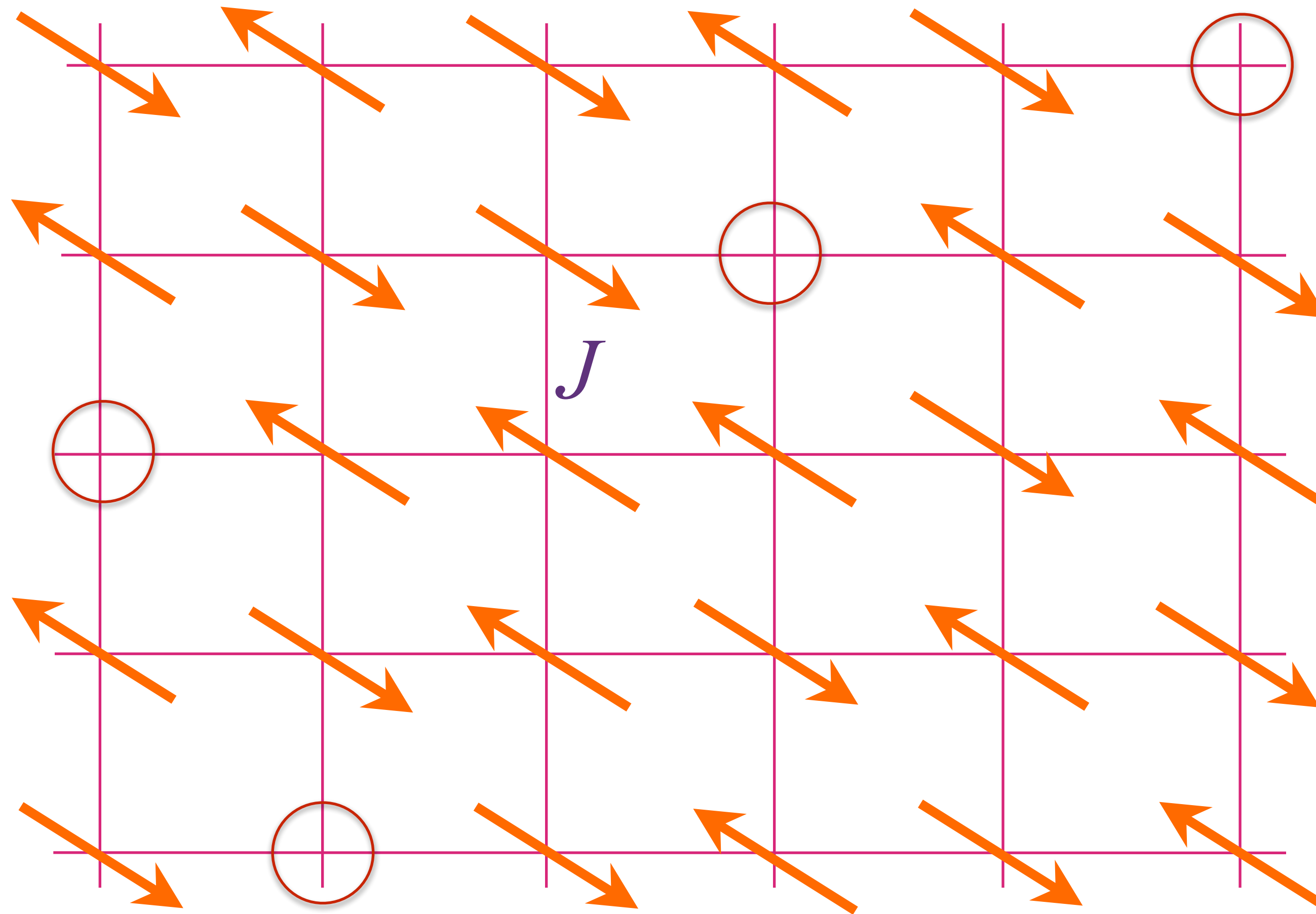
p mobile holes in a background of
fluctuating spins

Real-space view at small p



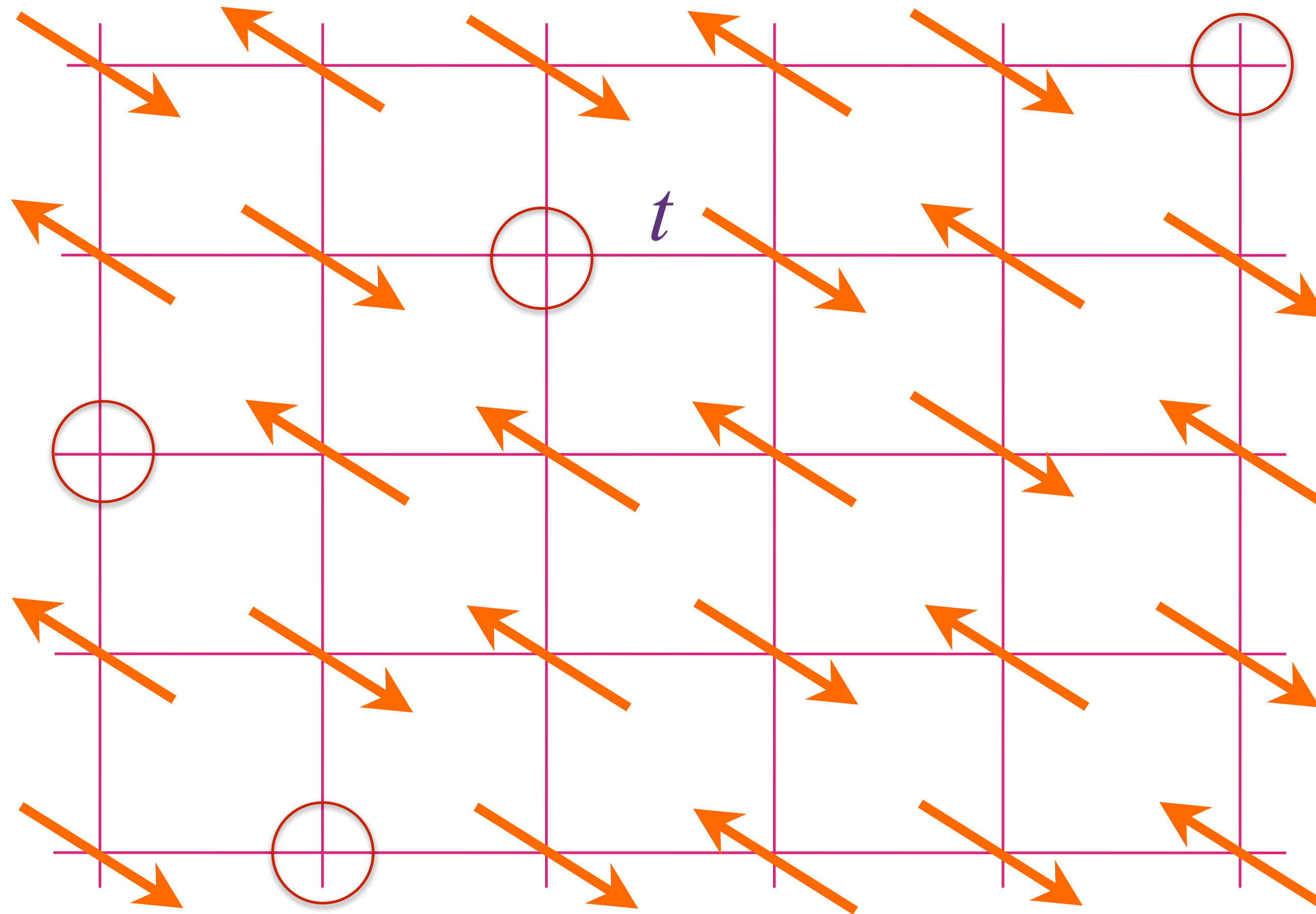
p mobile holes in a background of
fluctuating spins

Real-space view at small p



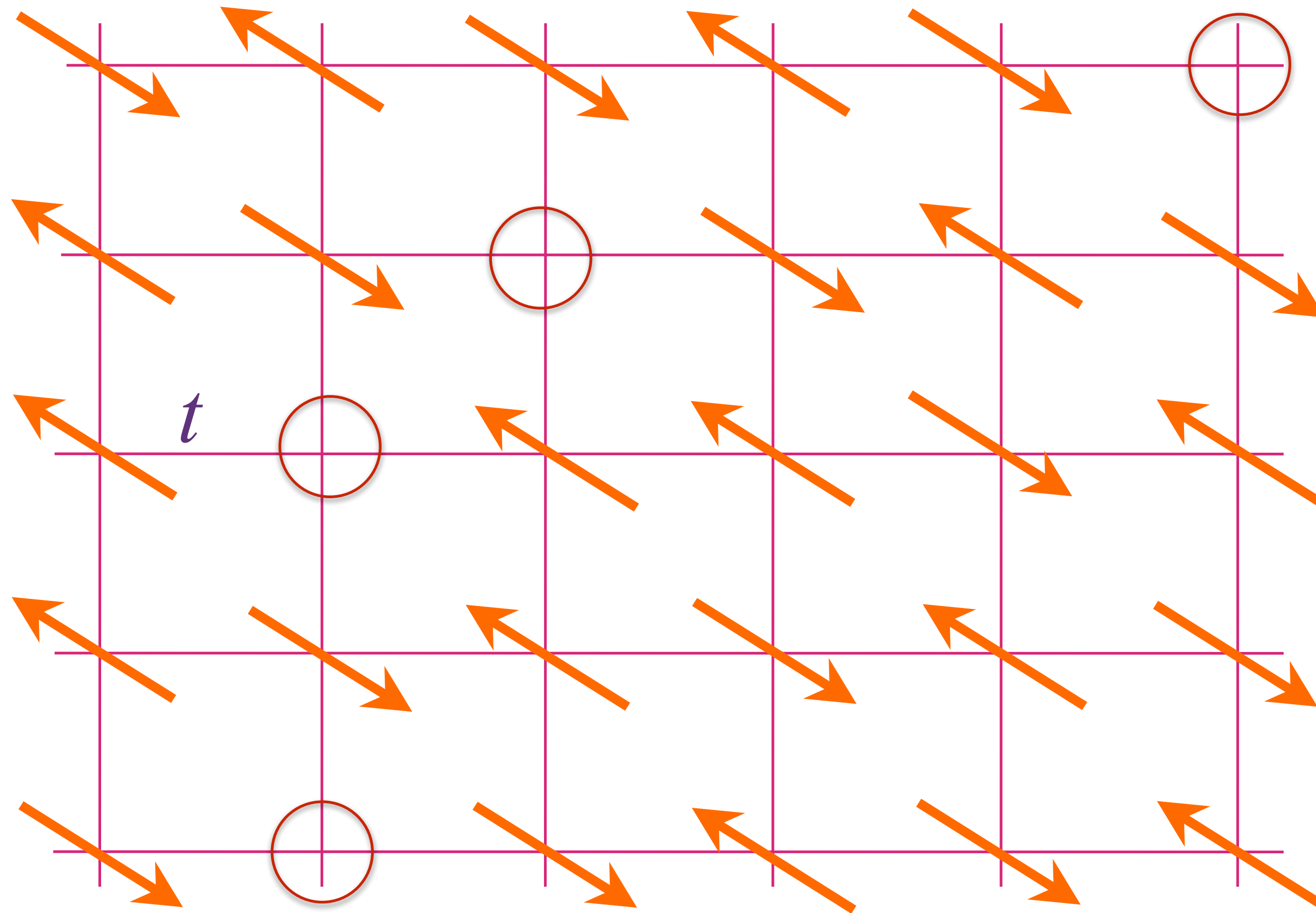
p mobile holes in a background of
fluctuating spins

Real-space view at small p



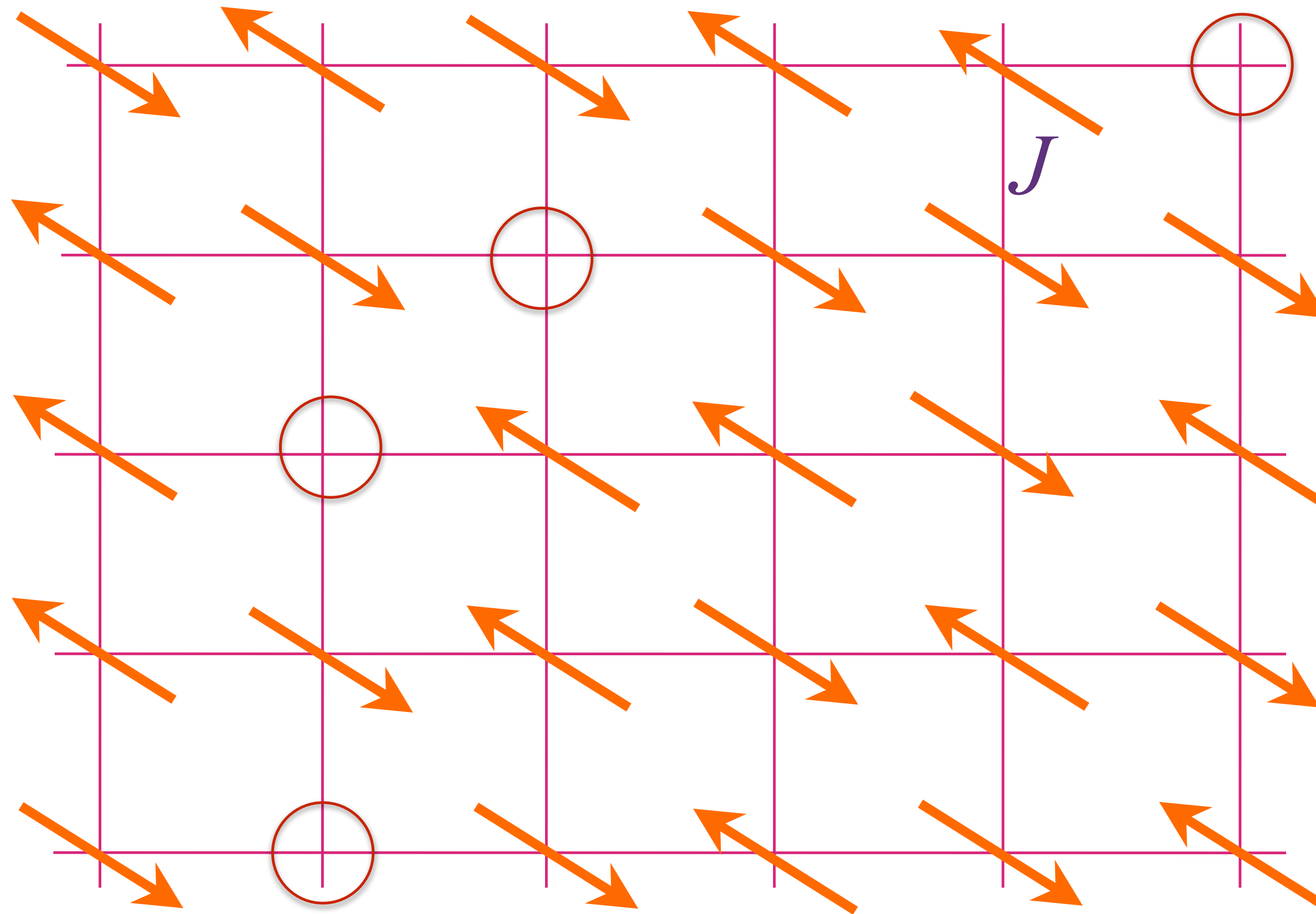
p mobile holes in a background of
fluctuating spins

Real-space view at small p



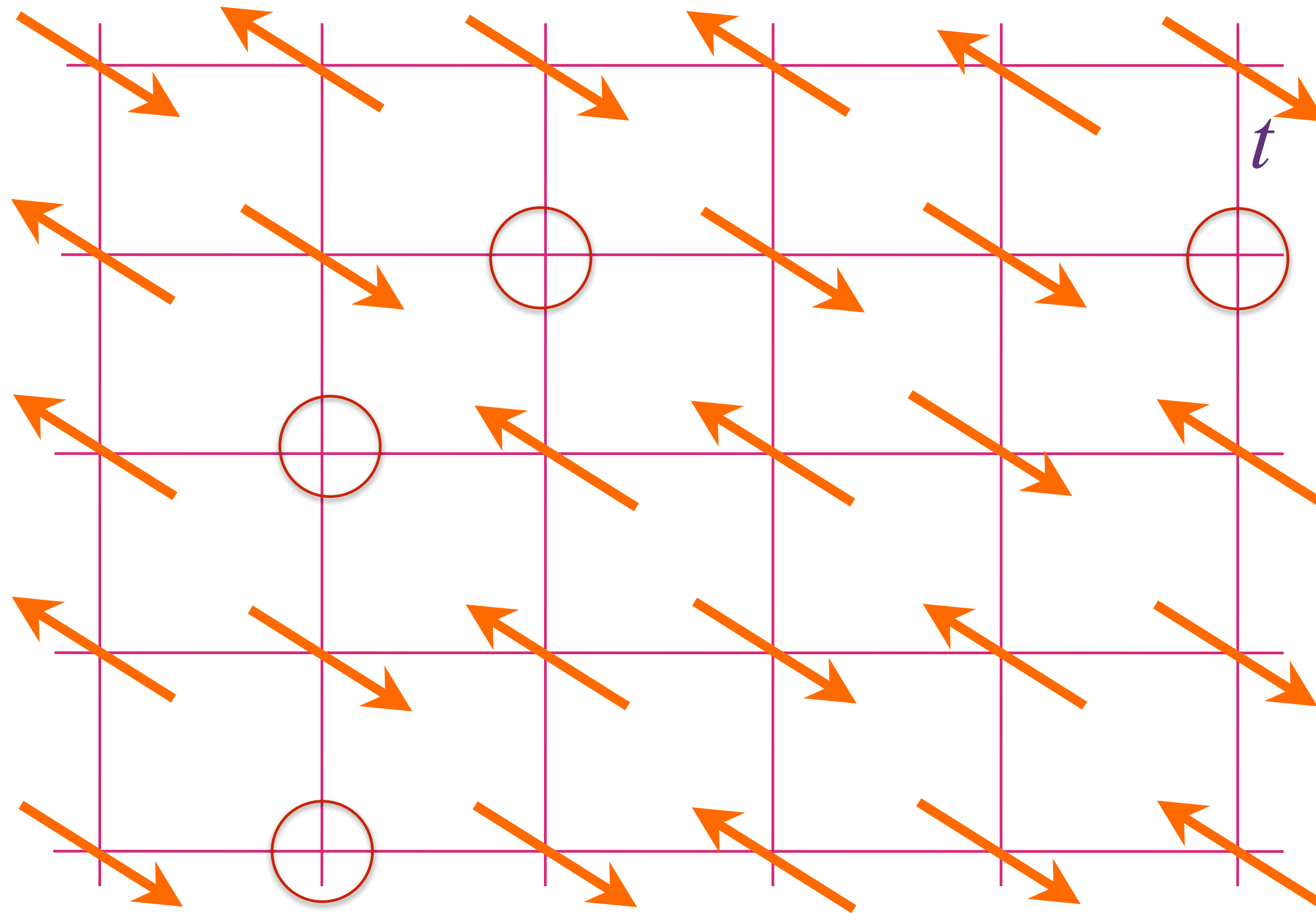
p mobile holes in a background of
fluctuating spins

Real-space view at small p



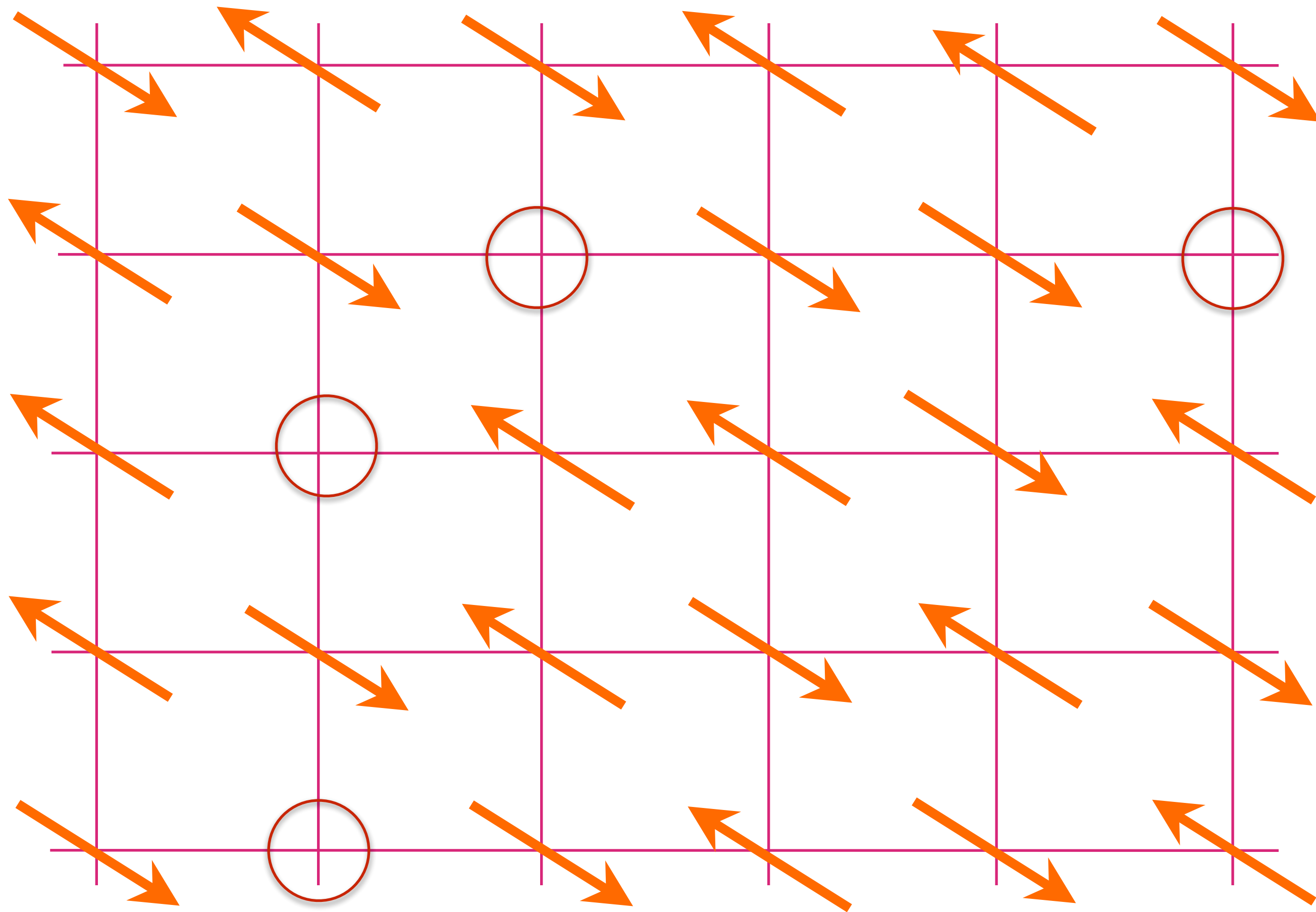
p mobile holes in a background of
fluctuating spins

Real-space view at small p



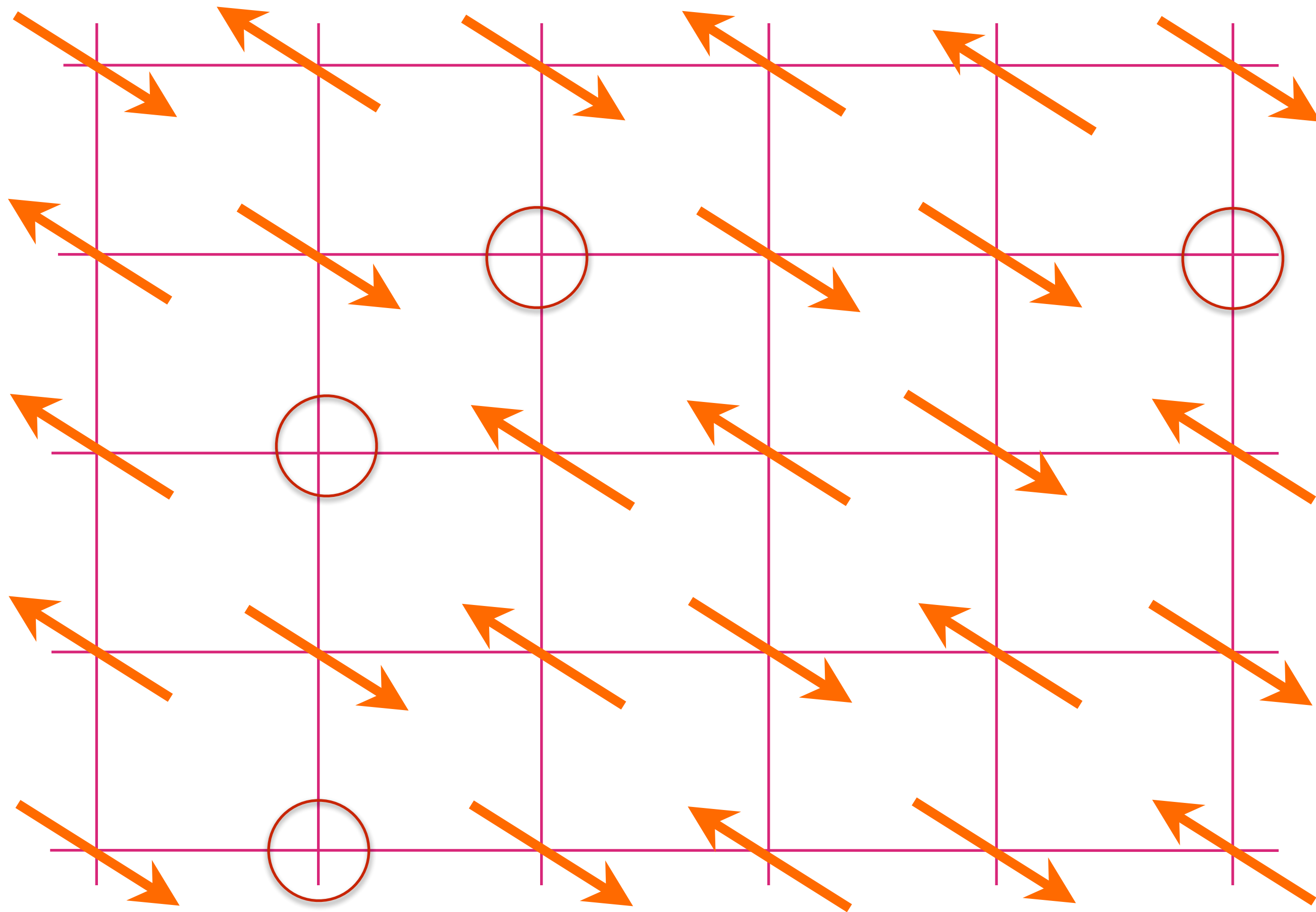
p mobile holes in a background of
fluctuating spins

Momentum-space view at large p



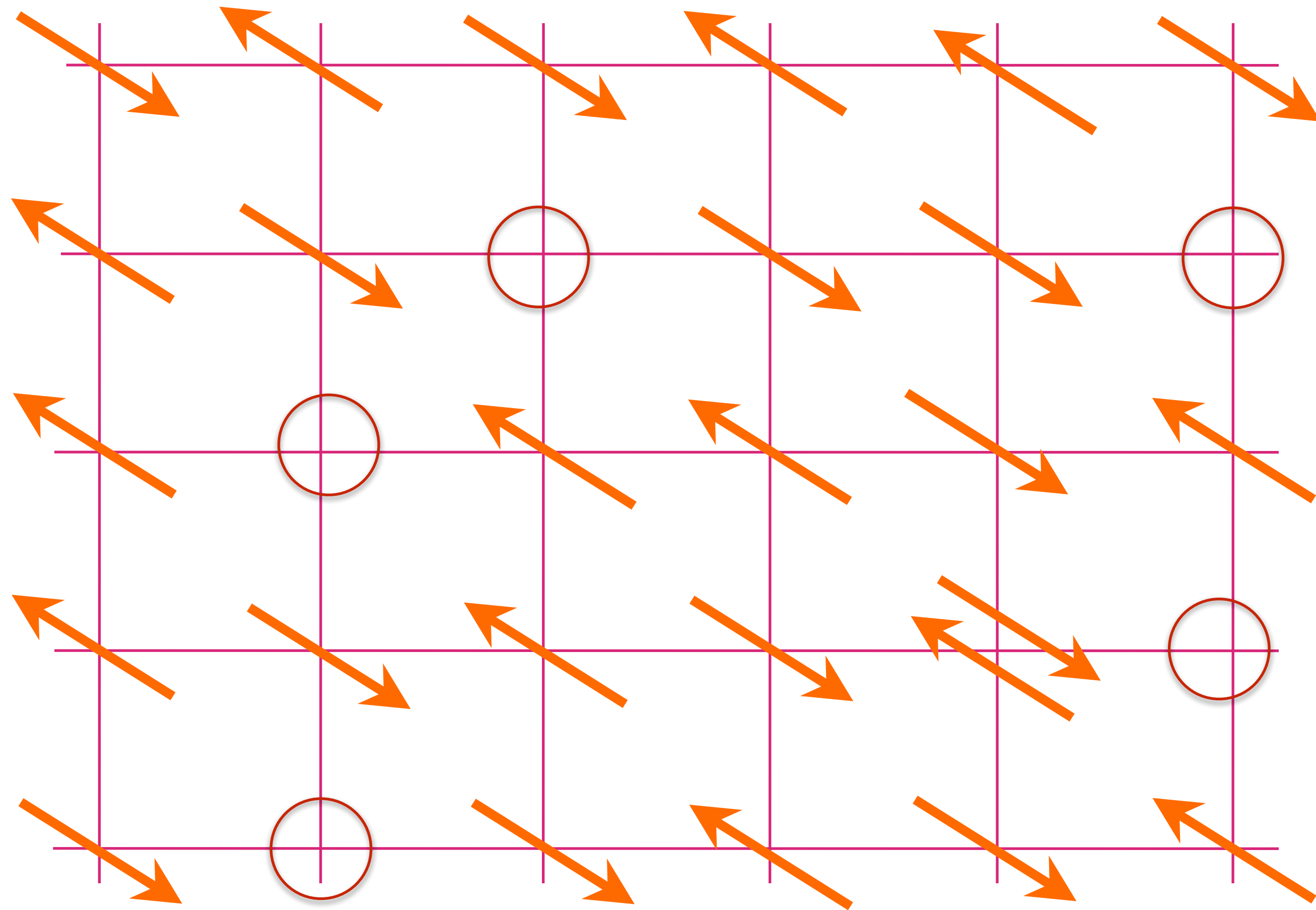
$1-p$ mobile electrons =
 $1+p$ mobile holes in a filled band

Momentum-space view at large p



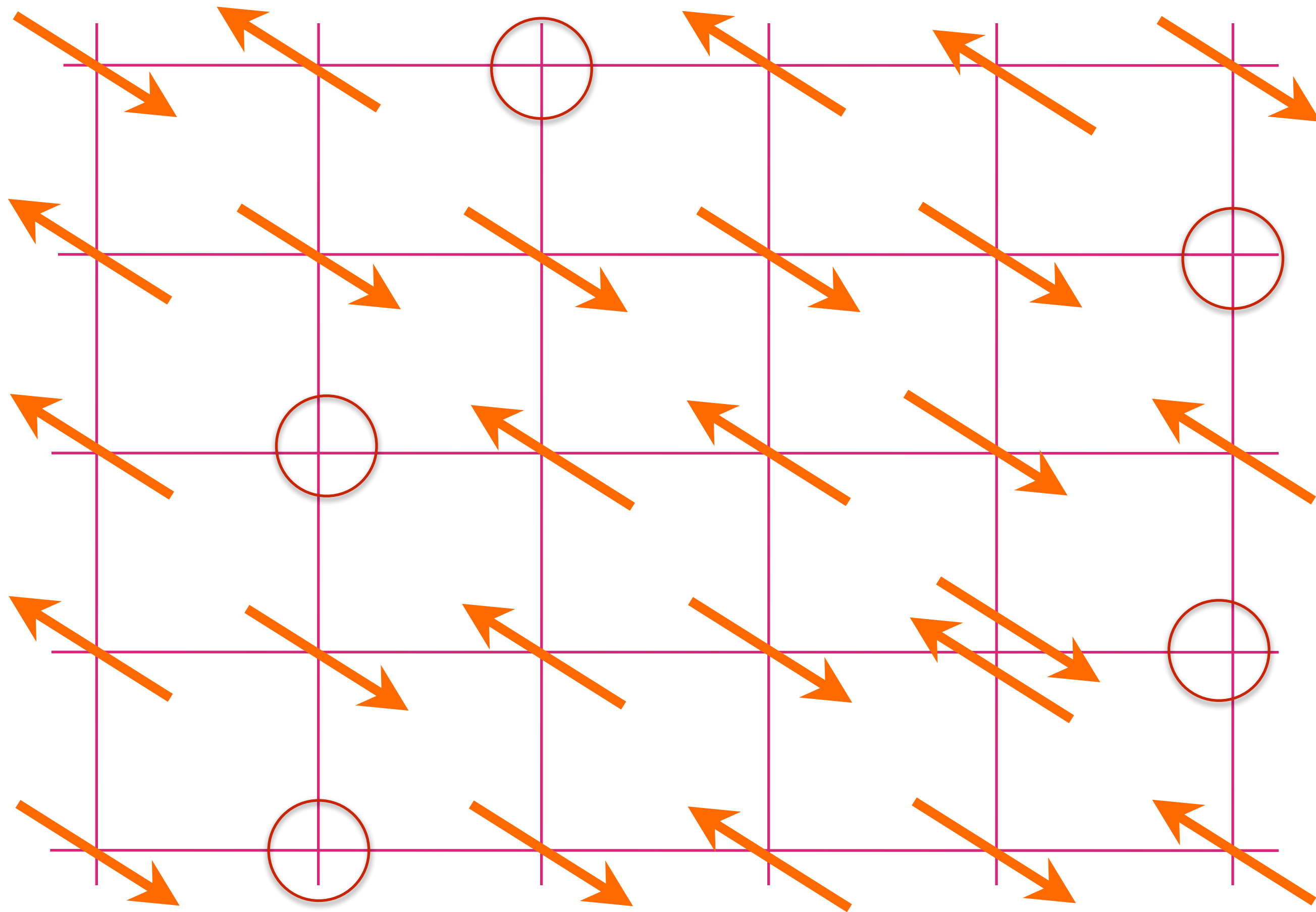
$1-p$ mobile electrons =
 $1+p$ mobile holes in a filled band

Momentum-space view at large p



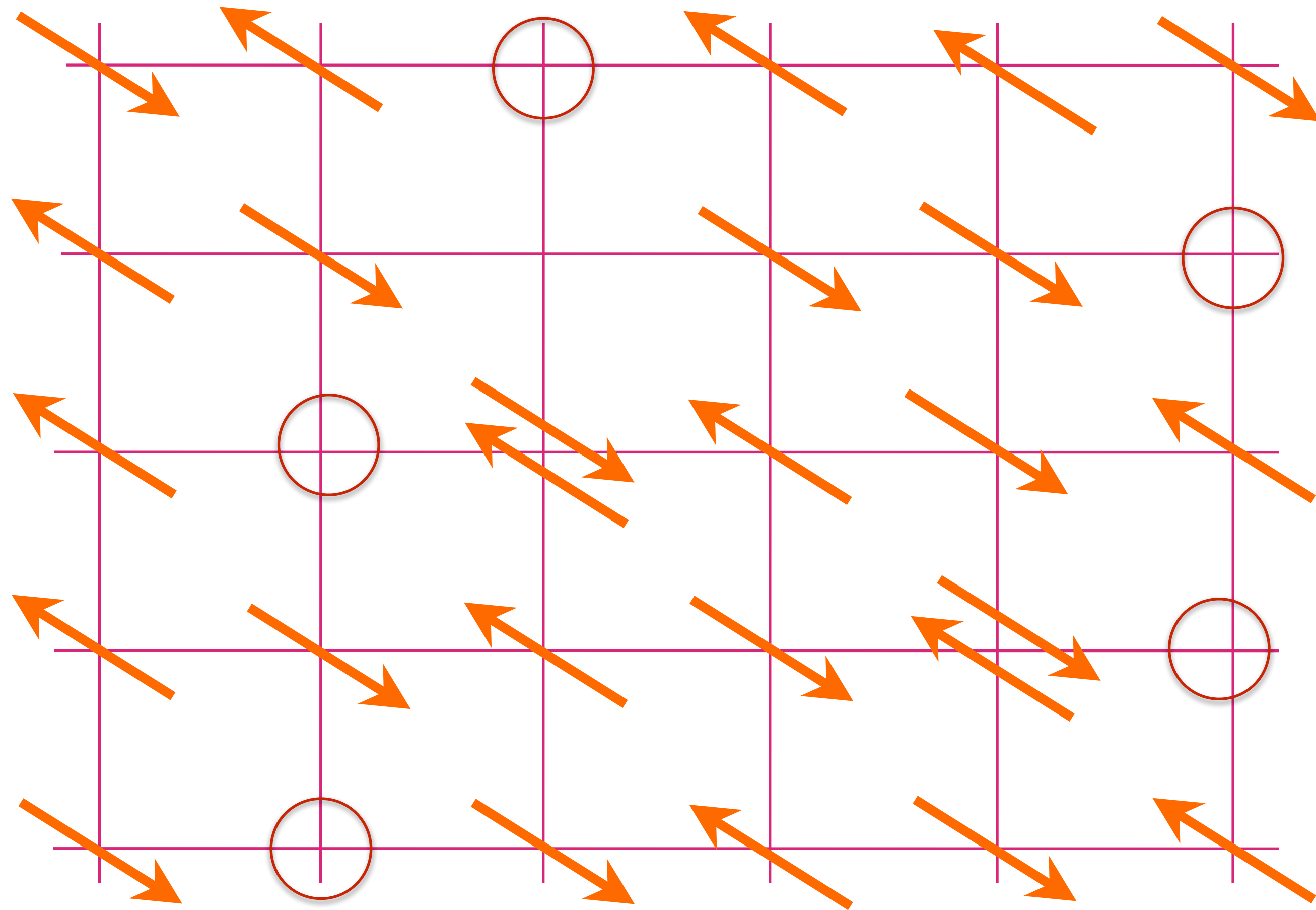
$1-p$ mobile electrons =
 $1+p$ mobile holes in a filled band

Momentum-space view at large p



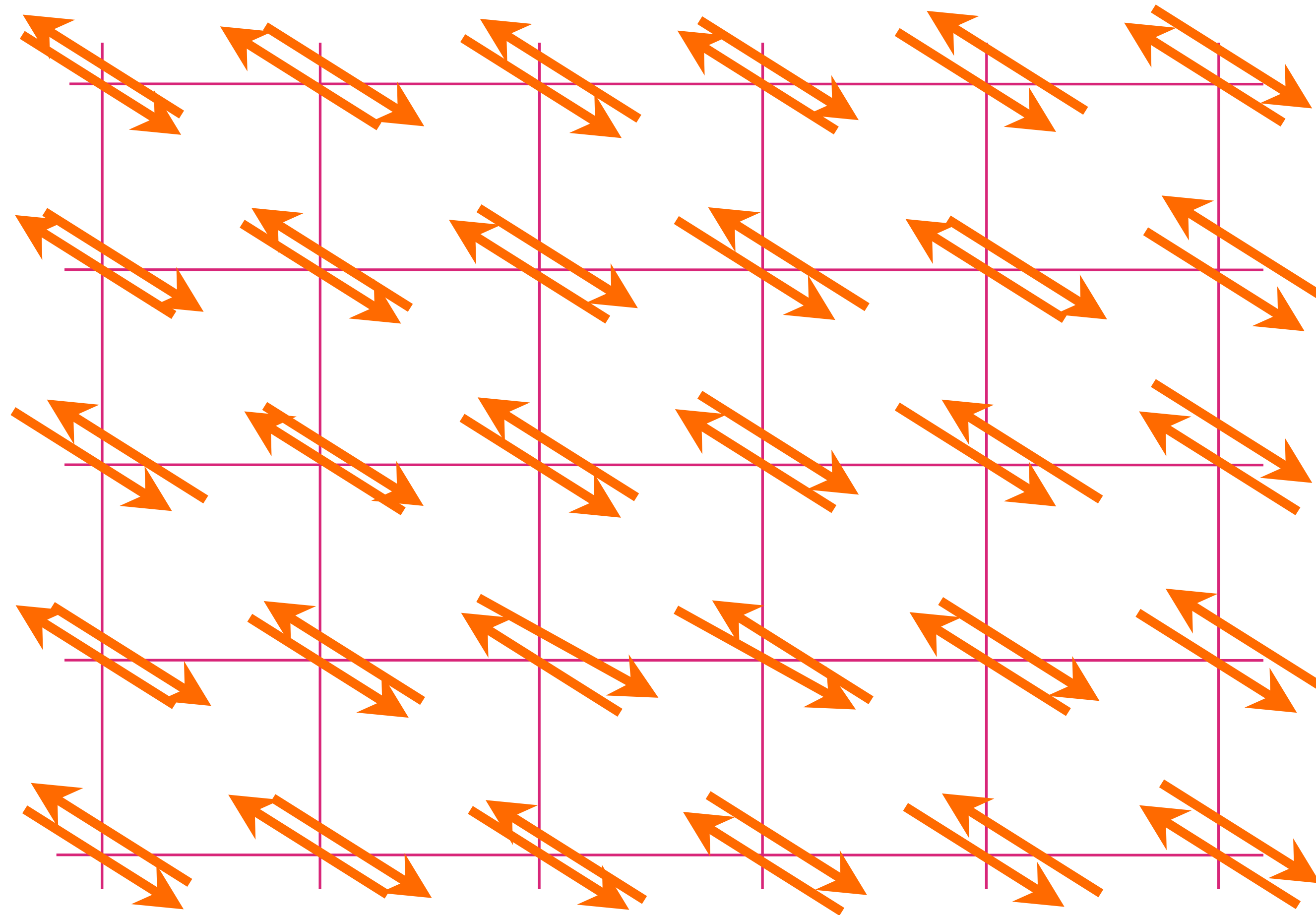
$1-p$ mobile electrons =
 $1+p$ mobile holes in a filled band

Momentum-space view at large p



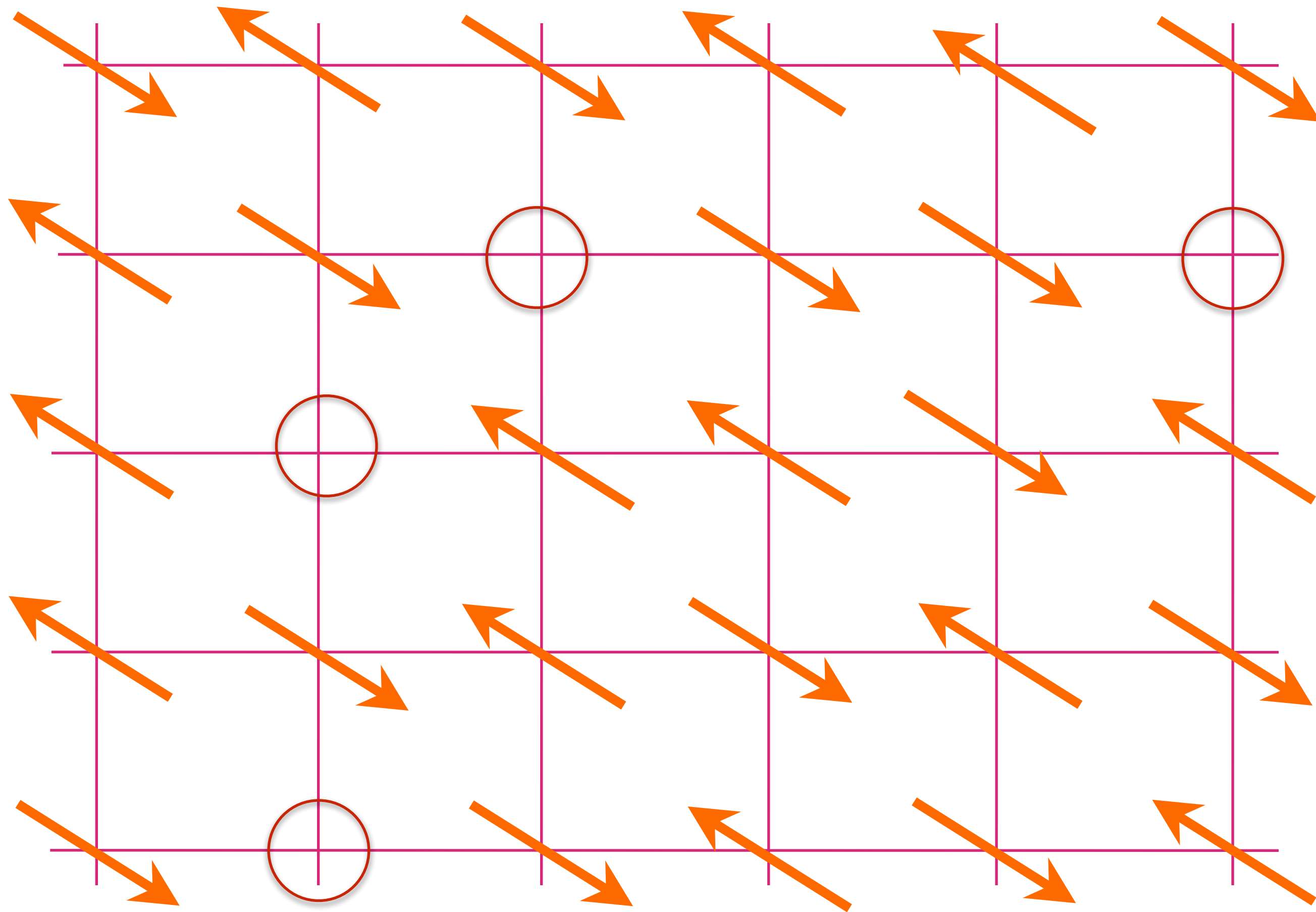
$1-p$ mobile electrons =
 $1+p$ mobile holes in a filled band

Momentum-space view at large p



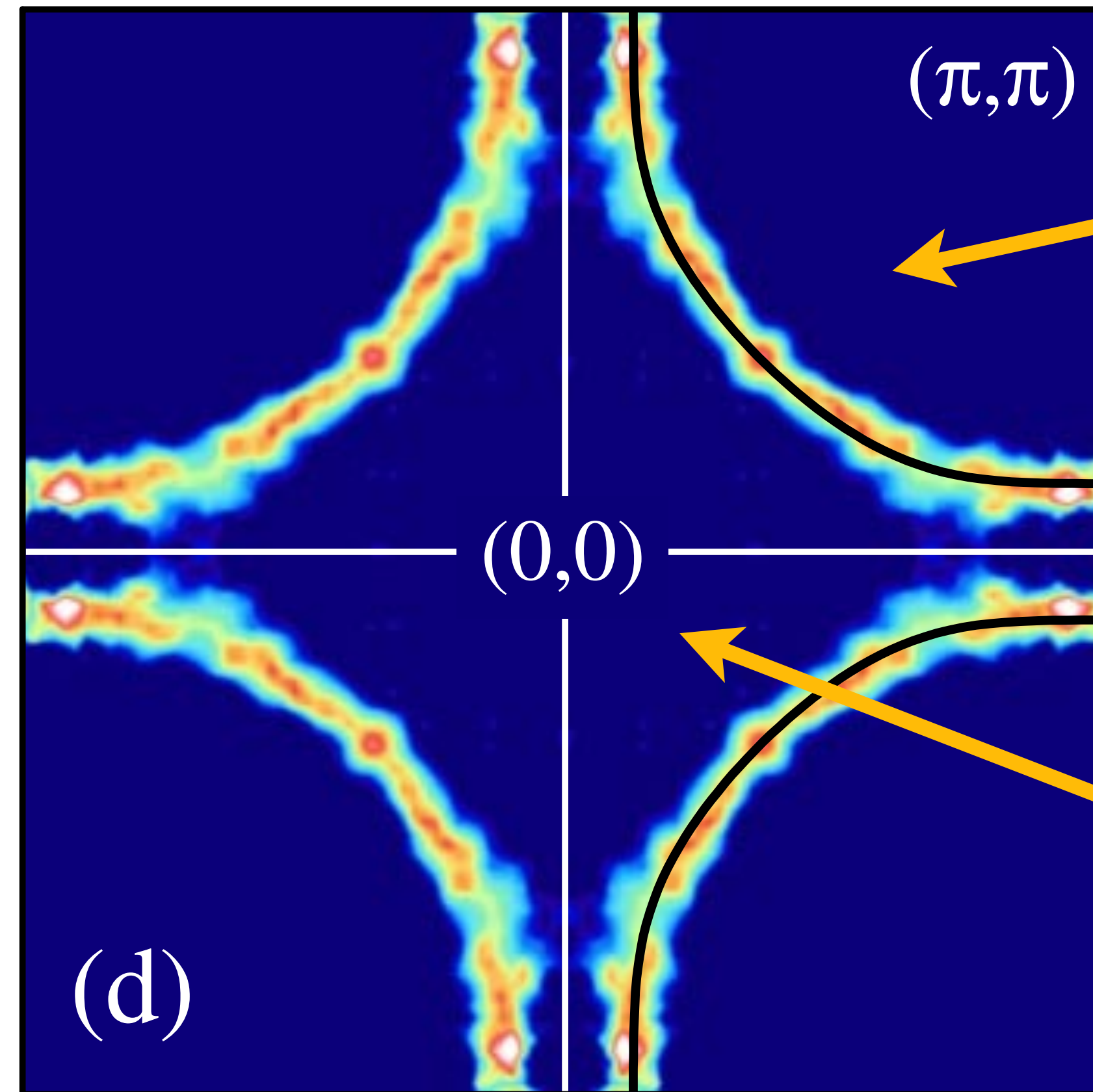
Filled
Band

Momentum-space view at large p



$1-p$ mobile electrons =
 $1+p$ mobile holes in a filled band

Momentum-space view at large p



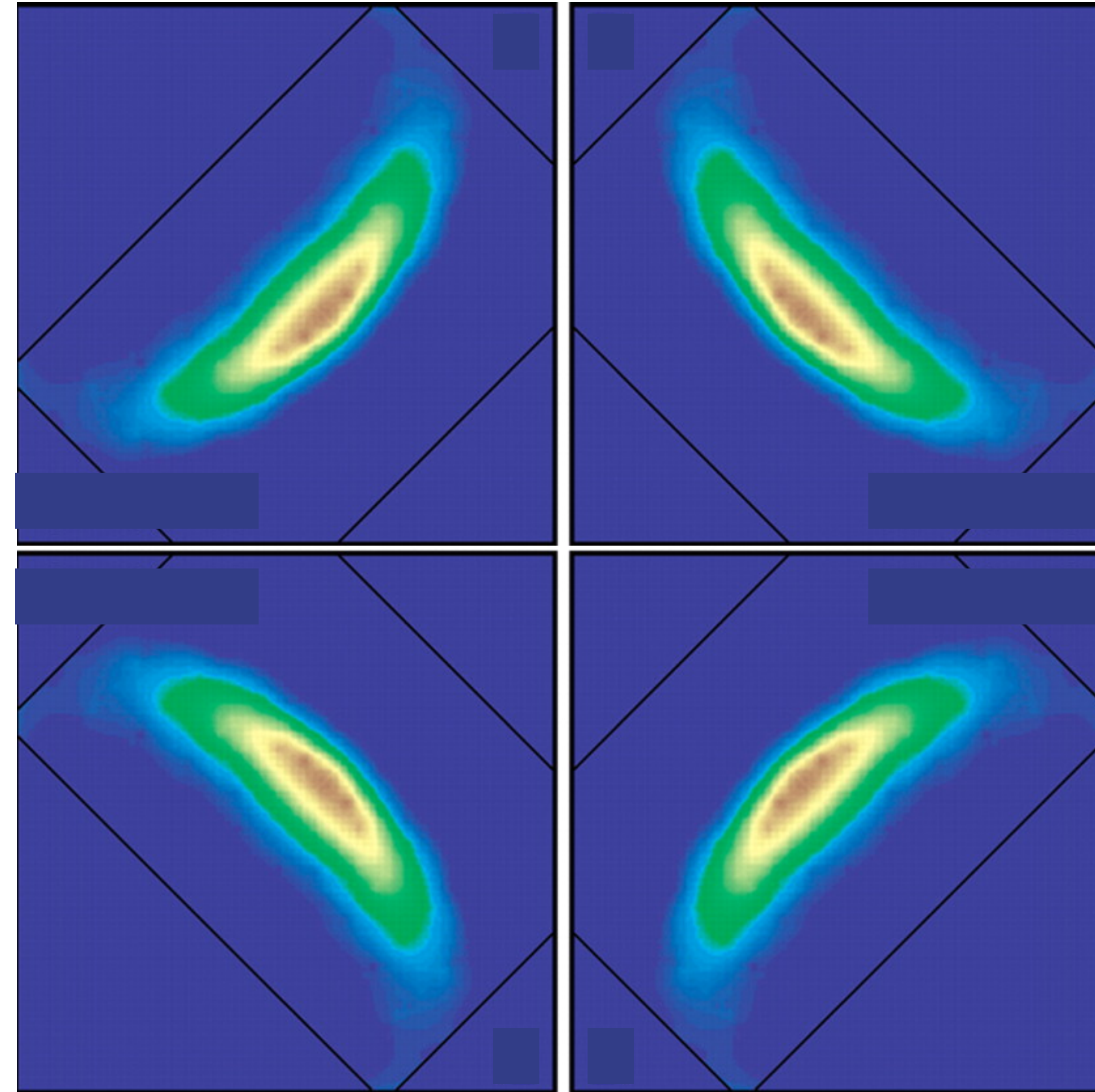
$l+p$ holes

Overdoped $\text{Tl}_2\text{Ba}_2\text{CuO}_{6+\delta}$
 $T_c = 30\text{K}$

$l-p$ electrons

$l+p$ mobile holes in a filled band

Momentum-space view at small p



$\text{Ca}_{2-x}\text{Na}_x\text{CuO}_2\text{Cl}_2$
at $x = 0.10$

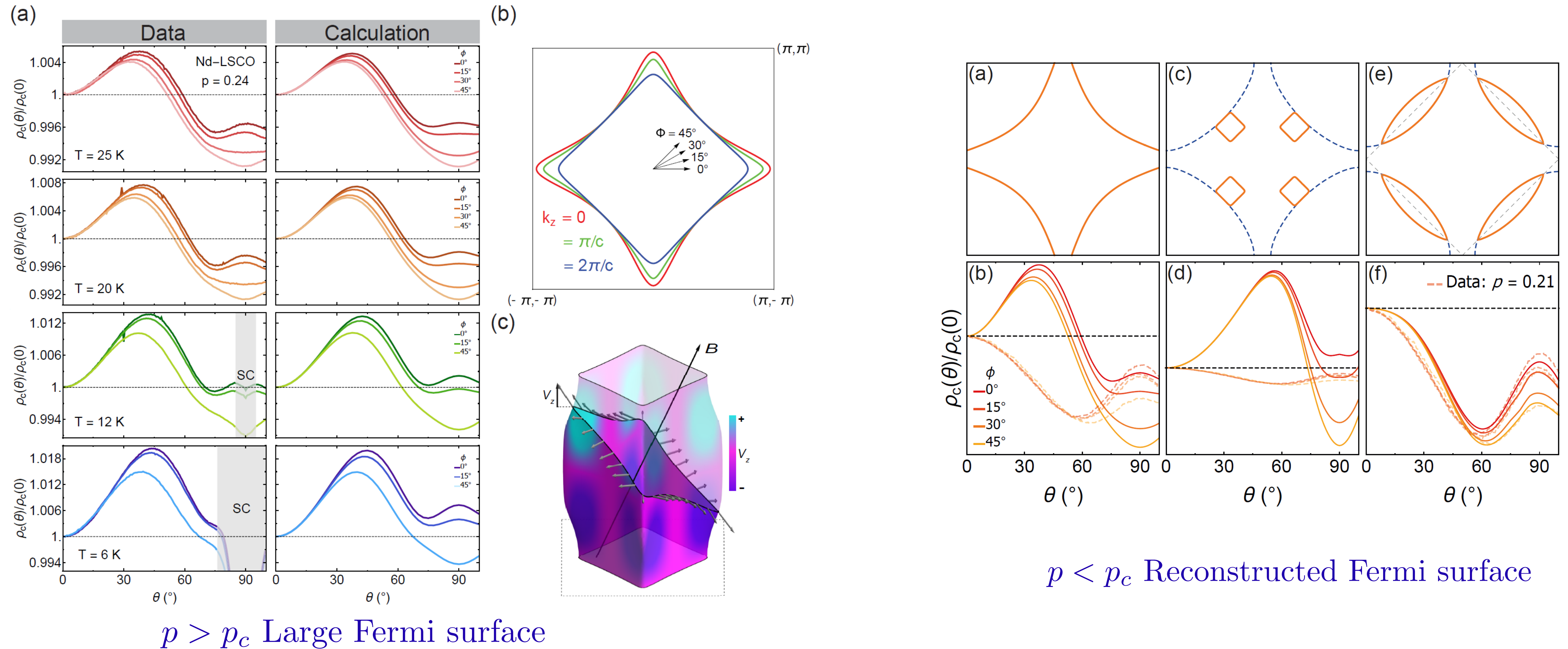
“Fermi arcs”

Kyle M. Shen, F. Ronning, D. H. Lu, F. Baumberger, N. J. C. Ingle, W. S. Lee, W. Meevasana, Y. Kohsaka, M. Azuma, M. Takano, H. Takagi, Z.-X. Shen, *Science* **307**, 901 (2005)

Fermi surface transformation at the pseudogap critical point of a cuprate superconductor

Yawen Fang, Gaël Grissonnanche, Anaëlle Legros, Simon Verret, Francis Laliberté, Clément Collignon, Amirreza Ataei, Maxime Dion, Jianshi Zhou, David Graf, M. J. Lawler, Paul Goddard, Louis Taillefer, and B. J. Ramshaw, arXiv:2004.01725

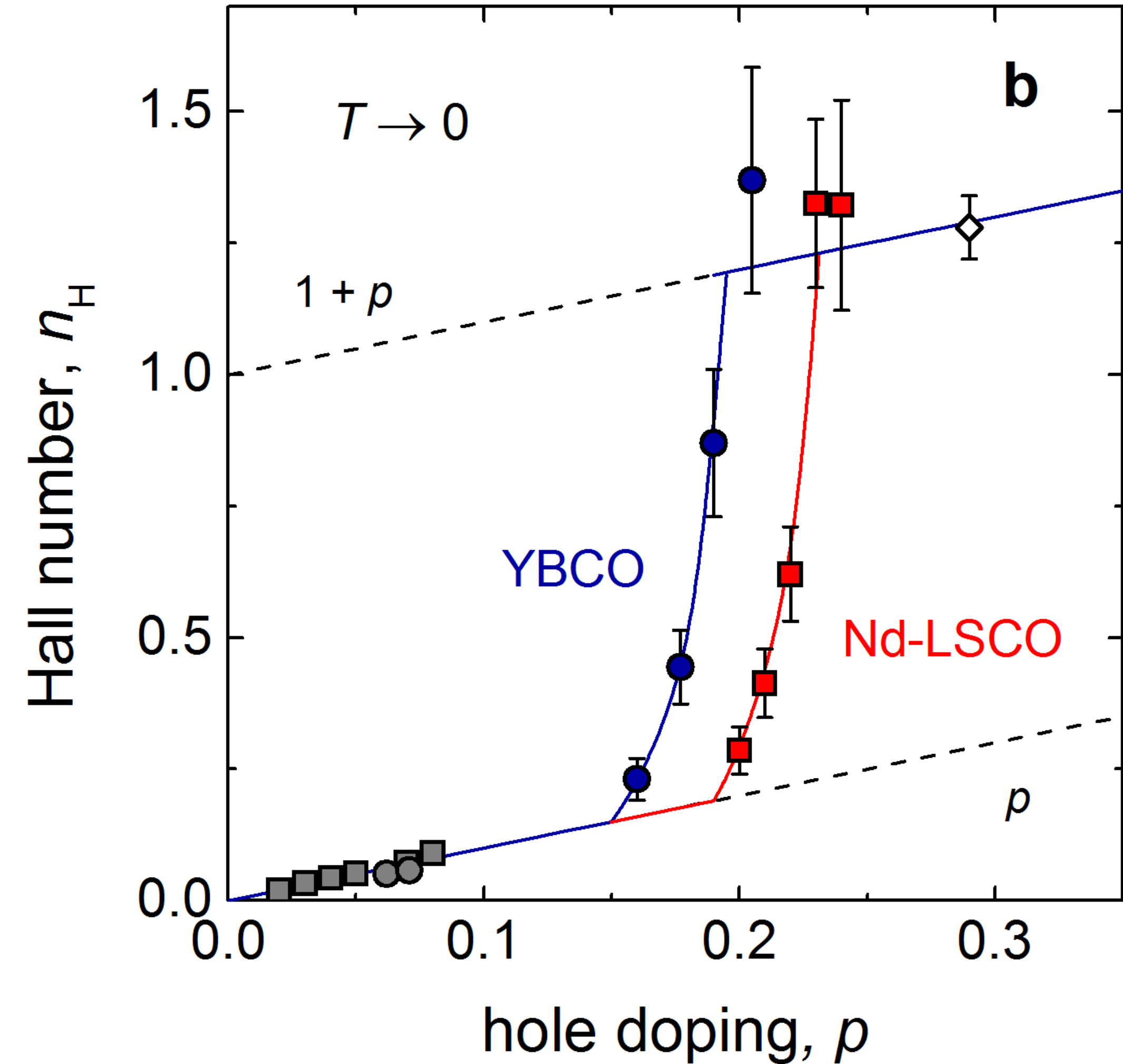
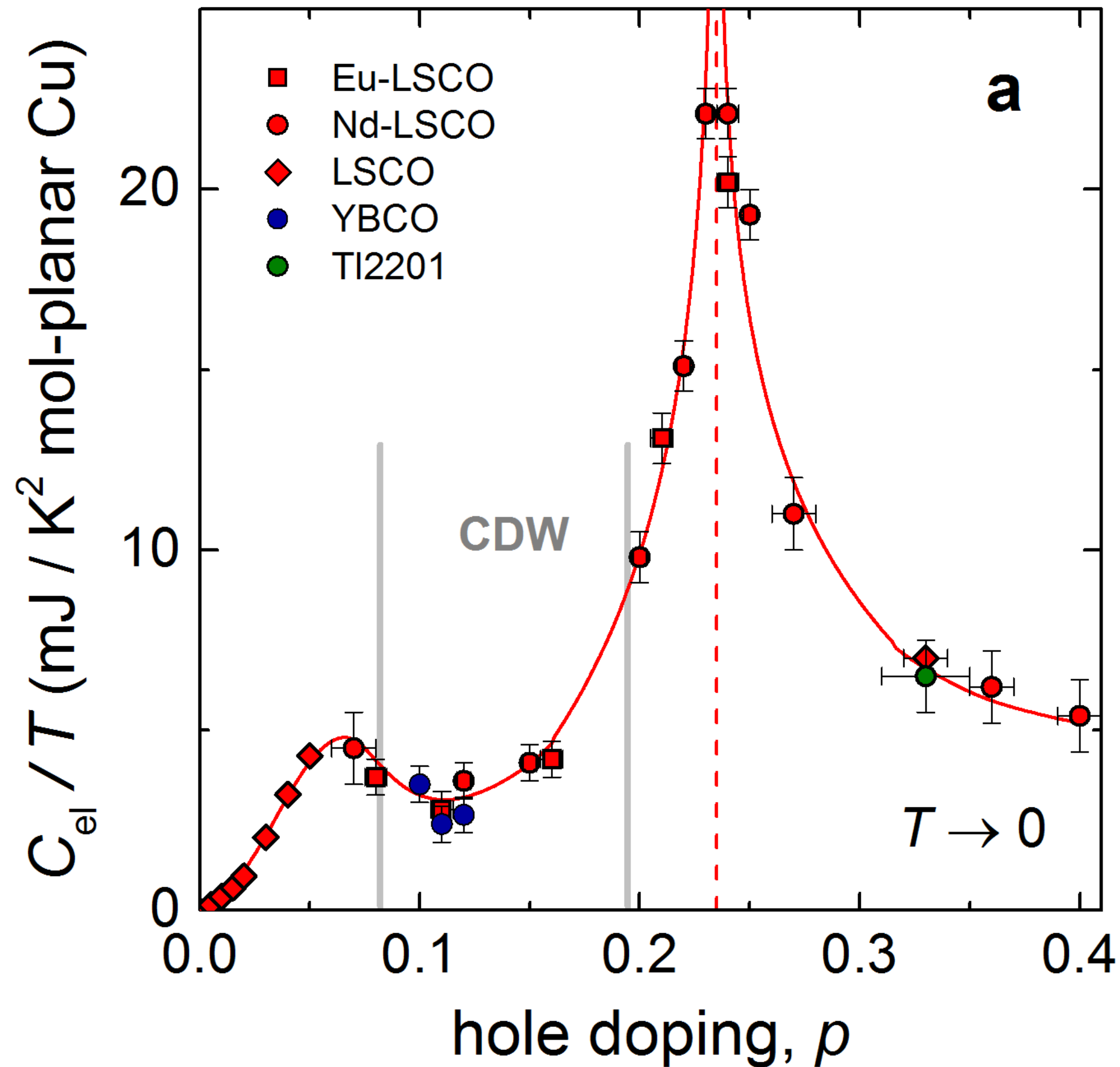
We use angle-dependent magnetoresistance (ADMR) to measure the Fermi surface of the cuprate $\text{La}_{1.6-x}\text{Nd}_{0.4}\text{Sr}_x\text{CuO}_4$. Above the critical doping p^* — outside of the pseudogap phase — we find a Fermi surface that is in quantitative agreement with angle-resolved photoemission. Below p^* , however, the ADMR is qualitatively different, revealing a clear change in Fermi surface topology. We find that our data is most consistent with a Fermi surface that has been reconstructed by a $Q = (\pi, \pi)$ wavevector. While static $Q = (\pi, \pi)$ antiferromagnetism is not found at these dopings, our results suggest that this wavevector is a fundamental organizing principle of the pseudogap phase.



Hole doped cuprates

The remarkable underlying ground states of cuprate superconductors

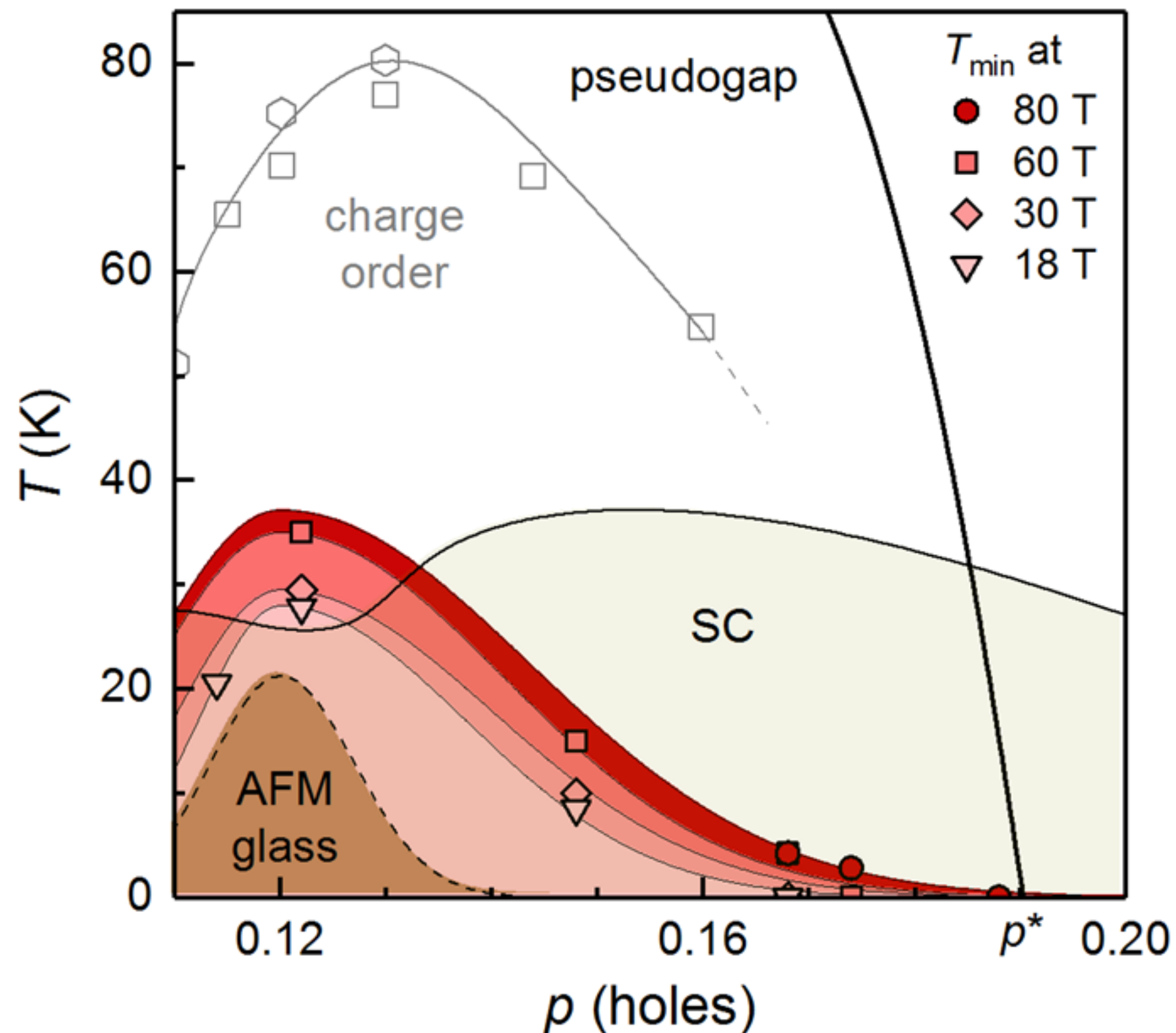
Cyril Proust and Louis Taillefer, Annual Review Condensed Matter Physics **10**, 409 (2019)



Hidden magnetism at the pseudogap critical point of a high temperature superconductor

Nature Physics doi: 10.1038/s41567-020-0950-5

Mehdi Frachet^{1†}, Igor Vinograd^{1†}, Rui Zhou^{1,2}, Siham Benhabib¹, Shangfei Wu¹, Hadrien Mayaffre¹, Steffen Krämer¹, Sanath K. Ramakrishna³, Arneil P. Reyes³, Jérôme Debray⁴, Tohru Kurosawa⁵, Naoki Momono⁶, Migaku Oda⁵, Seiki Komiya⁷, Shimpei Ono⁷, Masafumi Horio⁸, Johan Chang⁸, Cyril Proust¹, David LeBoeuf^{1*}, Marc-Henri Julien^{1*}



Quasi-static magnetism in the pseudogap state of $\text{La}_{2-x}\text{Sr}_x\text{CuO}_4$.

Temperature – doping phase diagram representing T_{min} , the temperature of the minimum in the sound velocity, at different fields. Since superconductivity precludes the observation of T_{min} in zero-field, the dashed line (brown area) represents the extrapolated $T_{min}(B=0)$. While not exactly equal to the freezing temperature T_f (see Fig. 2), T_{min} is closely tied to T_f and so is expected to have the same doping dependence, including a peak around $p = 0.12$ in zero/low fields (ref. 2). Onset temperatures of charge order are from ref. 33 (squares) and 35 (hexagons).

1. Metal-metal transition in the Kondo Lattice
2. Metal-metal transition in a one-band model
 - A. *FL* model of the pseudogap*
 - B. *Ancilla qubits and ghost Fermi surfaces*
3. Random J model (insulator)
RG analysis and exact exponent
4. Random t - J model (metals)
Numerics, RG analysis and exact exponents

1. Metal-metal transition in the Kondo Lattice

2. Metal-metal transition in a one-band model

A. FL model of the pseudogap*

B. Ancilla qubits and ghost Fermi surfaces

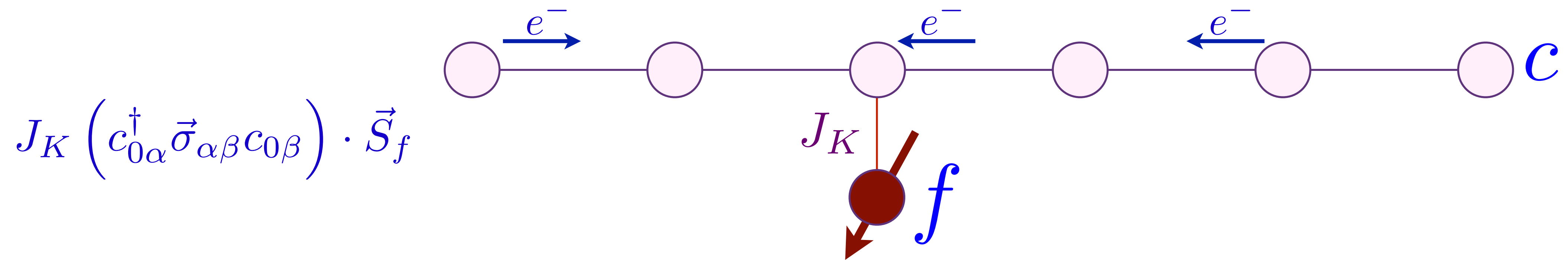
3. Random J model (insulator)

RG analysis and exact exponent

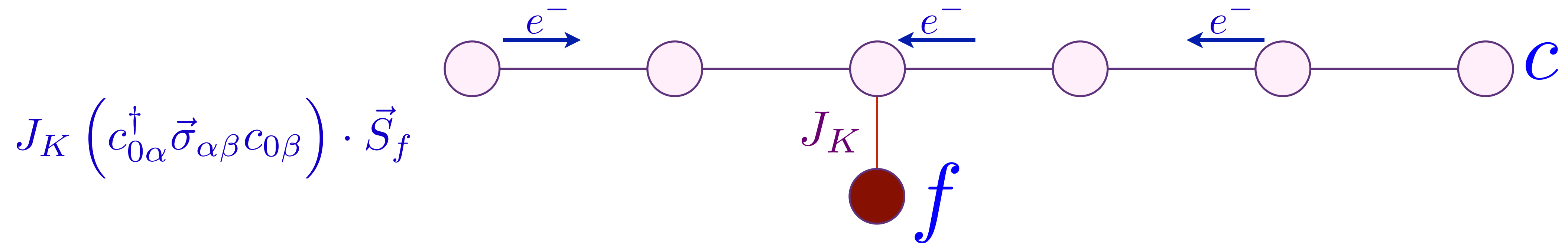
4. Random t - J model (metals)

Numerics, RG analysis and exact exponents

Kondo model



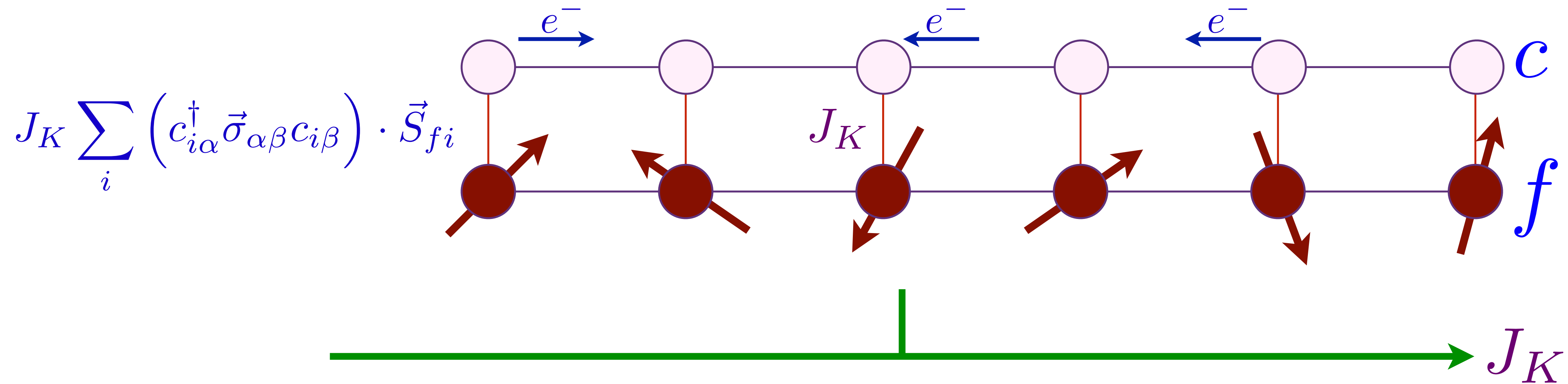
Kondo model



The c electrons ‘Kondo screen’ the f spin at low energies:
The f electron ‘dissolves’ into the Fermi sea.

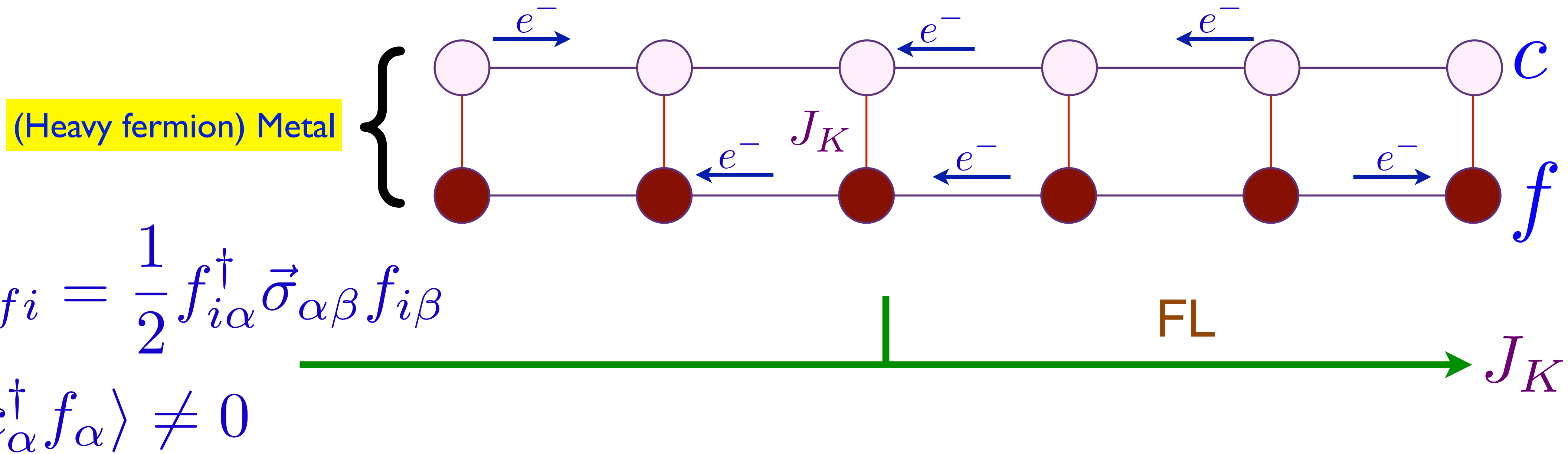
Metal-metal transitions in **Kondo lattice** models

Kondo lattice of f electron spins coupled to a conduction band of c electrons of density p .



Metal-metal transitions in **Kondo lattice** models

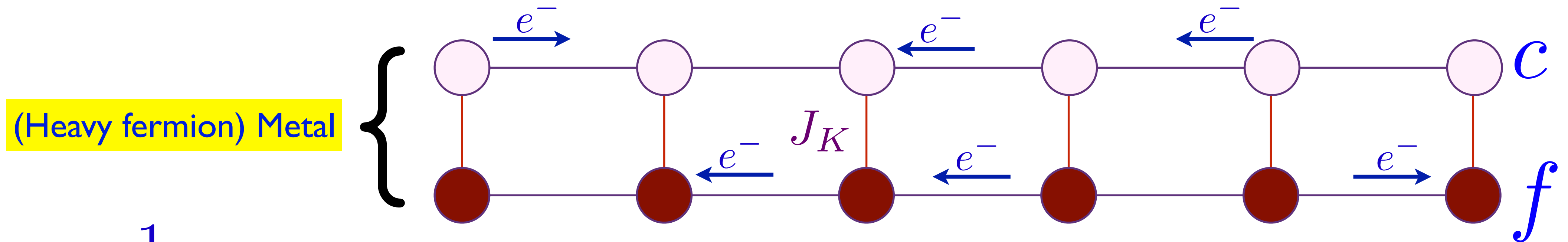
Kondo lattice of f electron spins coupled to a conduction band of c electrons of density p .



The c electrons ‘Kondo screen’ the f spins in the FL phase:
 The f electrons ‘dissolve’ into the Fermi sea.

Metal-metal transitions in **Kondo lattice** models

Kondo lattice of f electron spins coupled to a conduction band of c electrons of density p .



$$\vec{S}_{fi} = \frac{1}{2} f_{i\alpha}^\dagger \vec{\sigma}_{\alpha\beta} f_{i\beta}$$

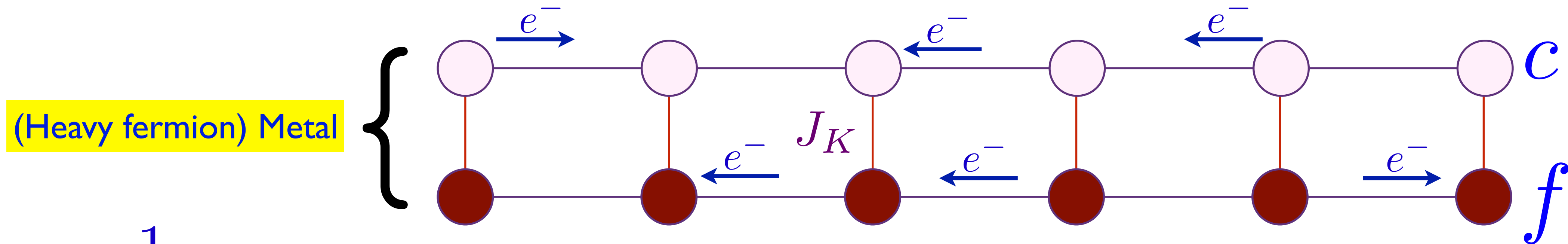
$$\langle c_\alpha^\dagger f_\alpha \rangle \neq 0$$

The Kondo lattice model has a gauge symmetry: $f_{i\alpha} \rightarrow e^{i\theta_i} f_{i\alpha}$

This gauge symmetry is fully broken by a Higgs condensate $\langle c_\alpha^\dagger f_\alpha \rangle$ in the FL phase.

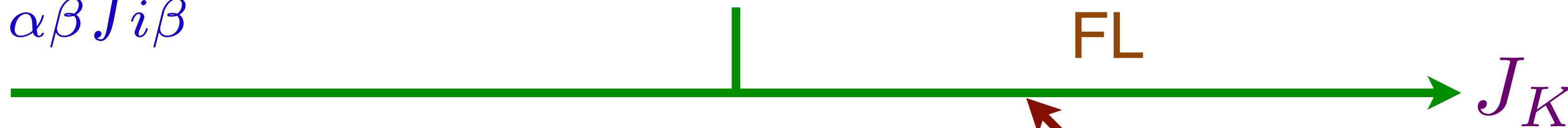
Metal-metal transitions in **Kondo lattice** models

Kondo lattice of f electron spins coupled to a conduction band of c electrons of density p .



$$\vec{S}_{fi} = \frac{1}{2} f_{i\alpha}^\dagger \vec{\sigma}_{\alpha\beta} f_{i\beta}$$

$$\langle c_\alpha^\dagger f_\alpha \rangle \neq 0$$

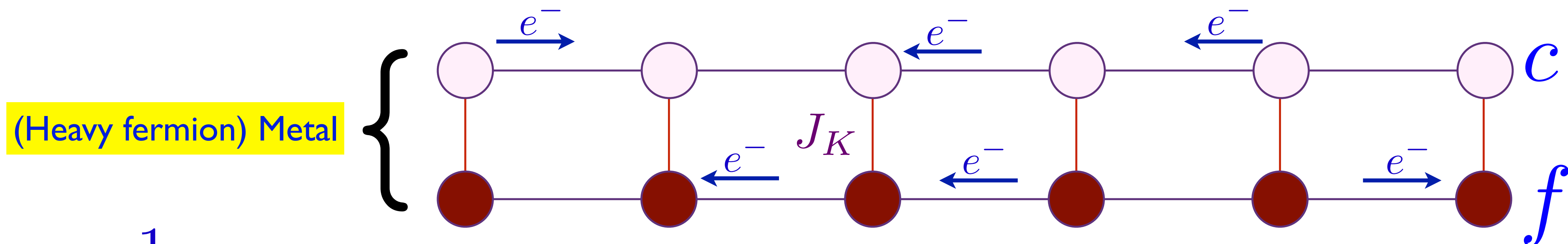


Large Fermi surface of size $1 + p$

$|\Phi\rangle = [\text{Projection onto one } f \text{ per site}]$
 $\otimes |\text{Slater determinant of } (c, f)\rangle$

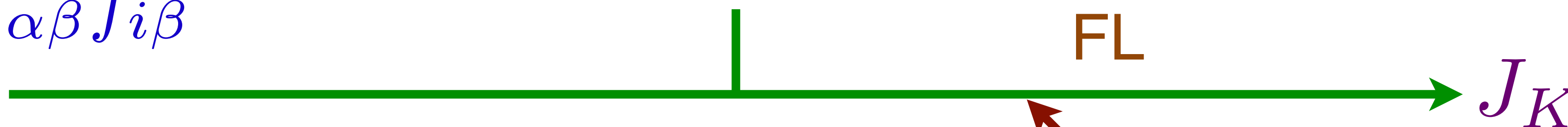
Metal-metal transitions in **Kondo lattice** models

Kondo lattice of f electron spins coupled to a conduction band of c electrons of density p .



$$\vec{S}_{fi} = \frac{1}{2} f_{i\alpha}^\dagger \vec{\sigma}_{\alpha\beta} f_{i\beta}$$

$$\langle c_\alpha^\dagger f_\alpha \rangle \neq 0$$



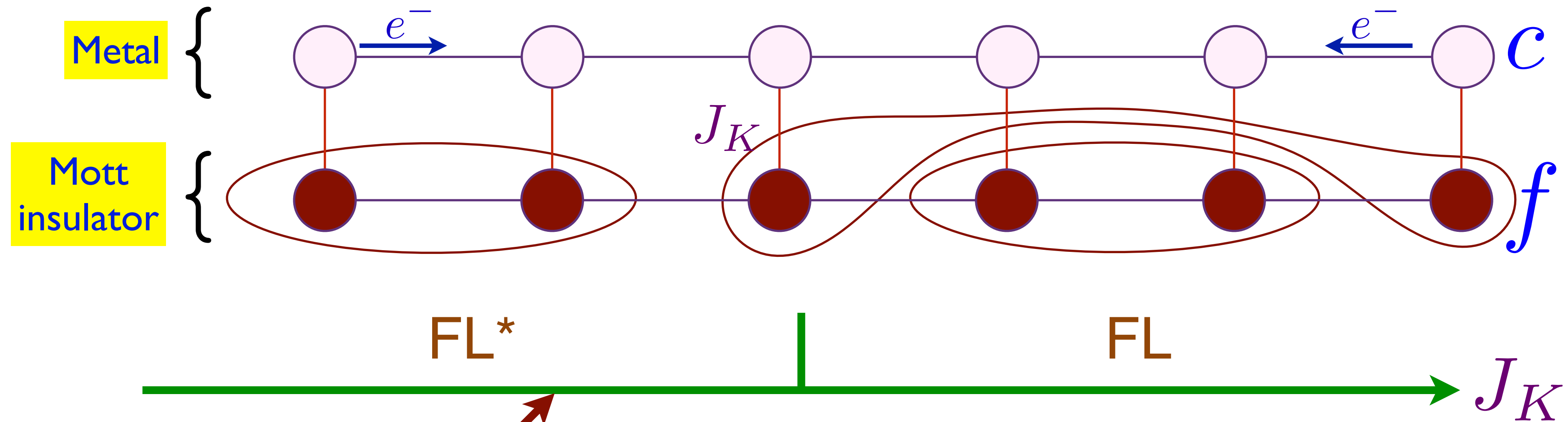
Luttinger
Theorem
obeyed

Large Fermi surface of size $1 + p$
 $|\Phi\rangle = [\text{Projection onto one } f \text{ per site}]$
 $\otimes |\text{Slater determinant of } (c, f)\rangle$

Metal-metal transitions in *Kondo lattice* models

Kondo lattice of f electron spins coupled to a conduction band of c electrons of density p .

Kondo-breakdown or 'selective Mott' transition



Small Fermi surface of size p

$|\Phi\rangle = |\text{Spin liquid insulator of } f\rangle$
 $\otimes |\text{Slater determinant of } c\rangle$

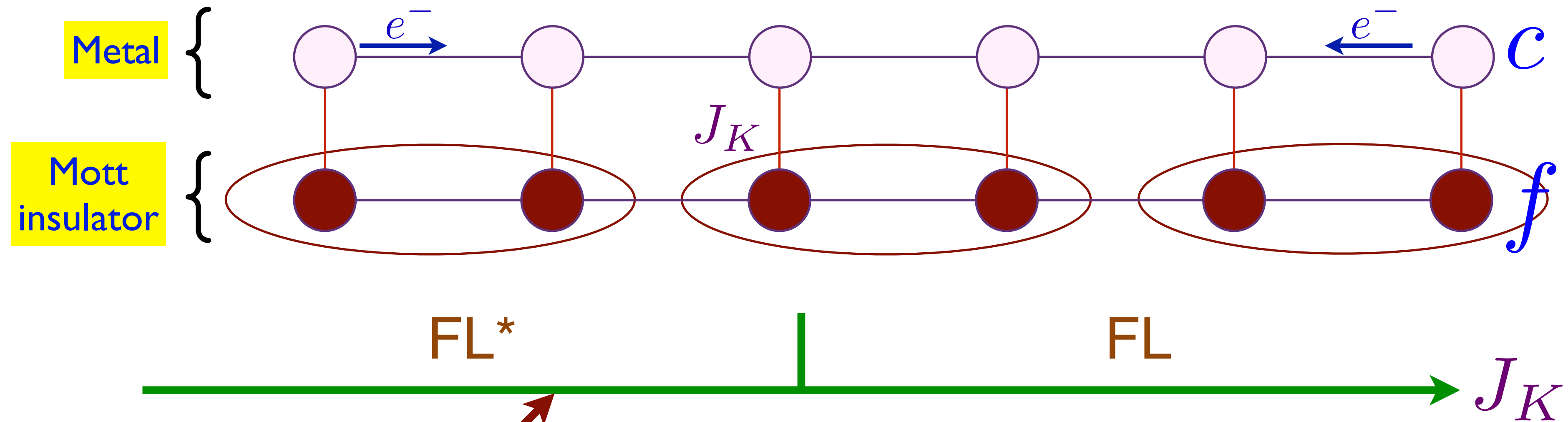
S. Burdin, D. R. Grempel, and A. Georges, PRB **66**, 045111 (2002)

T. Senthil, M. Vojta, and S. Sachdev, PRB **69**, 035111 (2004)

Metal-metal transitions in *Kondo lattice* models

Kondo lattice of f electron spins coupled to a conduction band of c electrons of density p .

Kondo-breakdown or ‘selective Mott’ transition



Small Fermi surface of size p

$|\Phi\rangle = |\text{Spin liquid insulator of } f\rangle$
 $\otimes |\text{Slater determinant of } c\rangle$

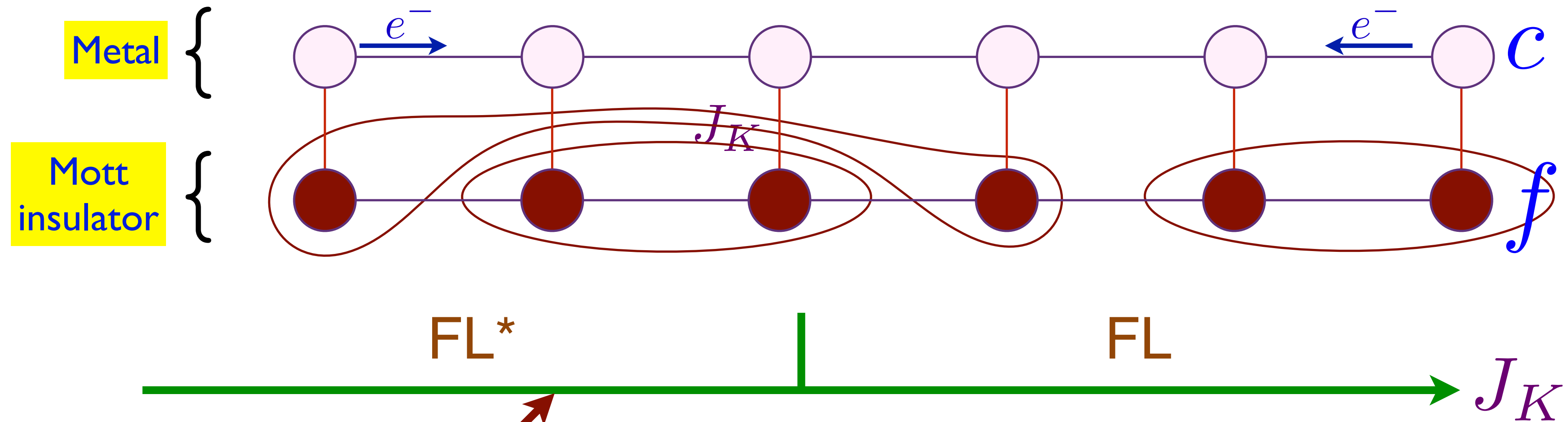
S. Burdin, D. R. Grempel, and A. Georges, PRB **66**, 045111 (2002)

T. Senthil, M. Vojta, and S. Sachdev, PRB **69**, 035111 (2004)

Metal-metal transitions in *Kondo lattice* models

Kondo lattice of f electron spins coupled to a conduction band of c electrons of density p .

Kondo-breakdown or ‘selective Mott’ transition



Small Fermi surface of size p

$|\Phi\rangle = |\text{Spin liquid insulator of } f\rangle$
 $\otimes |\text{Slater determinant of } c\rangle$

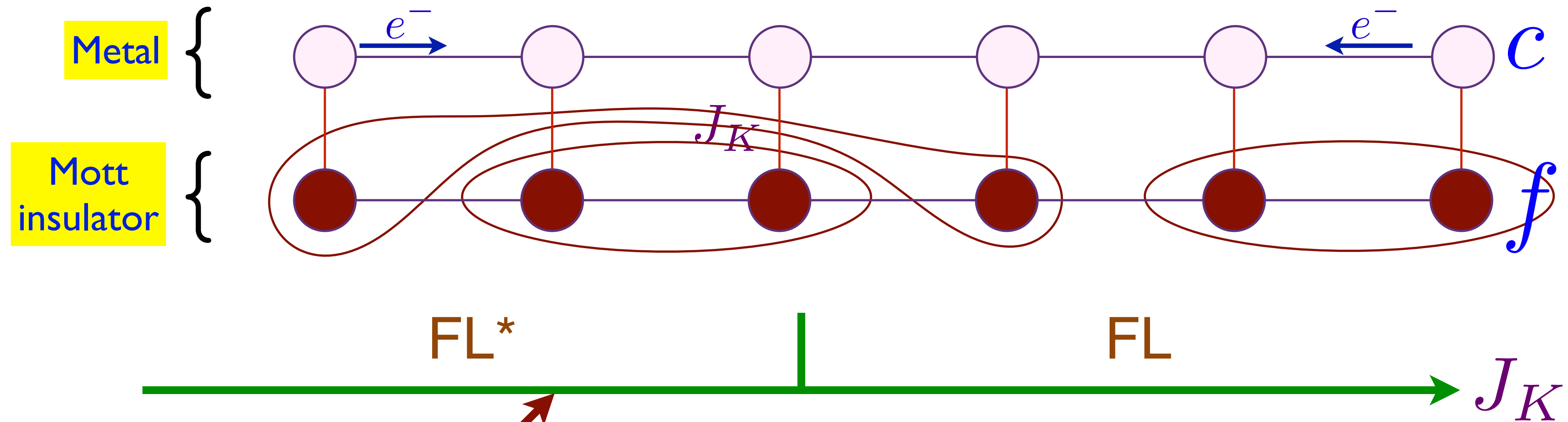
S. Burdin, D. R. Grempel, and A. Georges, PRB **66**, 045111 (2002)

T. Senthil, M. Vojta, and S. Sachdev, PRB **69**, 035111 (2004)

Metal-metal transitions in **Kondo lattice** models

Kondo lattice of f electron spins coupled to a conduction band of c electrons of density p .

Kondo-breakdown or ‘selective Mott’ transition



Small Fermi surface of size p

$|\Phi\rangle = |\text{Spin liquid insulator of } f\rangle \otimes |\text{Slater determinant of } c\rangle$

Luttinger Theorem violated; OK, because of topological order of f spins

Metal-metal transitions in *Kondo lattice* models

Kondo lattice of f electron spins coupled to a conduction band of c electrons of density p .

Kondo-breakdown or ‘selective Mott’ transition

U(1) gauge theory of a ‘hybridization-Higgs’ boson $b \sim f_{\alpha}^{\dagger} c_{\alpha}$ which condenses on the ‘Large Fermi surface’ side.

FL*

FL

J_K

Small Fermi surface of size p

$|\Phi\rangle = |\text{Spin liquid insulator of } f\rangle \otimes |\text{Slater determinant of } c\rangle$

Large Fermi surface of size $1 + p$

$|\Phi\rangle = [\text{Projection onto one } f \text{ per site}] \otimes |\text{Slater determinant of } (c, f)\rangle$

Metal-metal transitions in **Kondo lattice** models

Kondo lattice of f electron spins coupled to a conduction band of c electrons of density p .

Kondo-breakdown or ‘selective Mott’ transition

Shortcomings:

- Only works well for a particular spin liquid in the f band: the spinon Fermi surface with a trivial PSG.

Metal-metal transitions in **Kondo lattice** models

Kondo lattice of f electron spins coupled to a conduction band of c electrons of density p .

Kondo-breakdown or ‘selective Mott’ transition

Shortcomings:

- Only works well for a particular spin liquid in the f band: the spinon Fermi surface with a trivial PSG.
- No natural extension to the case where the non-FL state has magnetic order.

Metal-metal transitions in **Kondo lattice** models

Kondo lattice of f electron spins coupled to a conduction band of c electrons of density p .

Kondo-breakdown or ‘selective Mott’ transition

Shortcomings:

- Only works well for a particular spin liquid in the f band: the spinon Fermi surface with a trivial PSG.
- No natural extension to the case where the non-FL state has magnetic order.
- No simple extension to one-band model.

1. Metal-metal transition in the Kondo Lattice

2. Metal-metal transition in a one-band model

A. FL model of the pseudogap*

B. Ancilla qubits and ghost Fermi surfaces

3. Random J model (insulator)

RG analysis and exact exponent

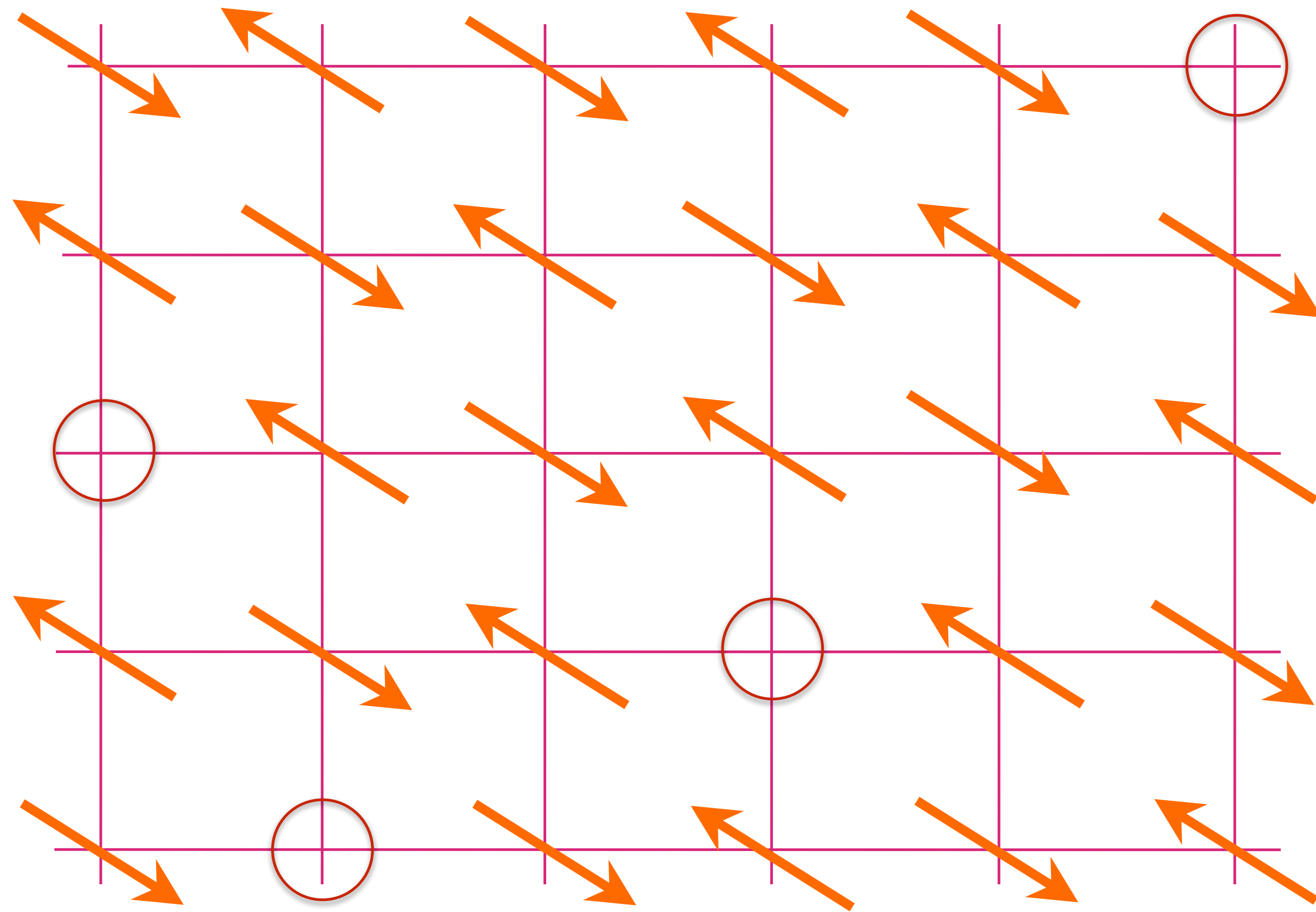
4. Random t - J model (metals)

Numerics, RG analysis and exact exponents

1. Metal-metal transition in the Kondo Lattice
2. Metal-metal transition in a one-band model
 - A. *FL* model of the pseudogap*
 - B. *Ancilla qubits and ghost Fermi surfaces*
3. Random J model (insulator)
RG analysis and exact exponent
4. Random t - J model (metals)
Numerics, RG analysis and exact exponents

Metal-metal transitions in a **one-band** model

- Can realize the FL* state as a doped spin liquid in which spinons and holons bind to form ‘electrons’, which then form a small Fermi surface (X.-G. Wen and P. A. Lee, PRL **76**, 503 (1996)); but there is no complete description of this process, except in the very strong binding limit of dimer ‘electrons’ (M. Punk, A. Allais, and S. Sachdev, PNAS **112**, 9552 (2015)). This approach does not yield a theory of the transition to the FL state.

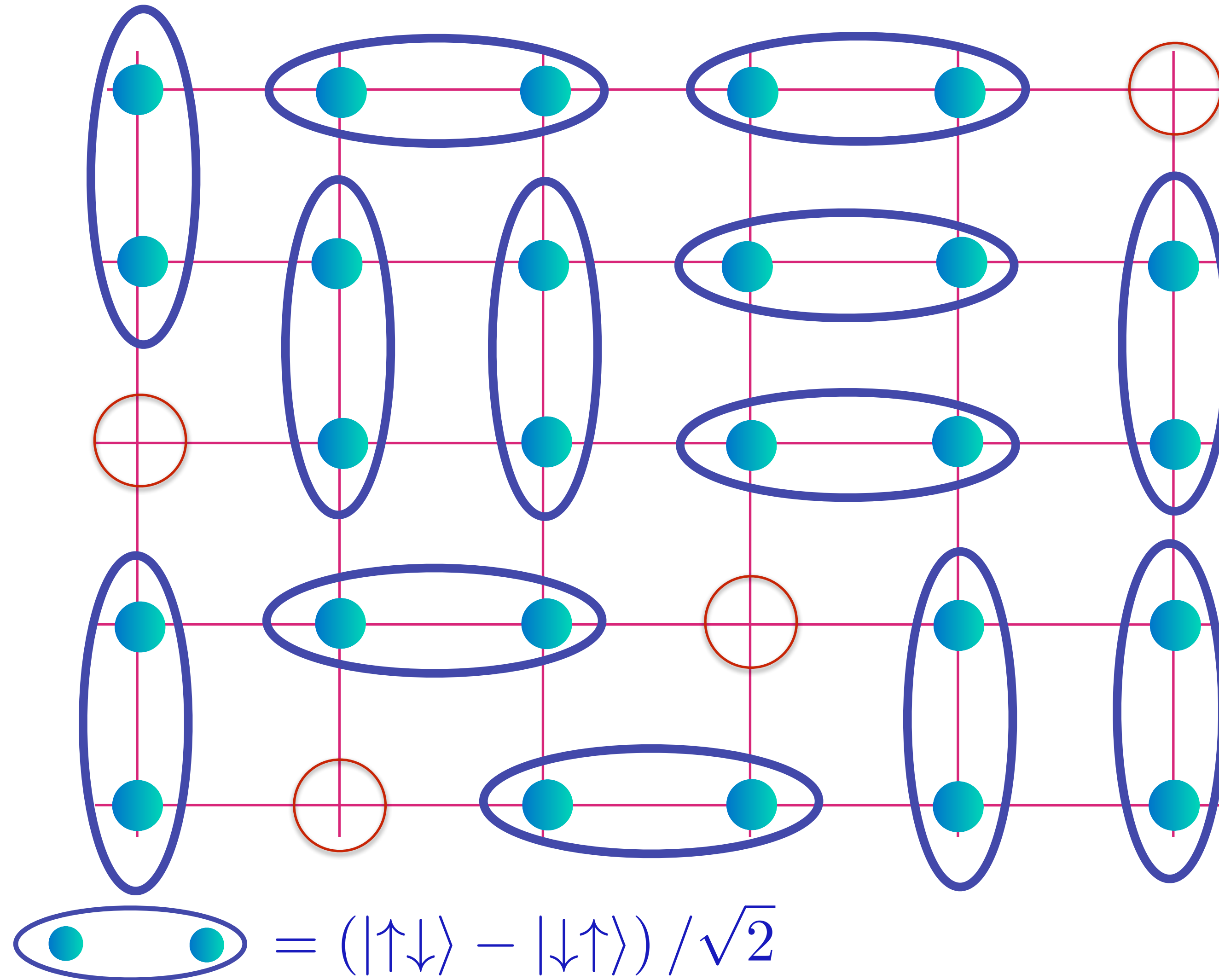


Anti-ferromagnet
with p holes
per square

Holon metal

S.A. Kivelson, D.S. Rokhsar and J.P. Sethna, PRB **35**, 8865 (1987)

D. Rokhsar and S.A. Kivelson, PRL **61**, 2376 (1988)

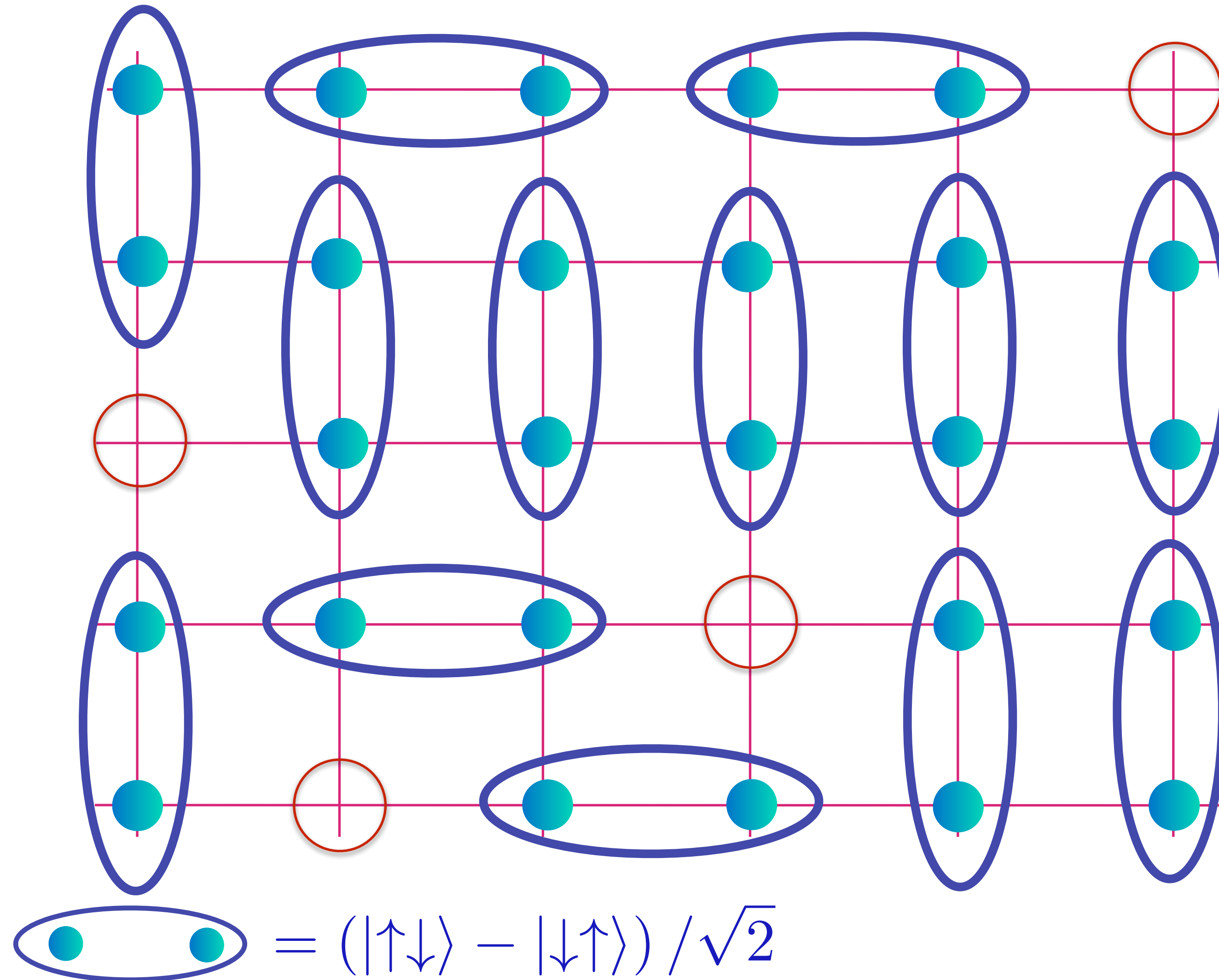


Spin liquid
with density
 ρ of spinless,
charge $+e$
“holons”.

Holon metal

S.A. Kivelson, D.S. Rokhsar and J.P. Sethna, PRB **35**, 8865 (1987)

D. Rokhsar and S.A. Kivelson, PRL **61**, 2376 (1988)

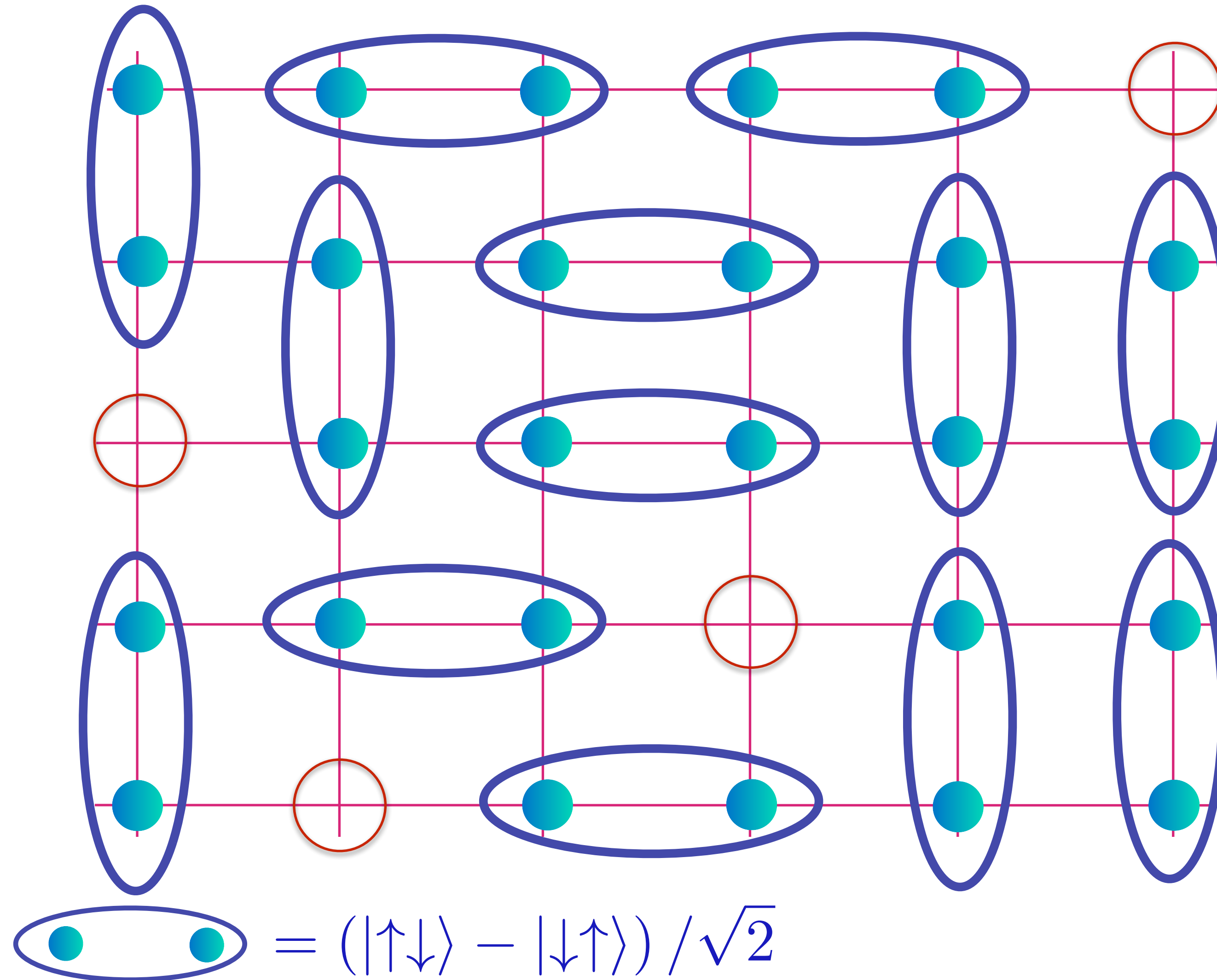


Spin liquid
with density
 p of spinless,
charge $+e$
“holons”.

Holon metal

S.A. Kivelson, D.S. Rokhsar and J.P. Sethna, PRB **35**, 8865 (1987)

D. Rokhsar and S.A. Kivelson, PRL **61**, 2376 (1988)

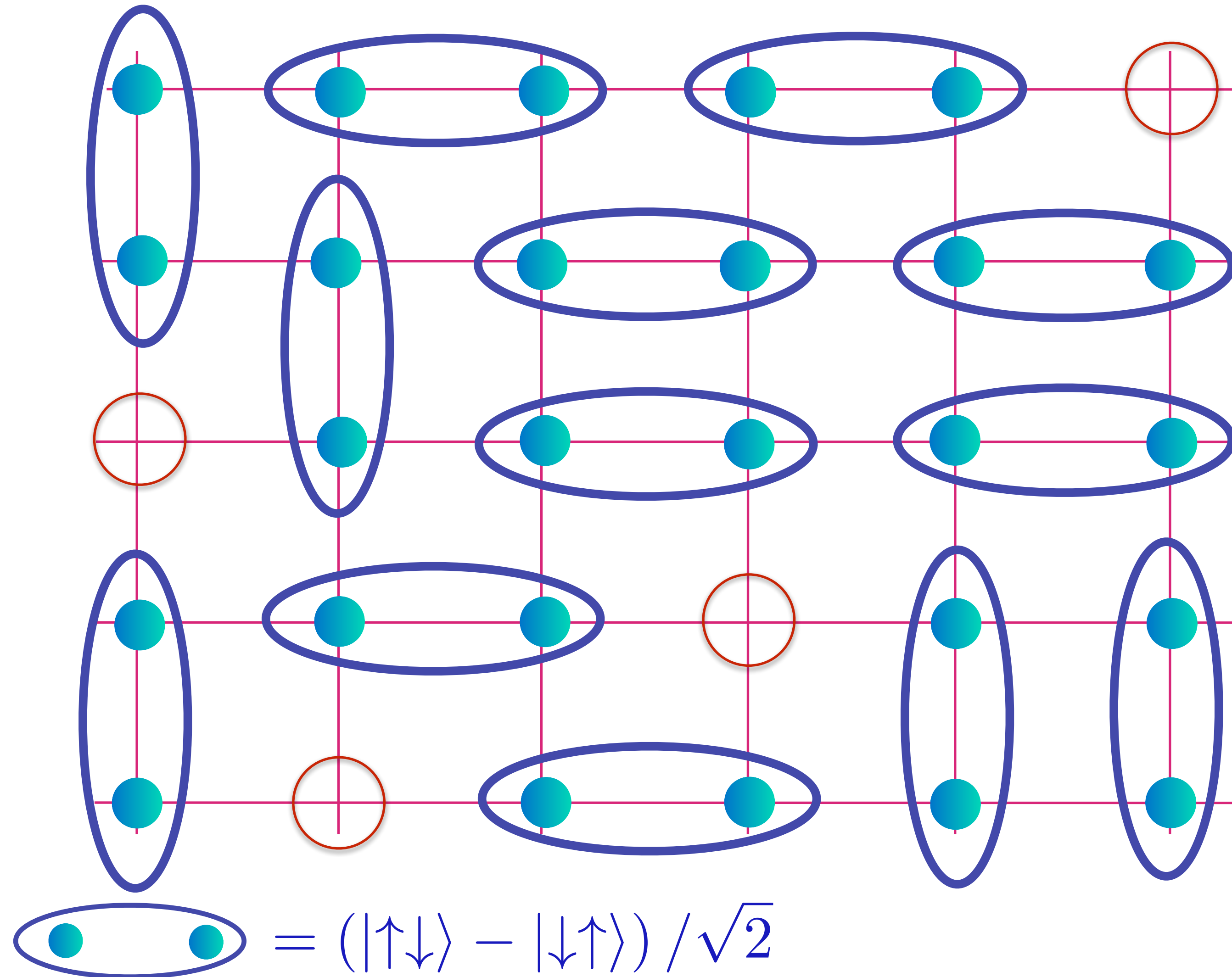


Spin liquid
with density
 ρ of spinless,
charge $+e$
“holons”.

Holon metal

S.A. Kivelson, D.S. Rokhsar and J.P. Sethna, PRB **35**, 8865 (1987)

D. Rokhsar and S.A. Kivelson, PRL **61**, 2376 (1988)

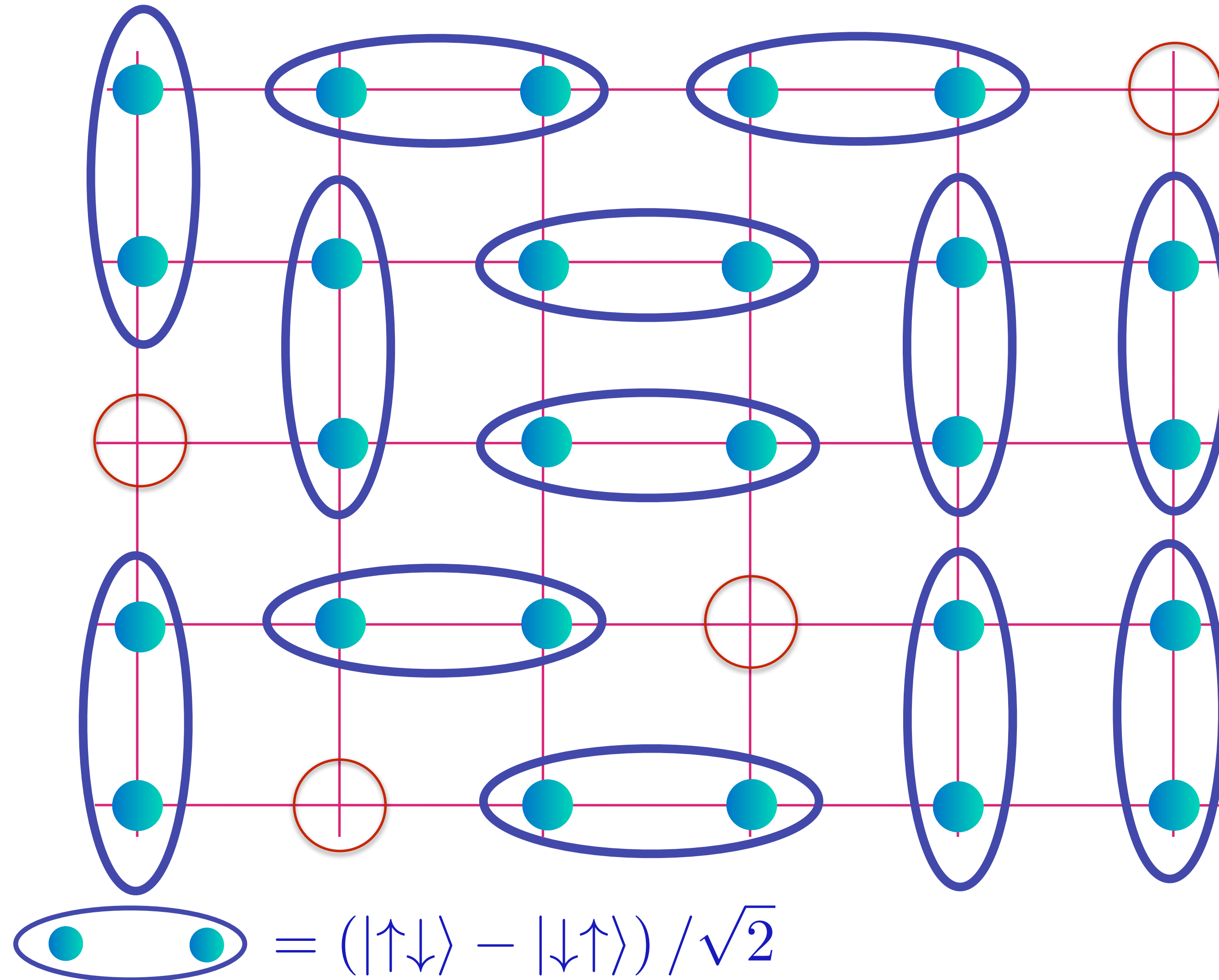


Spin liquid
with density
 ρ of spinless,
charge $+e$
“holons”.

Holon metal

S.A. Kivelson, D.S. Rokhsar and J.P. Sethna, PRB **35**, 8865 (1987)

D. Rokhsar and S.A. Kivelson, PRL **61**, 2376 (1988)

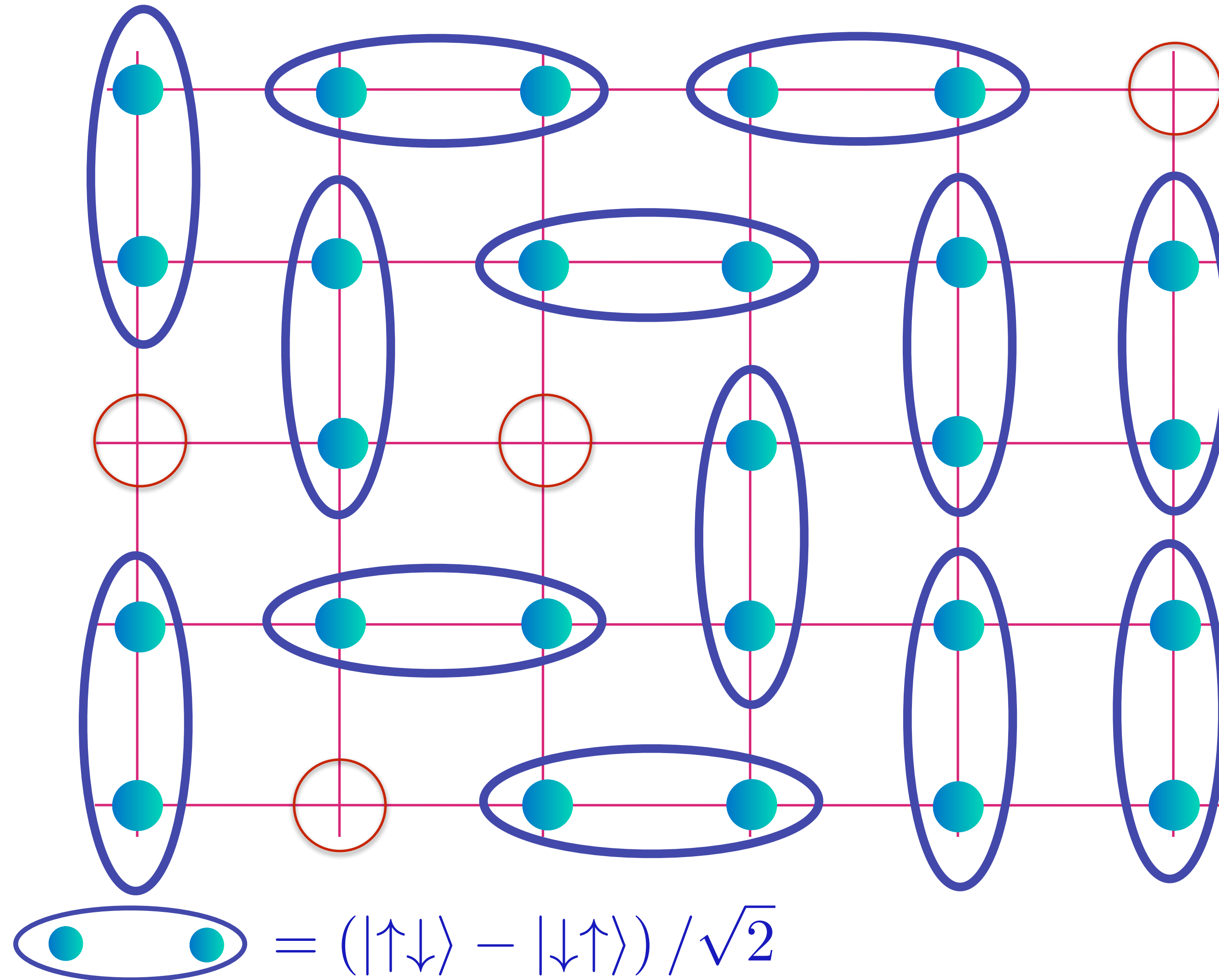


Spin liquid
with density
 ρ of spinless,
charge $+e$
“holons”.

Holon metal

S.A. Kivelson, D.S. Rokhsar and J.P. Sethna, PRB **35**, 8865 (1987)

D. Rokhsar and S.A. Kivelson, PRL **61**, 2376 (1988)

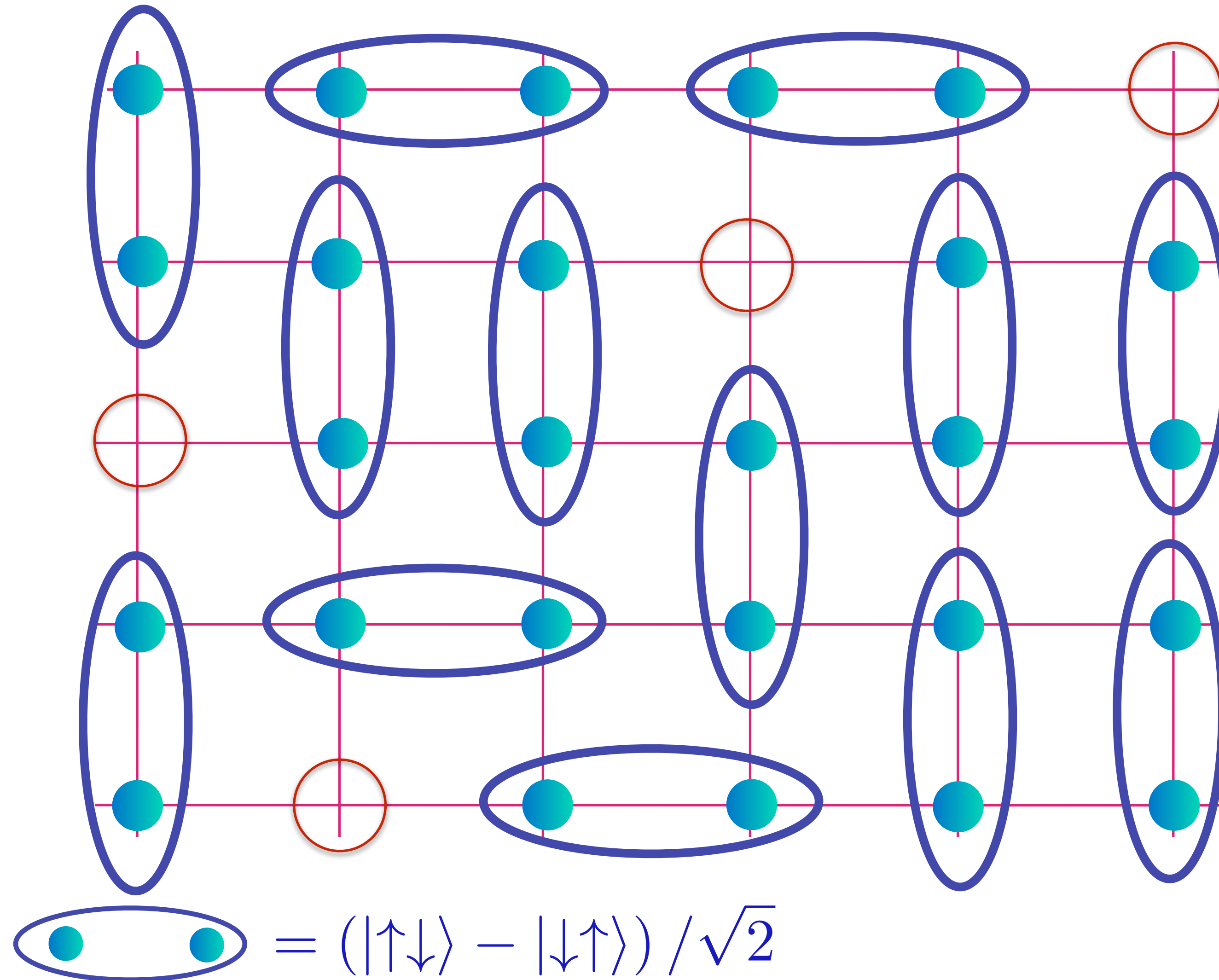


Spin liquid
with density
 ρ of spinless,
charge $+e$
“holons”.

Holon metal

S.A. Kivelson, D.S. Rokhsar and J.P. Sethna, PRB **35**, 8865 (1987)

D. Rokhsar and S.A. Kivelson, PRL **61**, 2376 (1988)

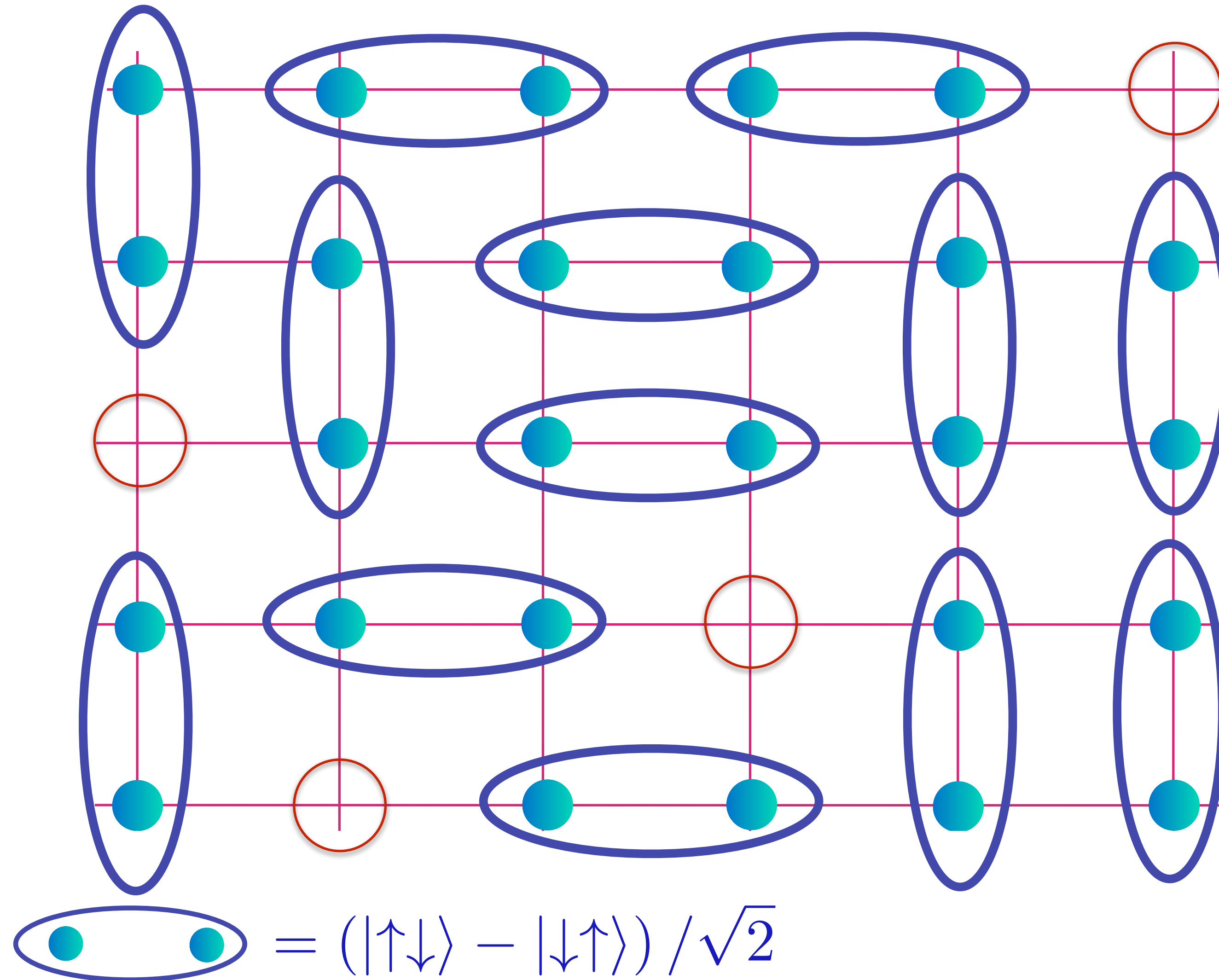


Spin liquid
with density
 ρ of spinless,
charge $+e$
“holons”.

Holon metal

S.A. Kivelson, D.S. Rokhsar and J.P. Sethna, PRB **35**, 8865 (1987)

D. Rokhsar and S.A. Kivelson, PRL **61**, 2376 (1988)

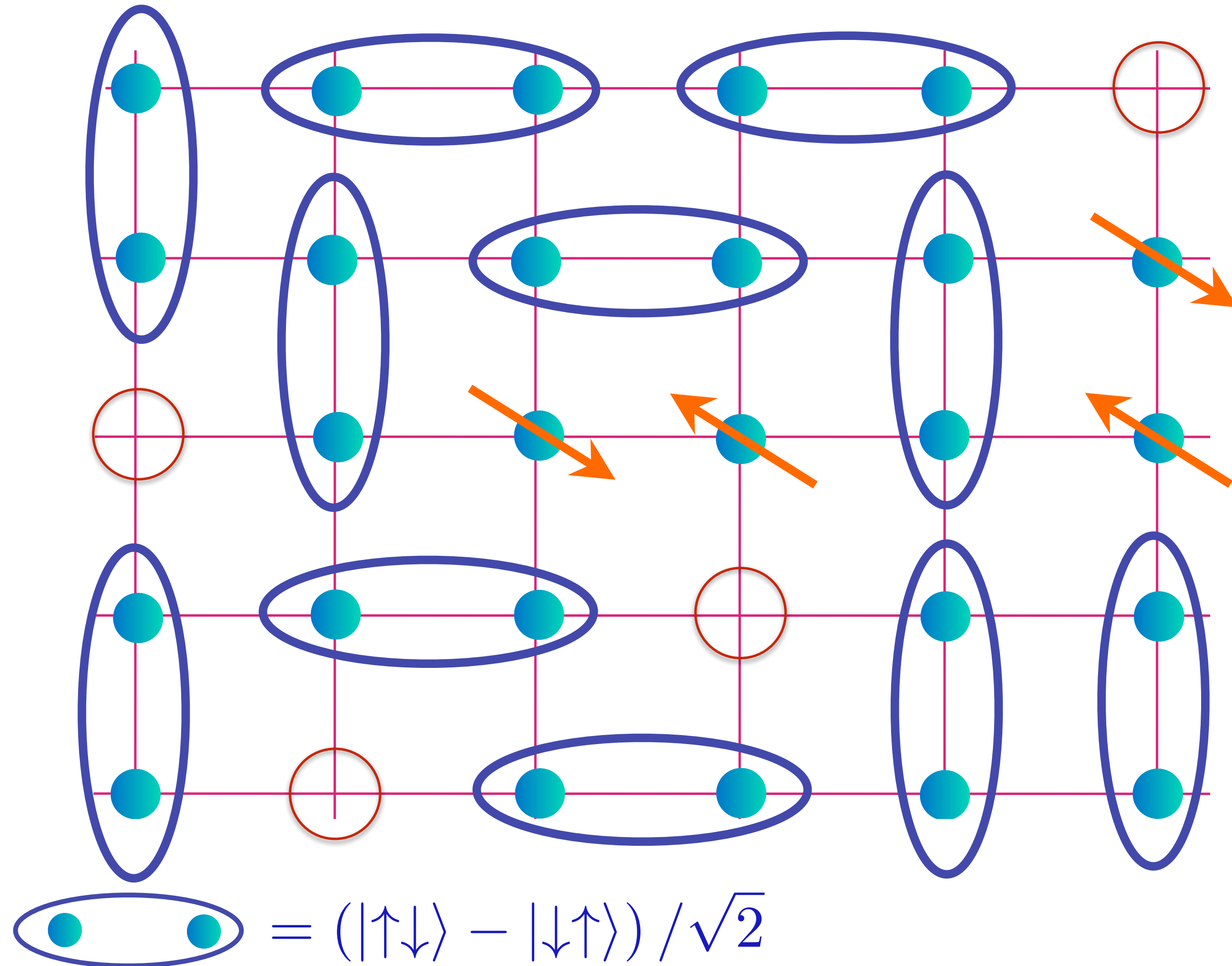


Spin liquid
with density
 ρ of spinless,
charge $+e$
“holons”.

Holon metal

S.A. Kivelson, D.S. Rokhsar and J.P. Sethna, PRB **35**, 8865 (1987)

D. Rokhsar and S.A. Kivelson, PRL **61**, 2376 (1988)

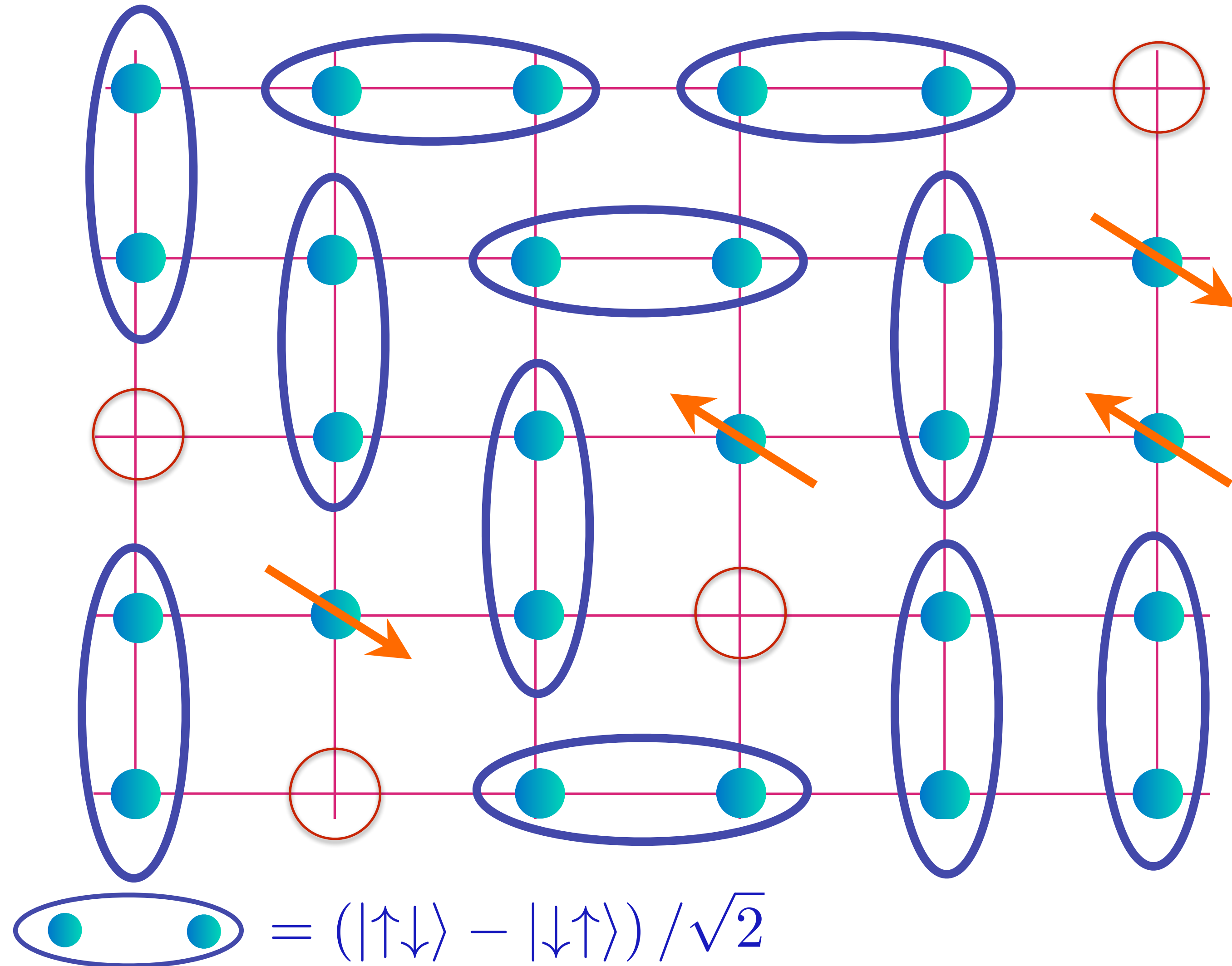


Spin liquid
with density
 ρ of spinless,
charge $+e$
“holons” and
charge 0, spin-1/2
“spinons”.

Holon metal

S.A. Kivelson, D.S. Rokhsar and J.P. Sethna, PRB **35**, 8865 (1987)

D. Rokhsar and S.A. Kivelson, PRL **61**, 2376 (1988)

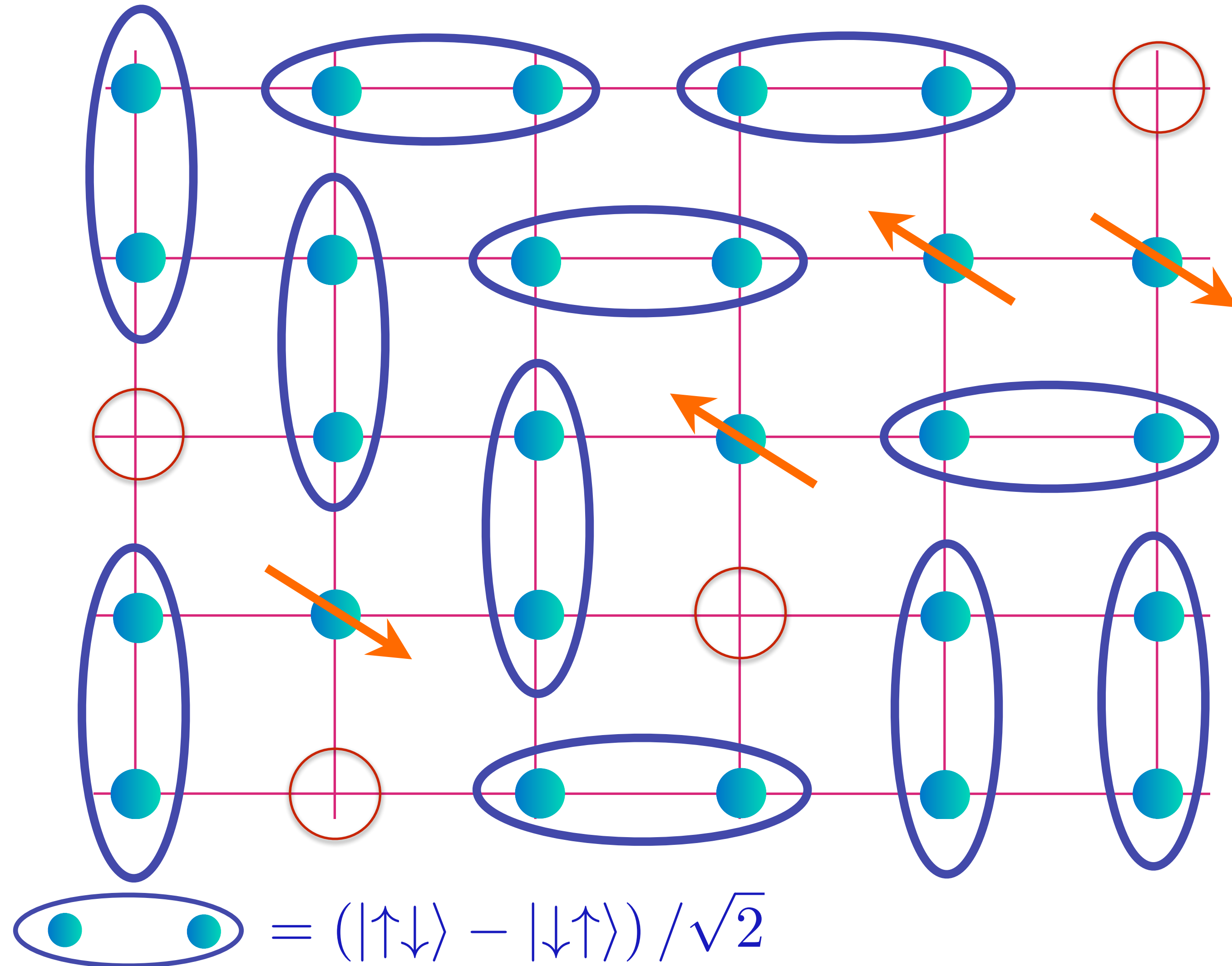


Spin liquid
with density
 ρ of spinless,
charge $+e$
“holons” and
charge 0, spin-1/2
“spinons”.

Holon metal

S.A. Kivelson, D.S. Rokhsar and J.P. Sethna, PRB **35**, 8865 (1987)

D. Rokhsar and S.A. Kivelson, PRL **61**, 2376 (1988)

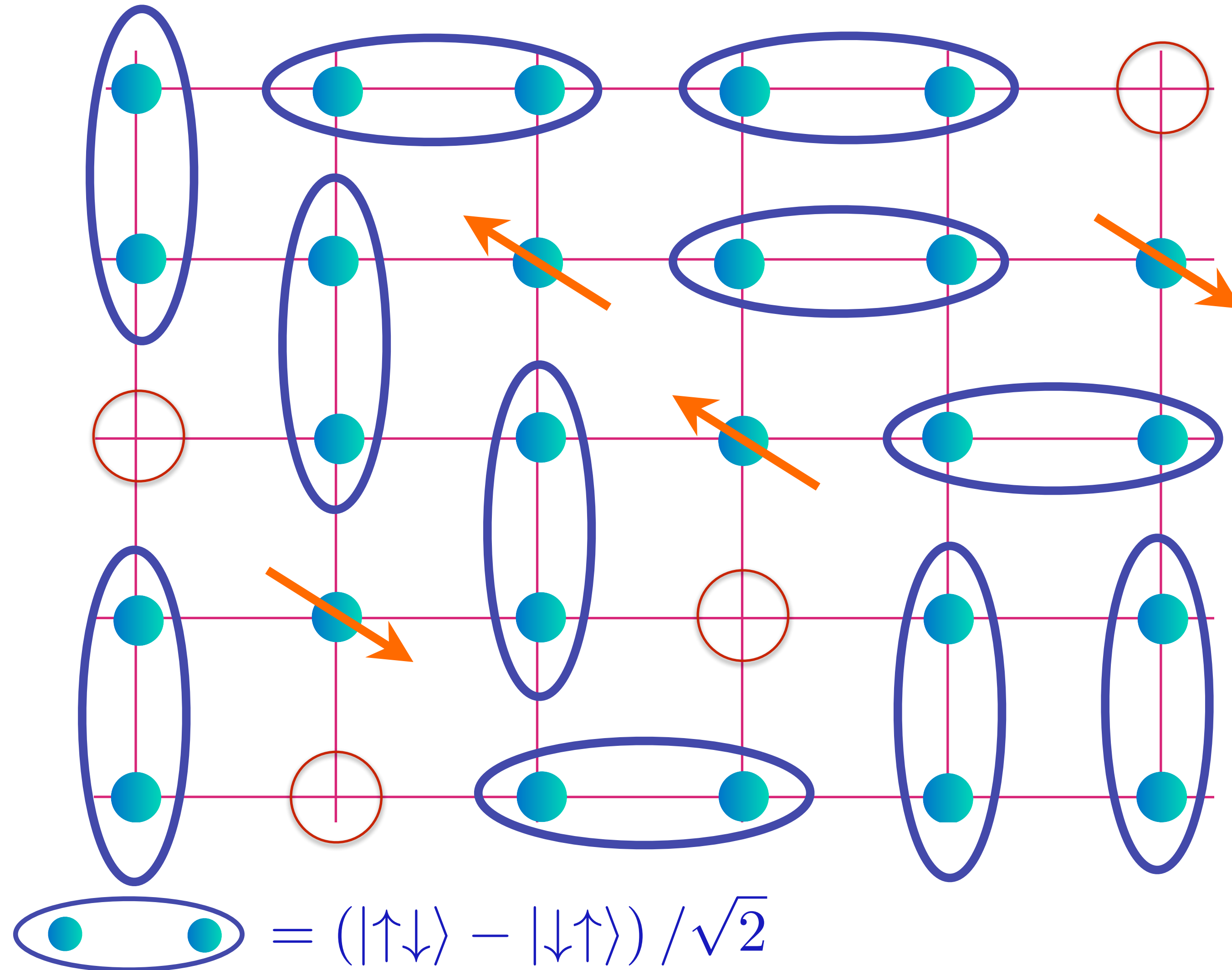


Spin liquid
with density
 ρ of spinless,
charge $+e$
“holons” and
charge 0, spin-1/2
“spinons”.

Holon metal

S.A. Kivelson, D.S. Rokhsar and J.P. Sethna, PRB **35**, 8865 (1987)

D. Rokhsar and S.A. Kivelson, PRL **61**, 2376 (1988)

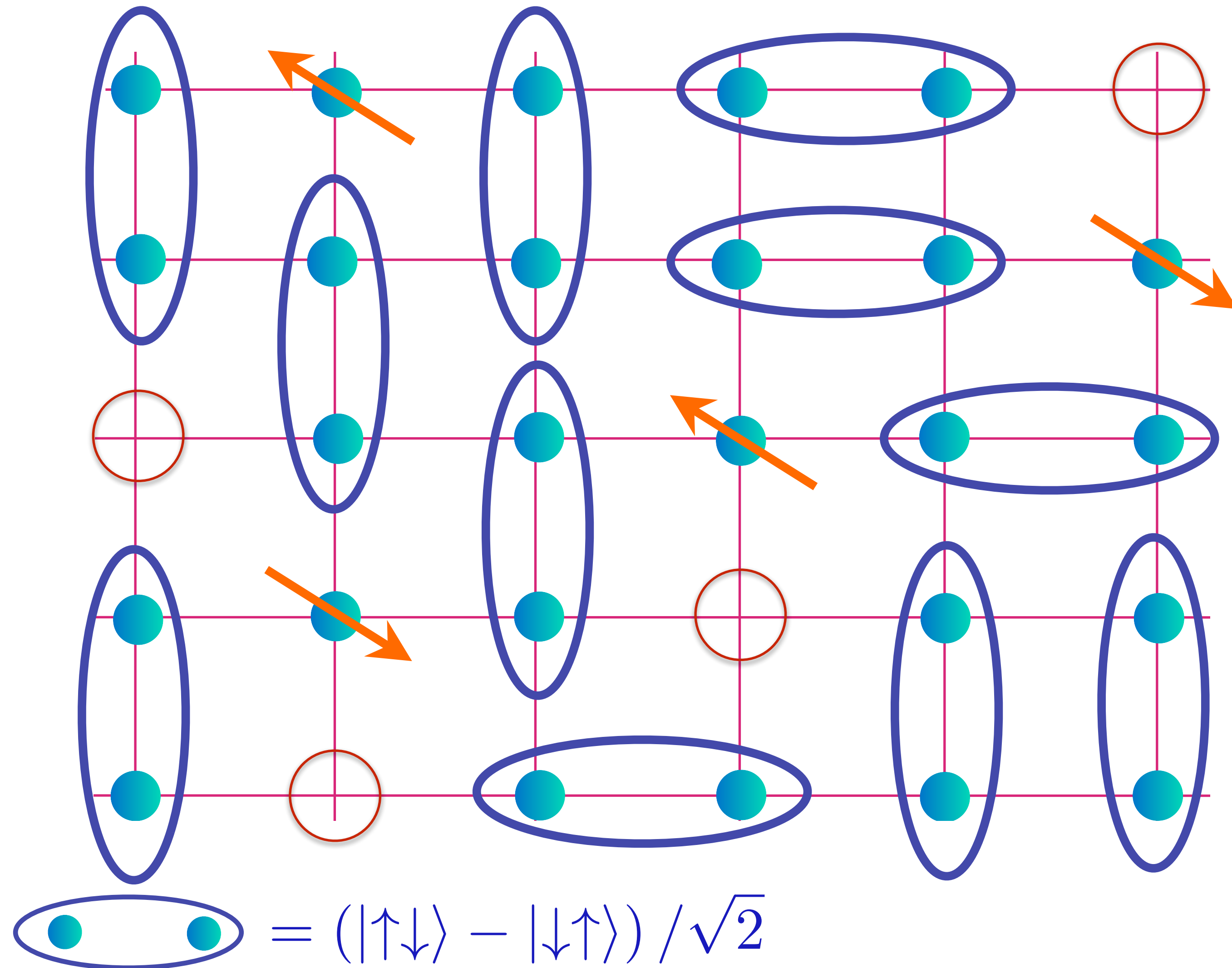


Spin liquid
with density
 ρ of spinless,
charge $+e$
“holons” and
charge 0, spin-1/2
“spinons”.

Holon metal

S.A. Kivelson, D.S. Rokhsar and J.P. Sethna, PRB **35**, 8865 (1987)

D. Rokhsar and S.A. Kivelson, PRL **61**, 2376 (1988)

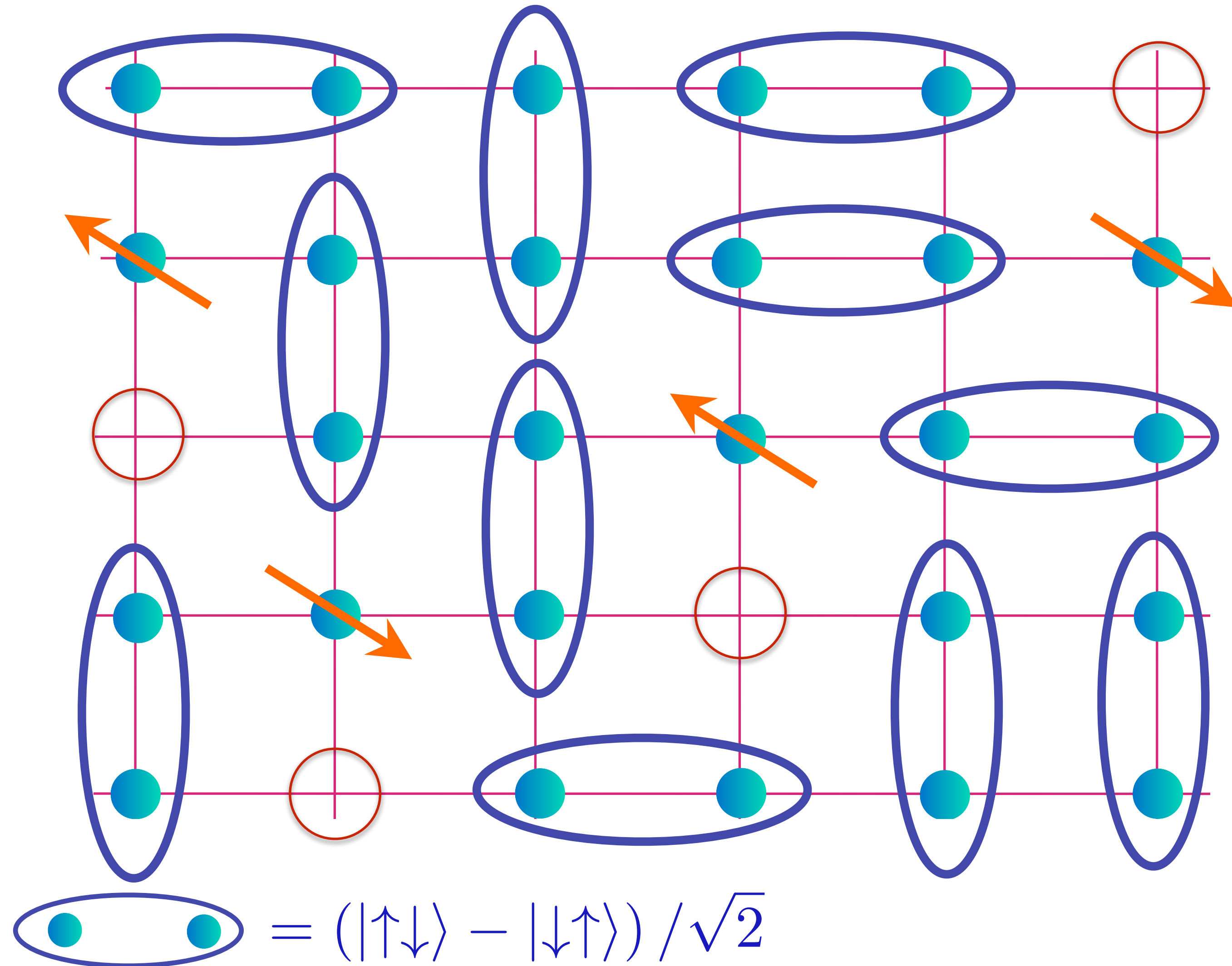


Spin liquid
with density
 ρ of spinless,
charge $+e$
“holons” and
charge 0, spin-1/2
“spinons”.

Holon metal

S.A. Kivelson, D.S. Rokhsar and J.P. Sethna, PRB **35**, 8865 (1987)

D. Rokhsar and S.A. Kivelson, PRL **61**, 2376 (1988)

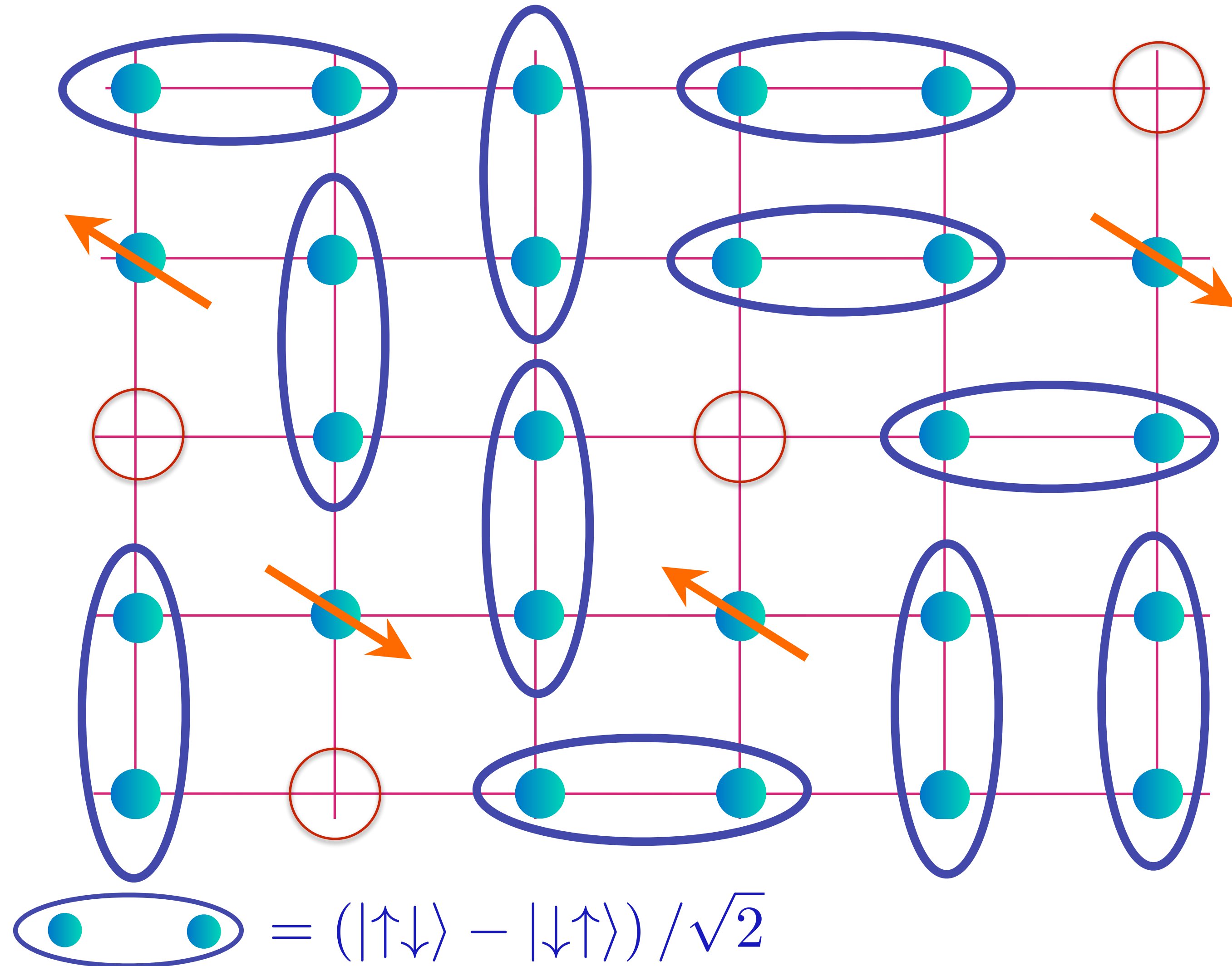


Spin liquid
with density
 ρ of spinless,
charge $+e$
“holons” and
charge 0, spin-1/2
“spinons”.

Holon metal

S.A. Kivelson, D.S. Rokhsar and J.P. Sethna, PRB **35**, 8865 (1987)

D. Rokhsar and S.A. Kivelson, PRL **61**, 2376 (1988)

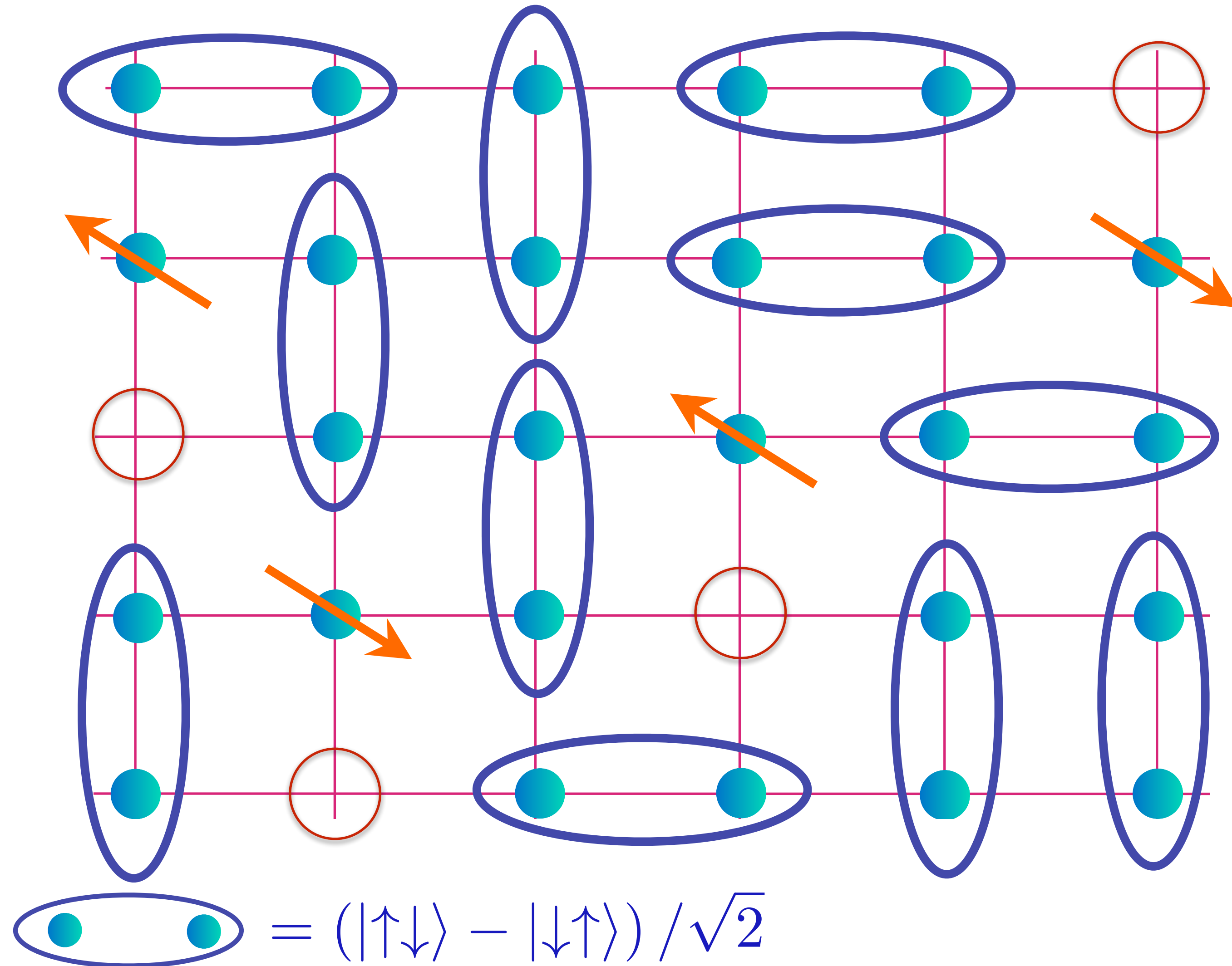


Spin liquid
with density ρ of spinless,
charge $+e$
“holons” and
charge 0, spin-1/2
“spinons”.

Holon metal

S.A. Kivelson, D.S. Rokhsar and J.P. Sethna, PRB **35**, 8865 (1987)

D. Rokhsar and S.A. Kivelson, PRL **61**, 2376 (1988)

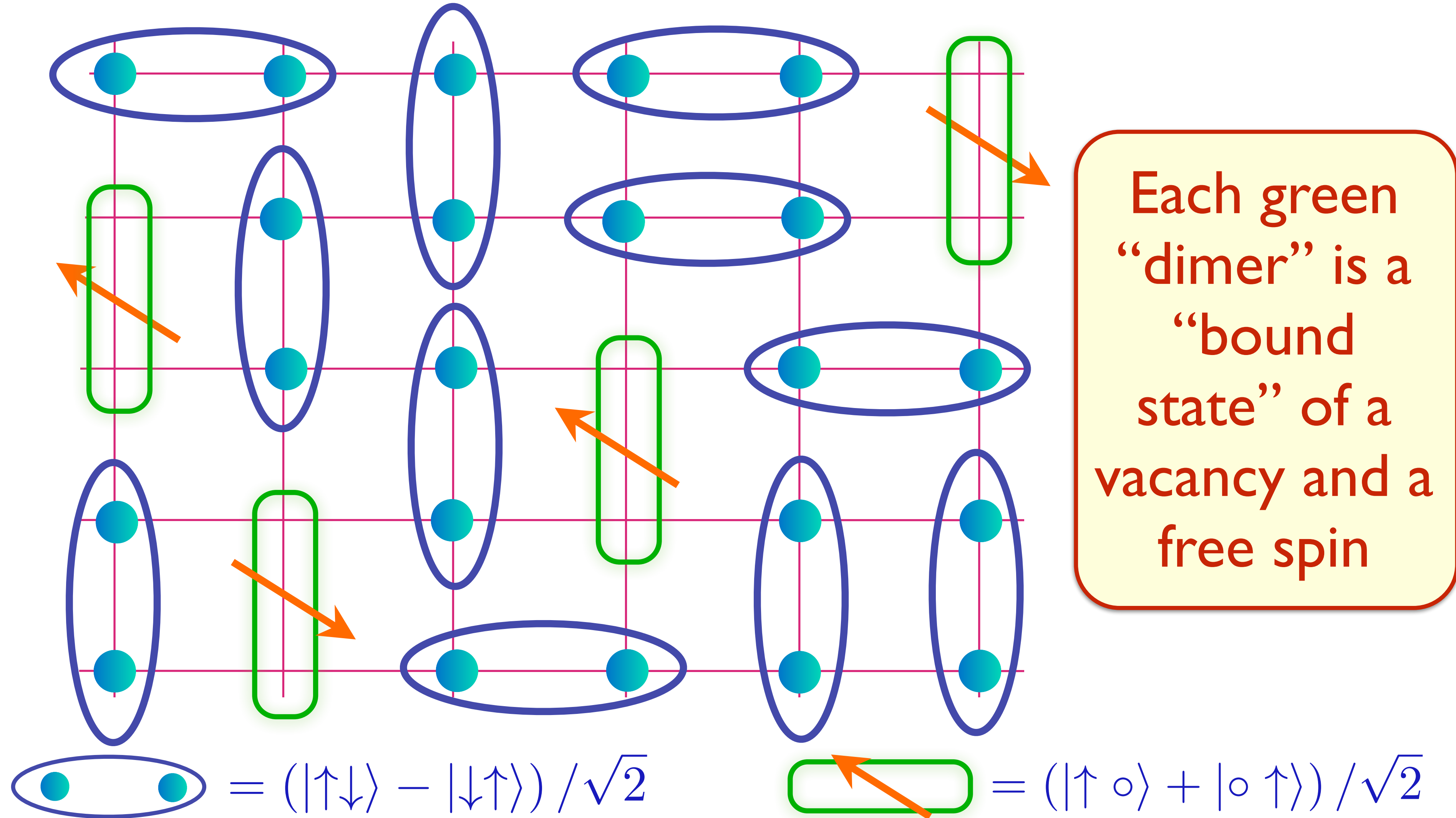


Spin liquid
with density
 ρ of spinless,
charge $+e$
“holons” and
charge 0, spin-1/2
“spinons”.

FL*

S. Sachdev PRB **49**, 6770 (1994); X.-G. Wen and P.A. Lee PRL **76**, 503 (1996)

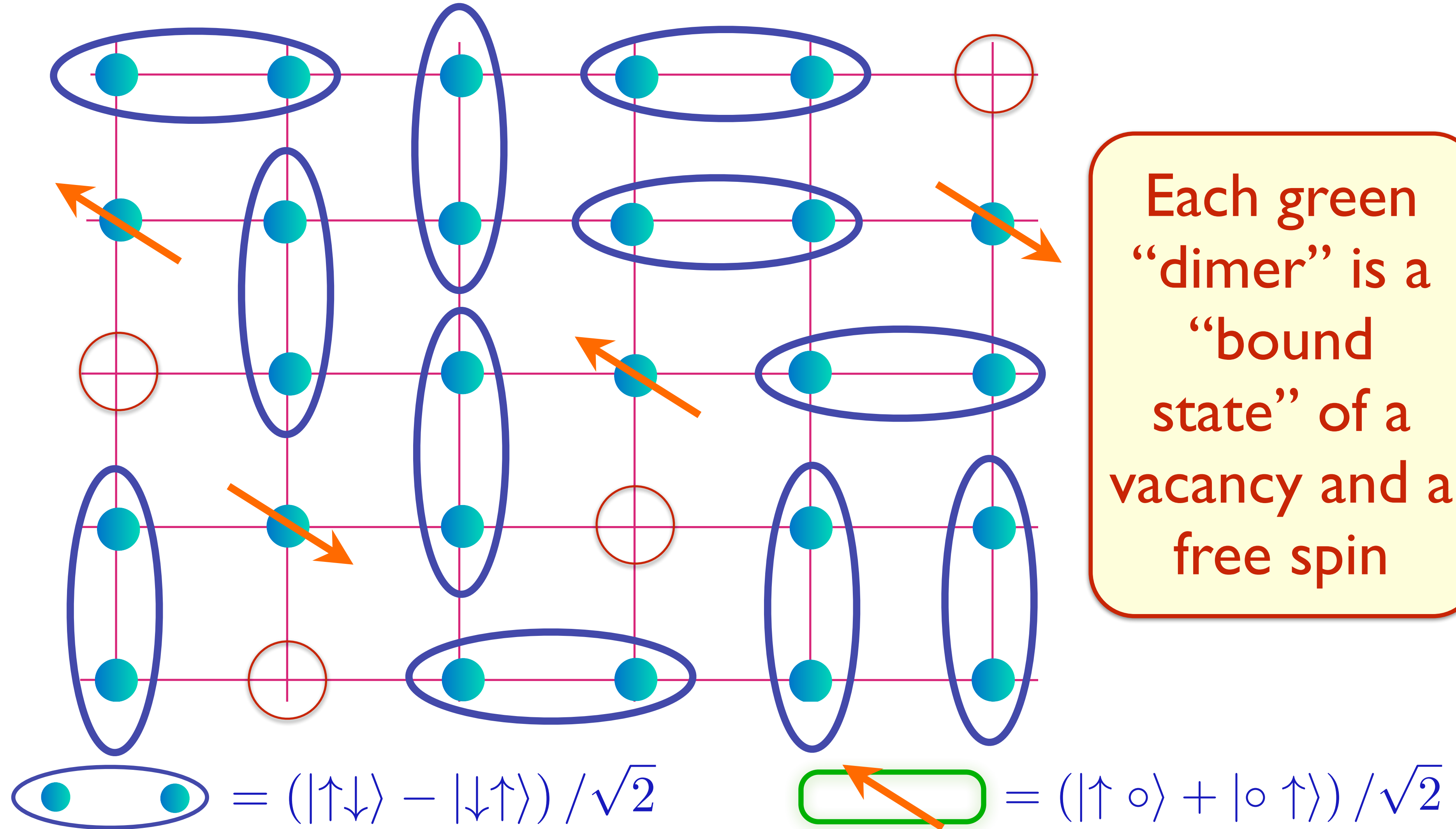
R. K. Kaul, A. Kolezhuk, M. Levin, S. Sachdev, and T. Senthil, PRB **75**, 235122 (2007)



FL*

S. Sachdev PRB **49**, 6770 (1994); X.-G. Wen and P.A. Lee PRL **76**, 503 (1996)

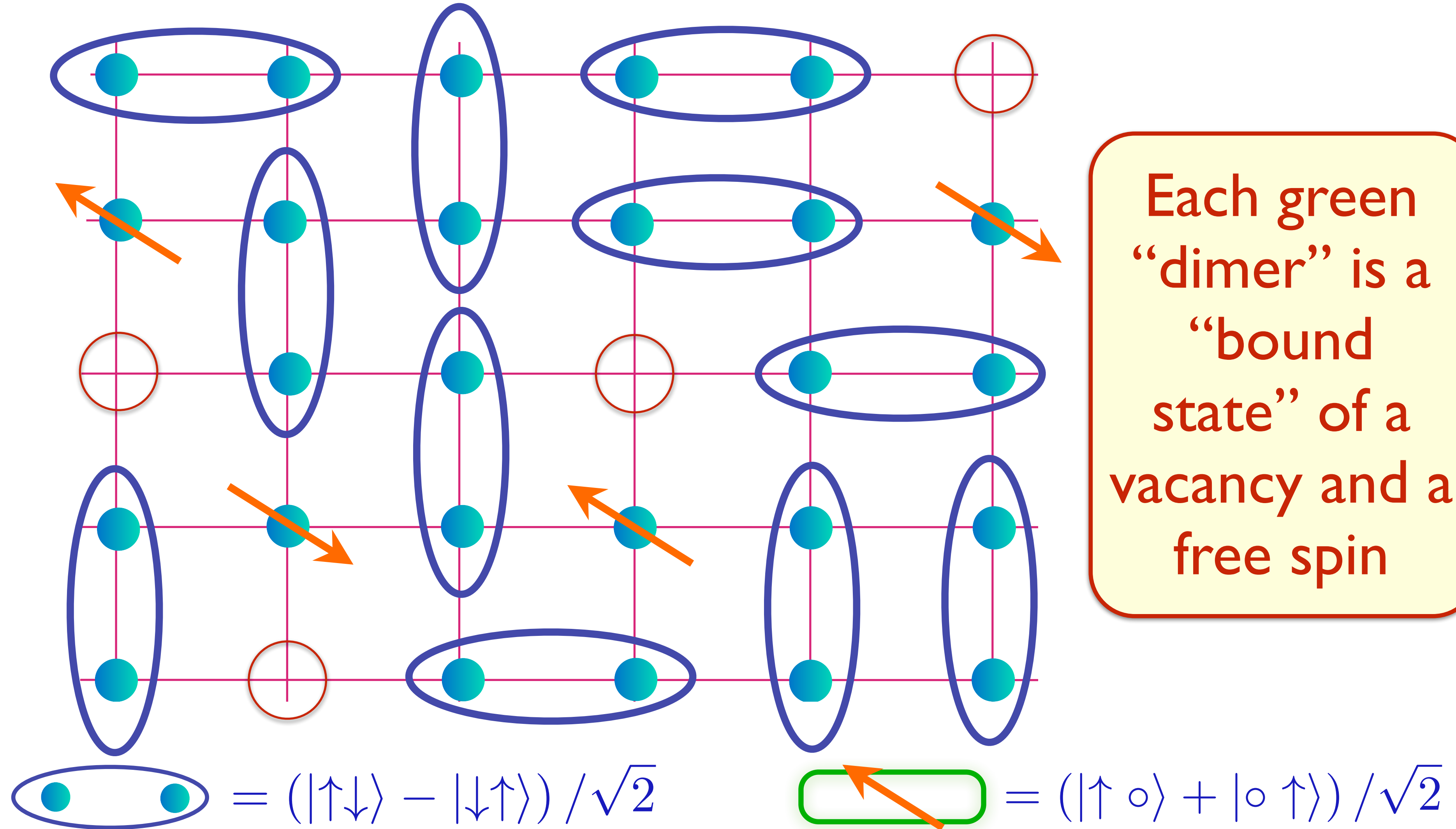
R. K. Kaul, A. Kolezhuk, M. Levin, S. Sachdev, and T. Senthil, PRB **75**, 235122 (2007)



FL*

S. Sachdev PRB **49**, 6770 (1994); X.-G. Wen and P.A. Lee PRL **76**, 503 (1996)

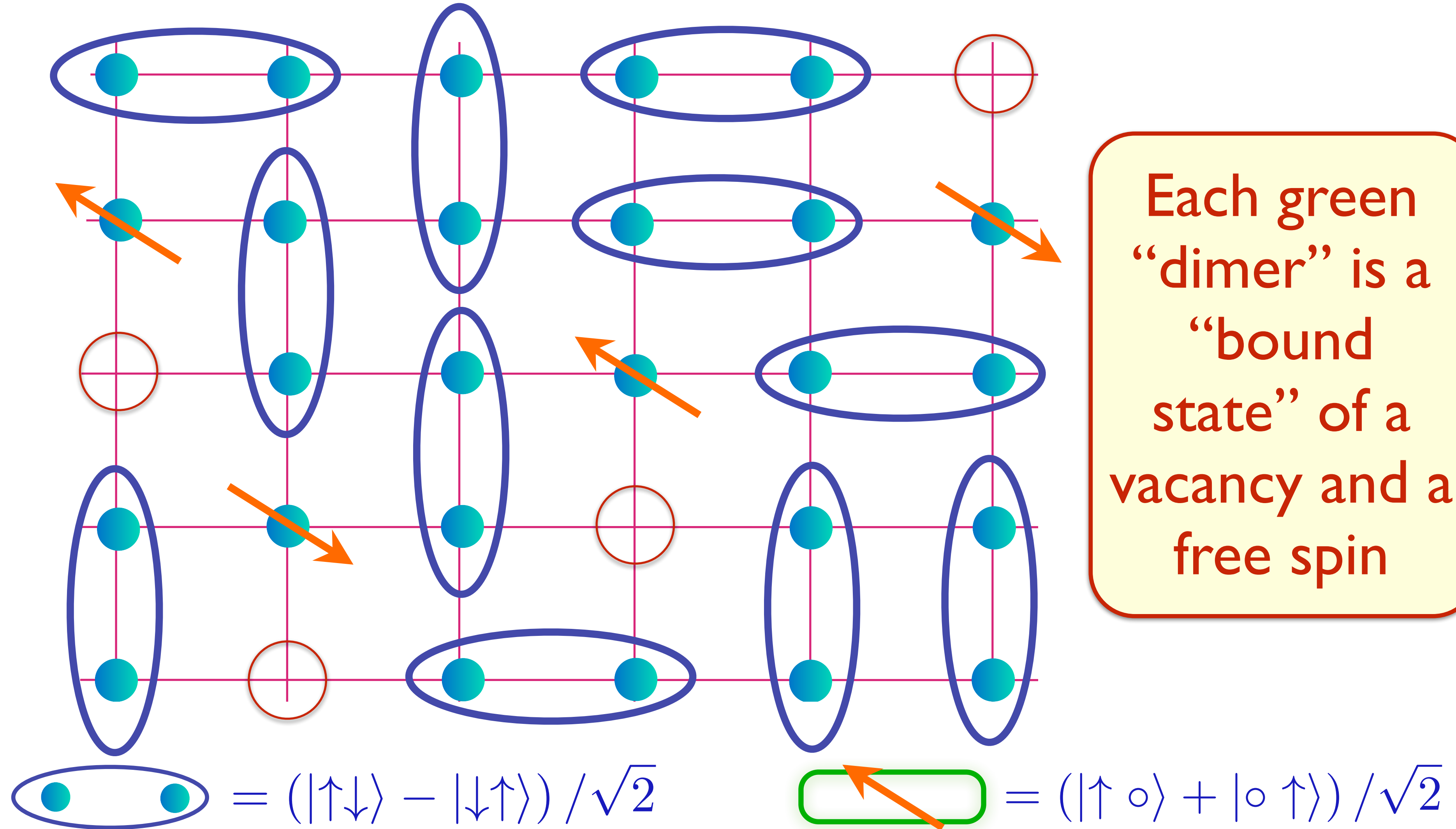
R. K. Kaul, A. Kolezhuk, M. Levin, S. Sachdev, and T. Senthil, PRB **75**, 235122 (2007)



FL*

S. Sachdev PRB **49**, 6770 (1994); X.-G. Wen and P.A. Lee PRL **76**, 503 (1996)

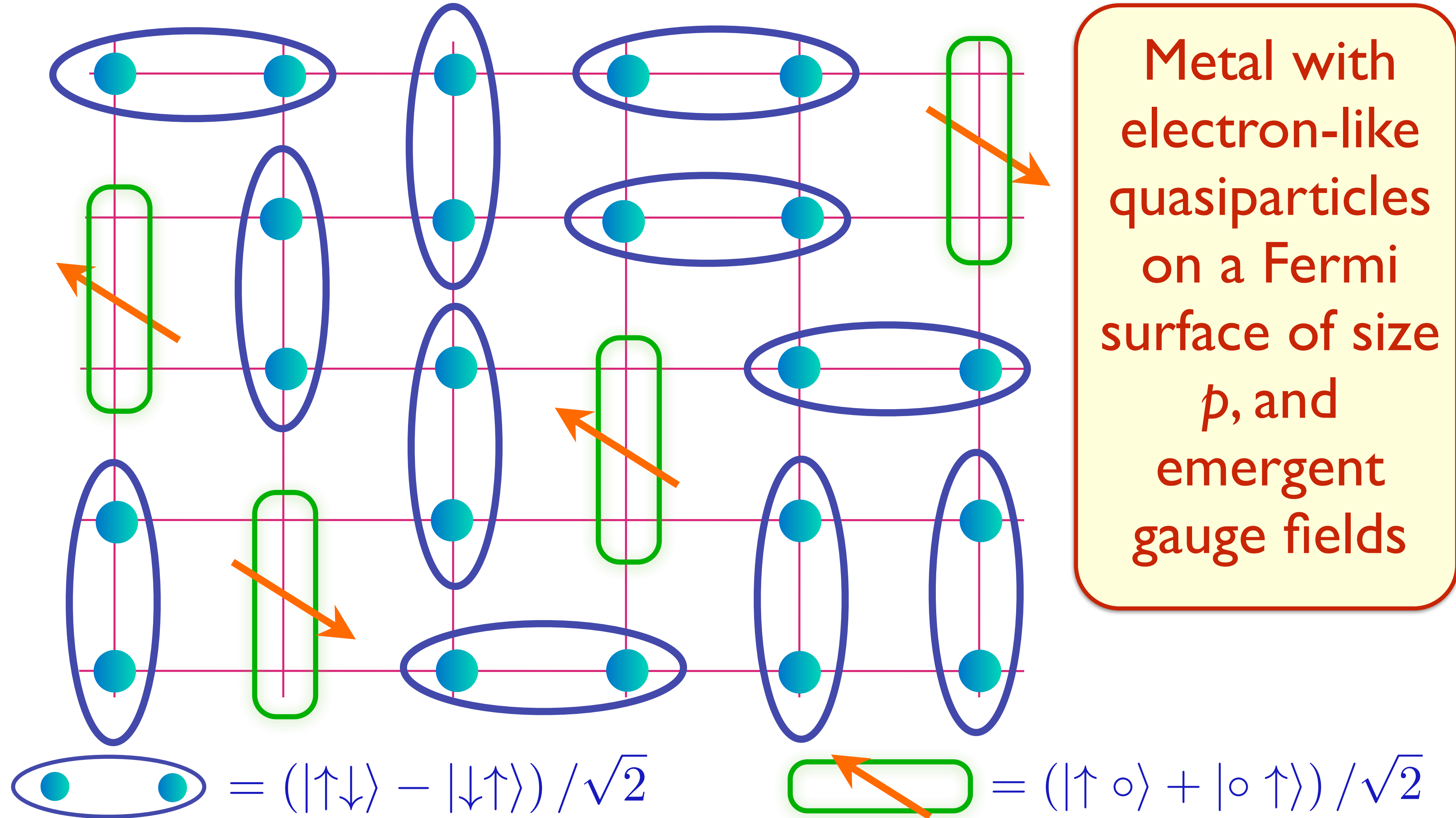
R. K. Kaul, A. Kolezhuk, M. Levin, S. Sachdev, and T. Senthil, PRB **75**, 235122 (2007)



FL*

S. Sachdev PRB **49**, 6770 (1994); X.-G. Wen and P.A. Lee PRL **76**, 503 (1996)

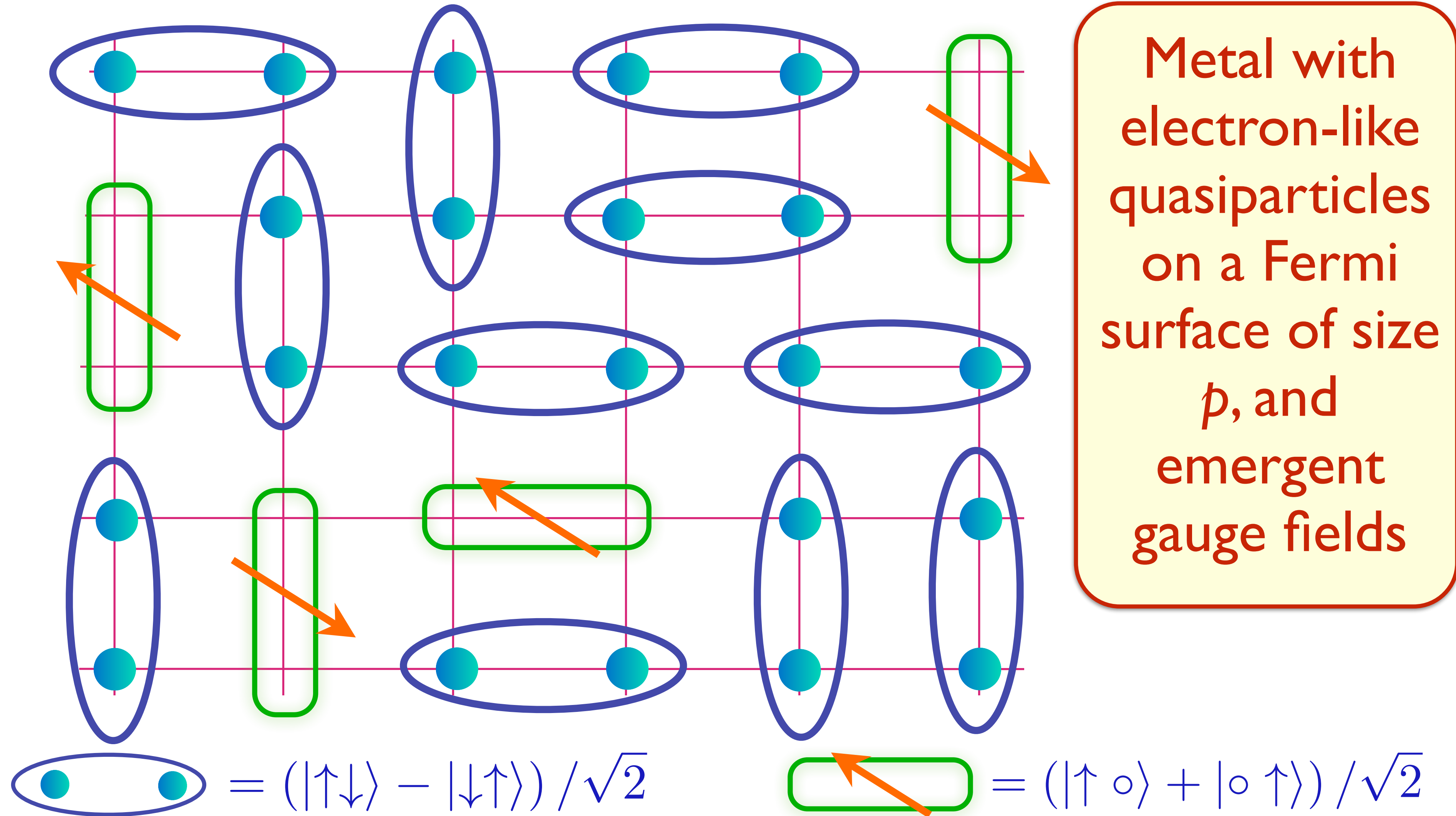
R. K. Kaul, A. Kolezhuk, M. Levin, S. Sachdev, and T. Senthil, PRB **75**, 235122 (2007)



FL*

S. Sachdev PRB **49**, 6770 (1994); X.-G. Wen and P.A. Lee PRL **76**, 503 (1996)

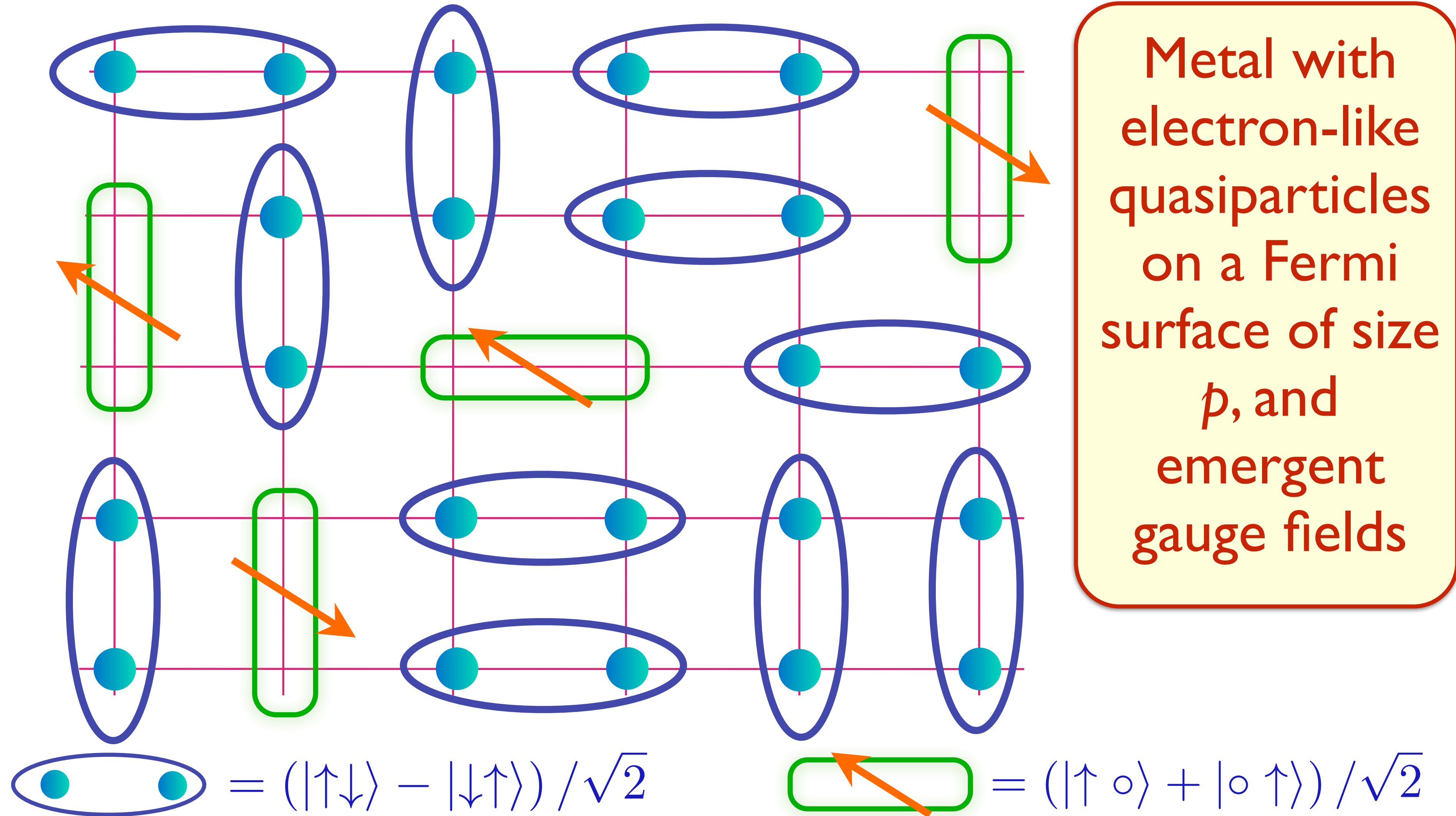
R. K. Kaul, A. Kolezhuk, M. Levin, S. Sachdev, and T. Senthil, PRB **75**, 235122 (2007)



FL*

S. Sachdev PRB **49**, 6770 (1994); X.-G. Wen and P.A. Lee PRL **76**, 503 (1996)

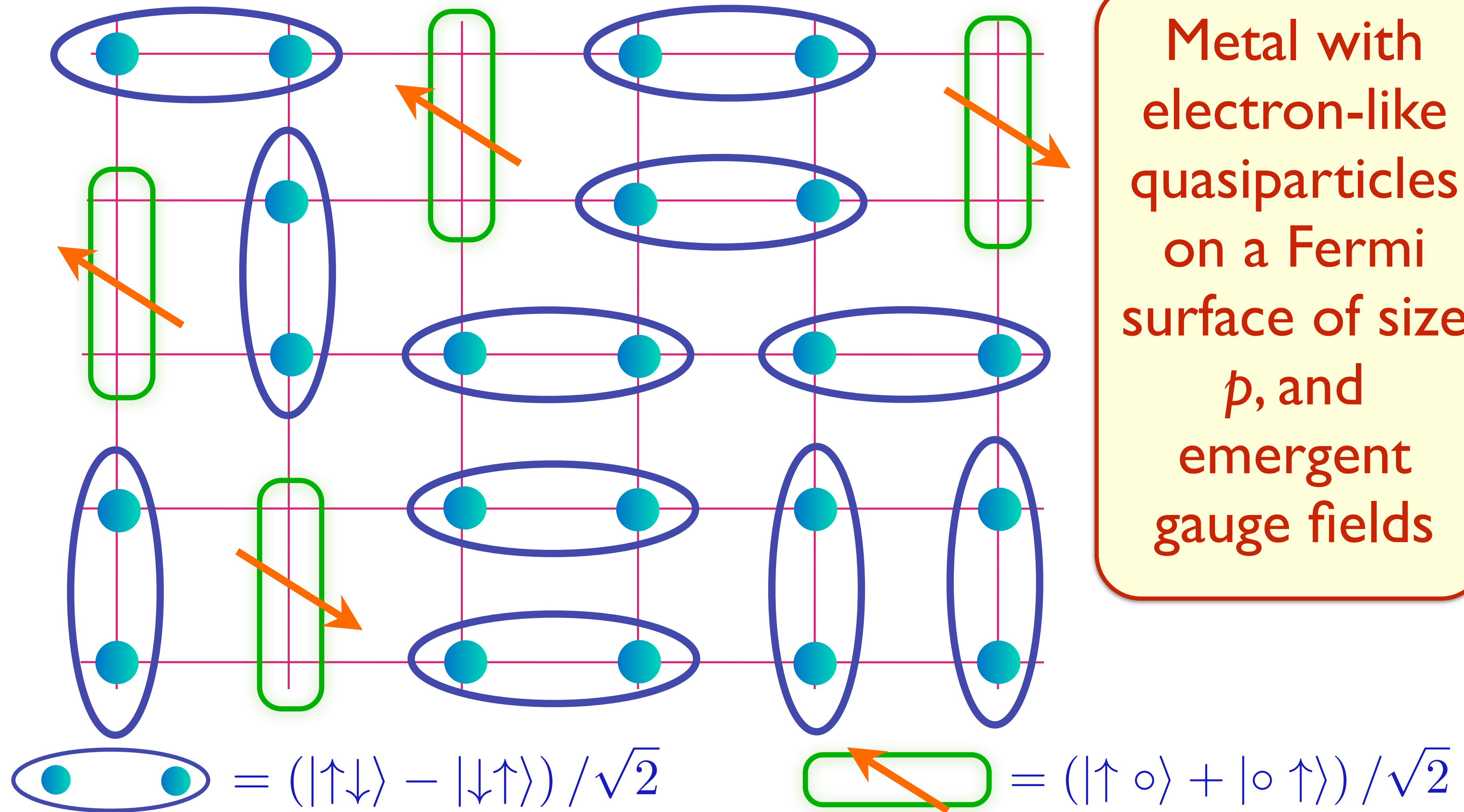
R. K. Kaul, A. Kolezhuk, M. Levin, S. Sachdev, and T. Senthil, PRB **75**, 235122 (2007)



FL*

S. Sachdev PRB **49**, 6770 (1994); X.-G. Wen and P.A. Lee PRL **76**, 503 (1996)

R. K. Kaul, A. Kolezhuk, M. Levin, S. Sachdev, and T. Senthil, PRB **75**, 235122 (2007)

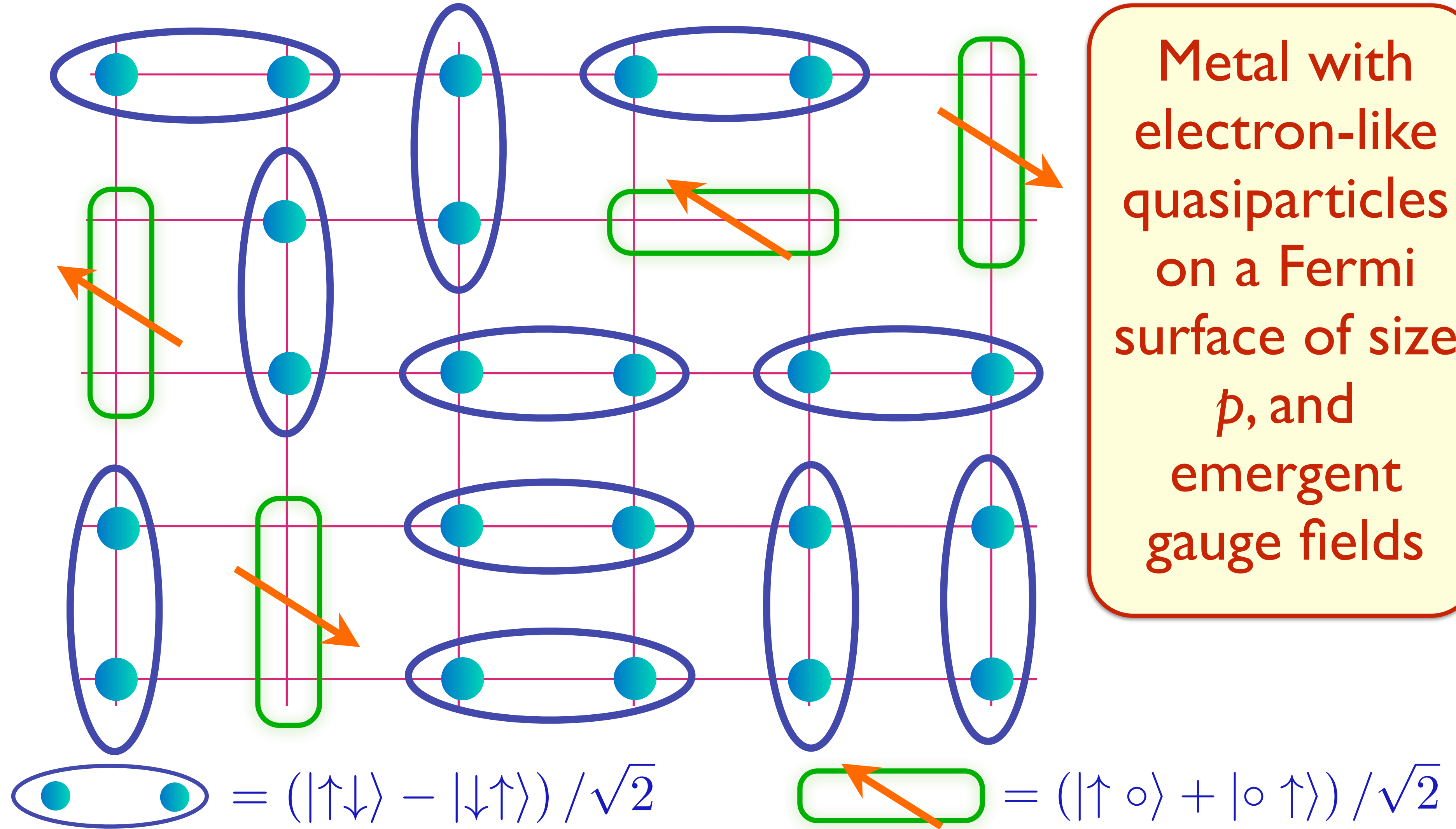


M. Punk, A. Allais, and S. Sachdev, PNAS **112**, 9552 (2015)

FL*

S. Sachdev PRB **49**, 6770 (1994); X.-G. Wen and P.A. Lee PRL **76**, 503 (1996)

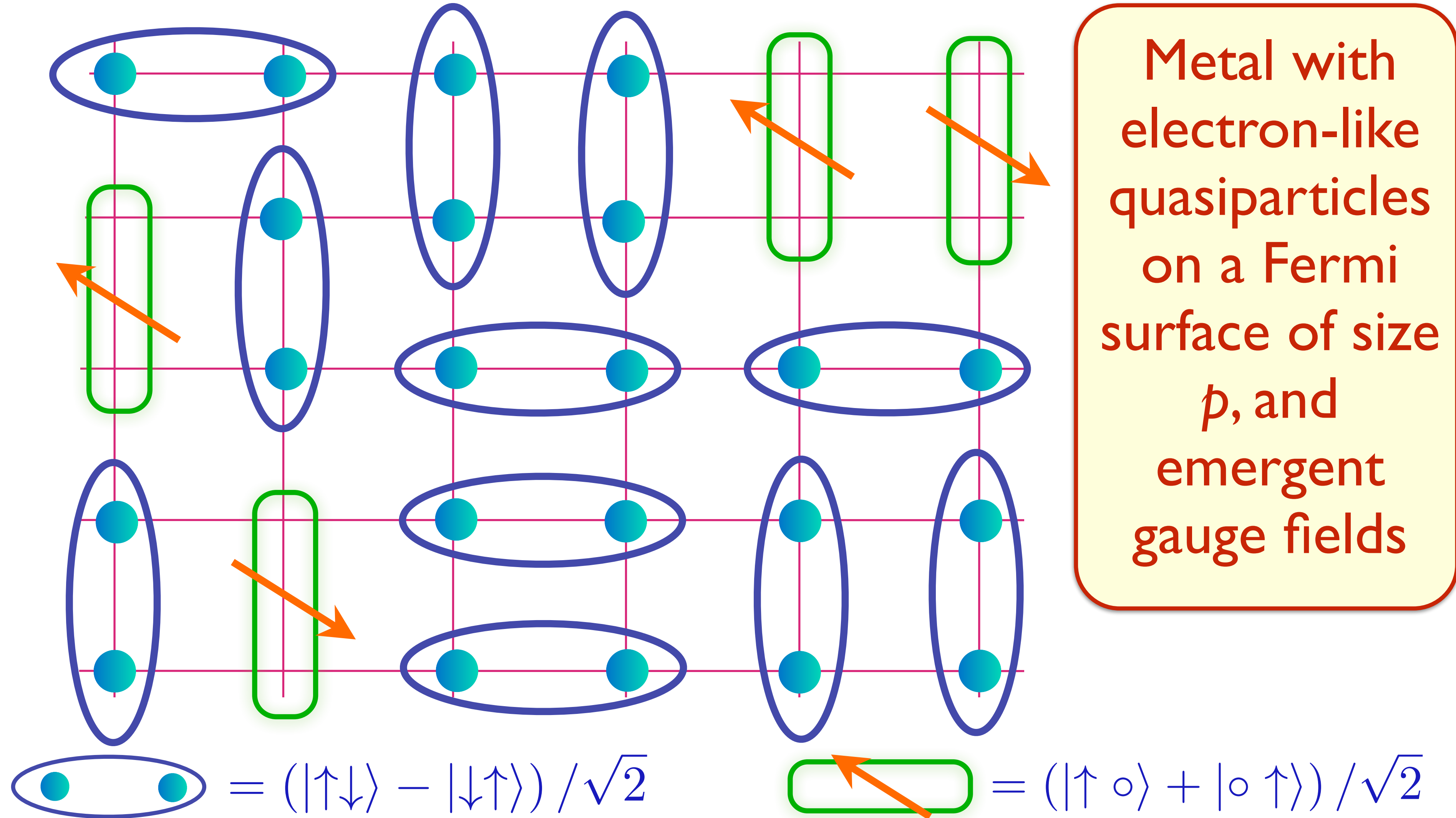
R. K. Kaul, A. Kolezhuk, M. Levin, S. Sachdev, and T. Senthil, PRB **75**, 235122 (2007)



FL*

S. Sachdev PRB **49**, 6770 (1994); X.-G. Wen and P.A. Lee PRL **76**, 503 (1996)

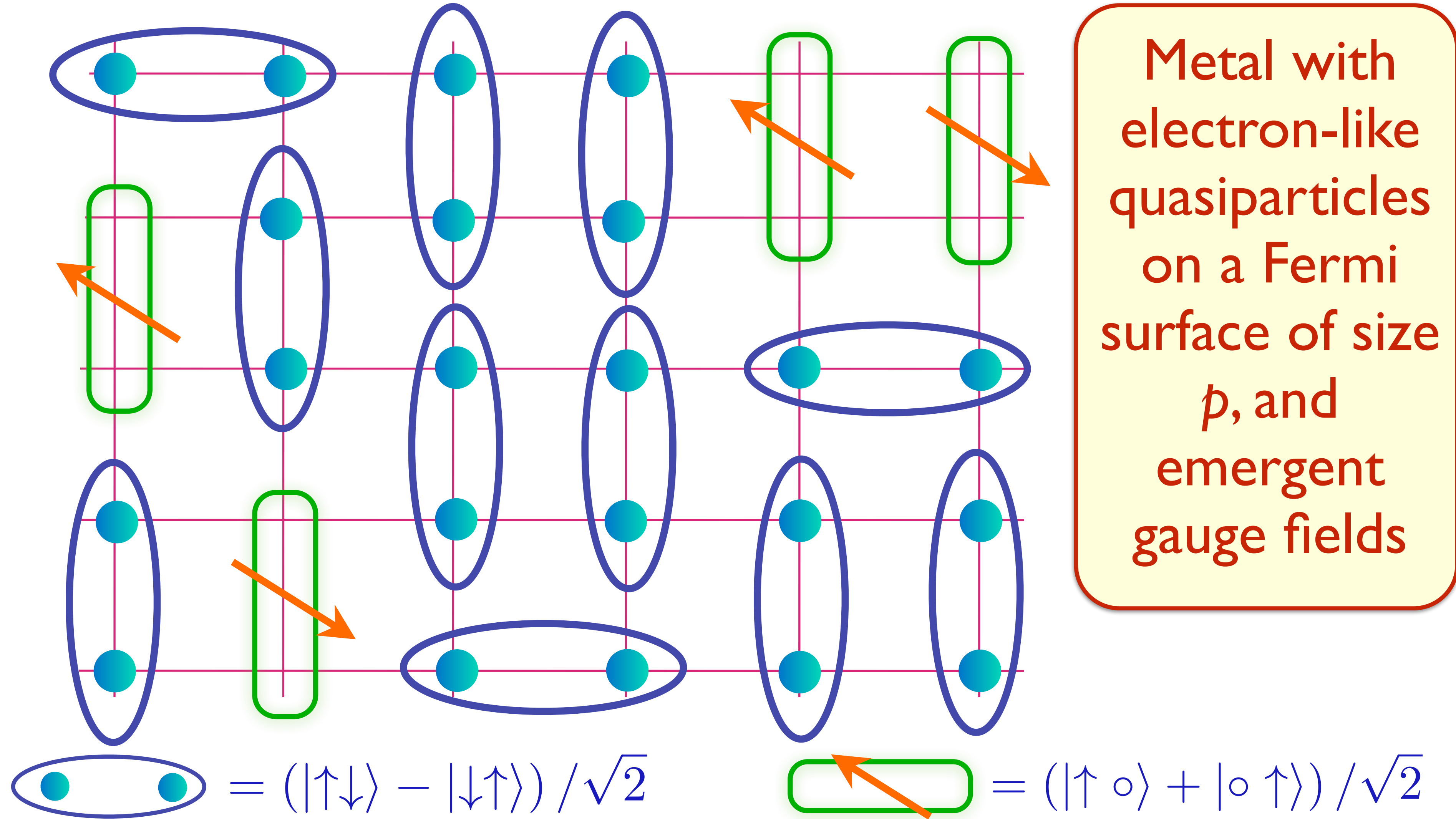
R. K. Kaul, A. Kolezhuk, M. Levin, S. Sachdev, and T. Senthil, PRB **75**, 235122 (2007)



FL*

S. Sachdev PRB **49**, 6770 (1994); X.-G. Wen and P.A. Lee PRL **76**, 503 (1996)

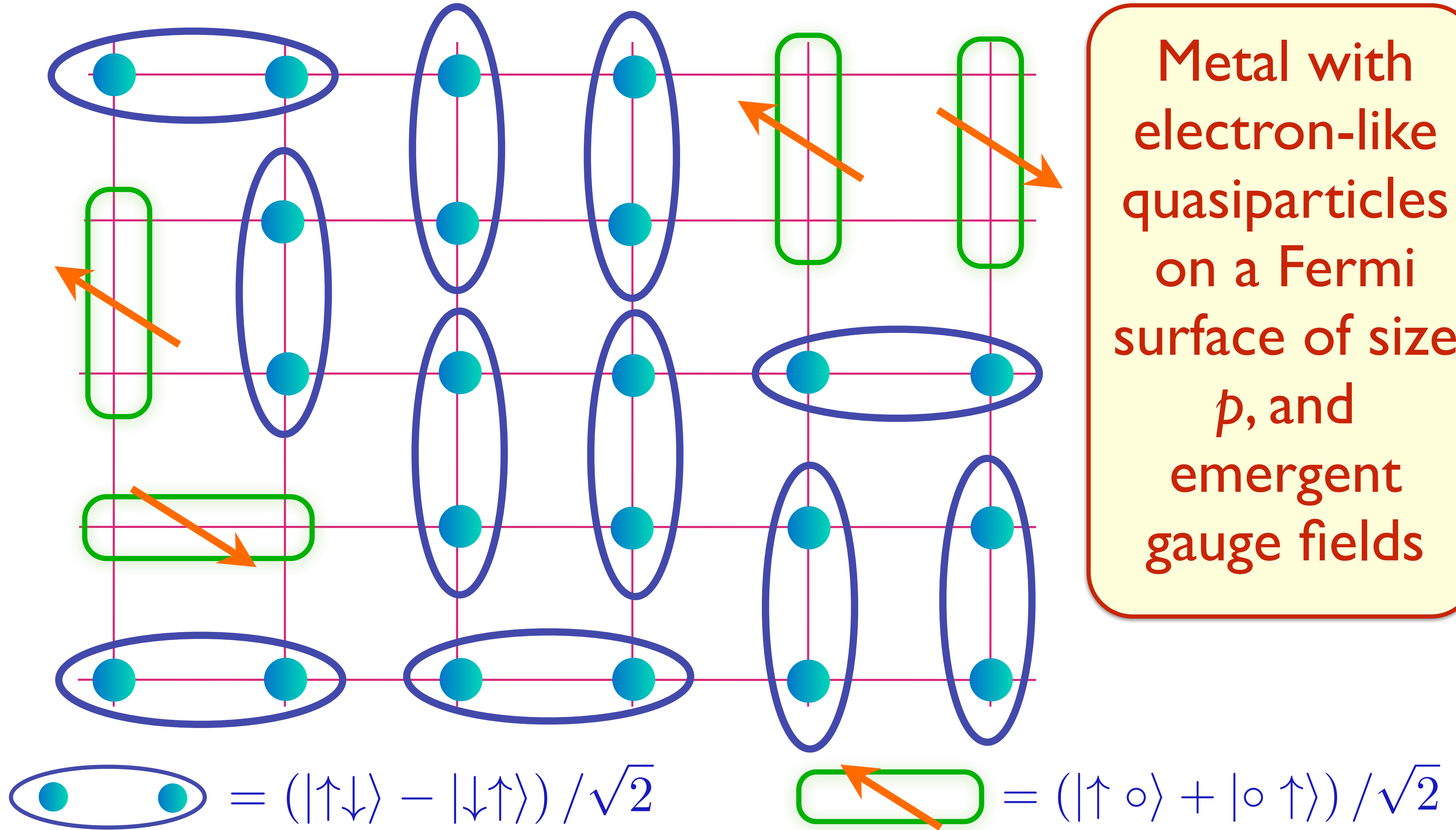
R. K. Kaul, A. Kolezhuk, M. Levin, S. Sachdev, and T. Senthil, PRB **75**, 235122 (2007)



FL*

S. Sachdev PRB **49**, 6770 (1994); X.-G. Wen and P.A. Lee PRL **76**, 503 (1996)

R. K. Kaul, A. Kolezhuk, M. Levin, S. Sachdev, and T. Senthil, PRB **75**, 235122 (2007)



Metal-metal transitions in a **one-band** model

- Can realize the FL* state as a doped spin liquid in which spinons and holons bind to form ‘electrons’, which then form a small Fermi surface (X.-G. Wen and P. A. Lee, PRL **76**, 503 (1996)); but there is no complete description of this process, except in the very strong binding limit of dimer ‘electrons’ (M. Punk, A. Allais, and S. Sachdev, PNAS **112**, 9552 (2015)). This approach does not yield a theory of the transition to the FL state.

Metal-metal transitions in a **one-band** model

- Can realize the FL* state as a doped spin liquid in which spinons and holons bind to form ‘electrons’, which then form a small Fermi surface (X.-G. Wen and P. A. Lee, PRL **76**, 503 (1996)); but there is no complete description of this process, except in the very strong binding limit of dimer ‘electrons’ (M. Punk, A. Allais, and S. Sachdev, PNAS **112**, 9552 (2015)). This approach does not yield a theory of the transition to the FL state.
- There is a proposal (S. Sachdev, H. D. Scammell, M. S. Scheurer, and G. Tarnopolsky, PRB **99**, 054516 (2019)) for a transition from FL* to FL using a $SU(2)_S$ gauge theory, but some ‘hand-waving’ is required to produce the FL* Fermi surface.

1. Metal-metal transition in the Kondo Lattice

2. Metal-metal transition in a one-band model

A. FL model of the pseudogap*

B. Ancilla qubits and ghost Fermi surfaces

3. Random J model (insulator)

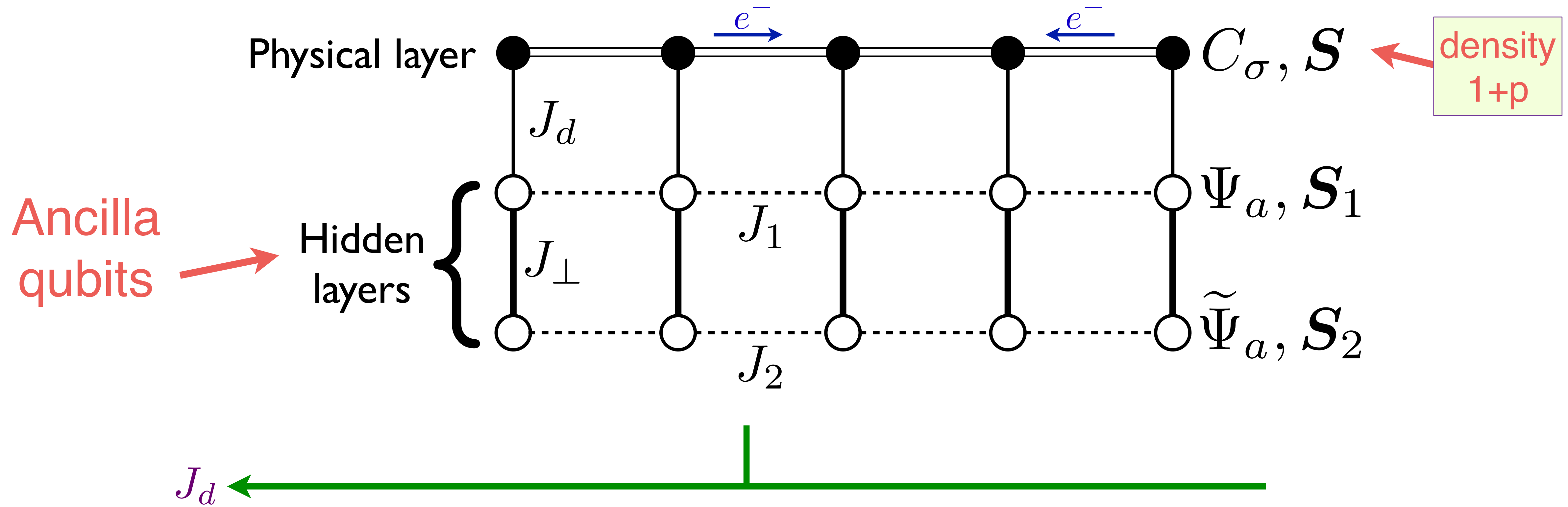
RG analysis and exact exponent

4. Random t - J model (metals)

Numerics, RG analysis and exact exponents

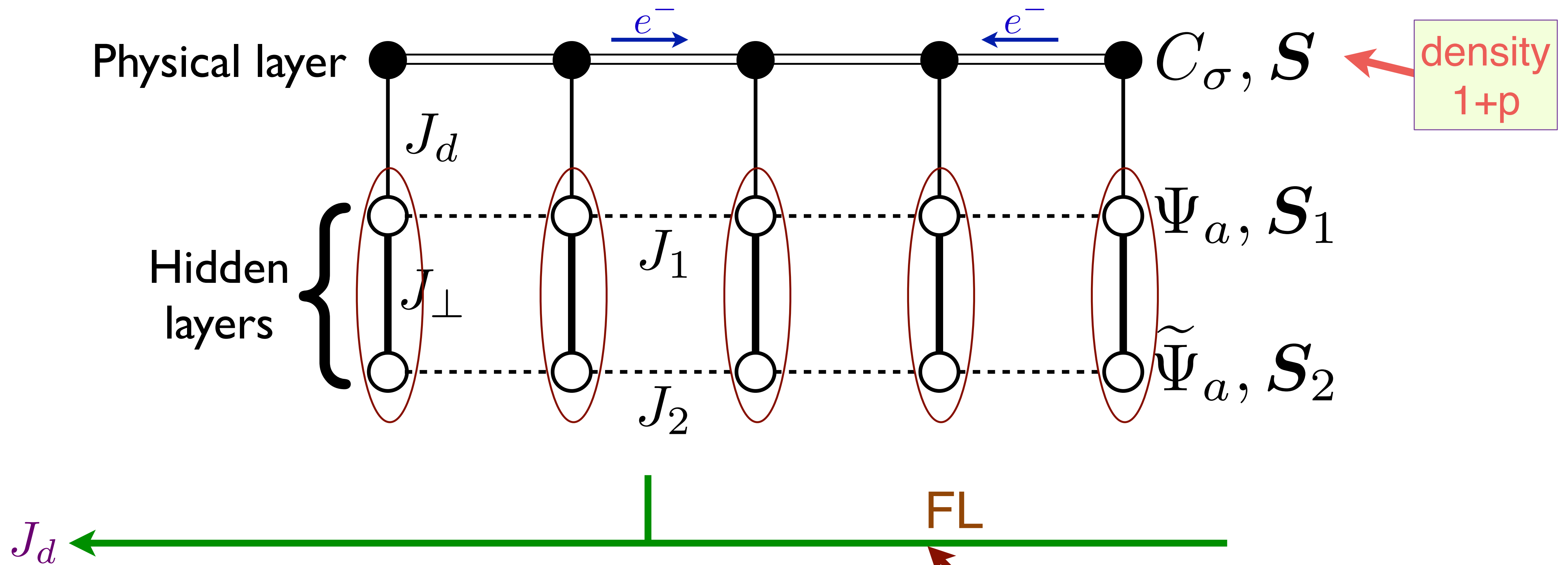
1. Metal-metal transition in the Kondo Lattice
2. Metal-metal transition in a one-band model
 - A. *FL* model of the pseudogap*
 - B. *Ancilla qubits and ghost Fermi surfaces*
3. Random J model (insulator)
RG analysis and exact exponent
4. Random t - J model (metals)
Numerics, RG analysis and exact exponents

Metal-metal transitions in a **one-band** model



Ya-Hui Zhang

Metal-metal transitions in a **one-band** model

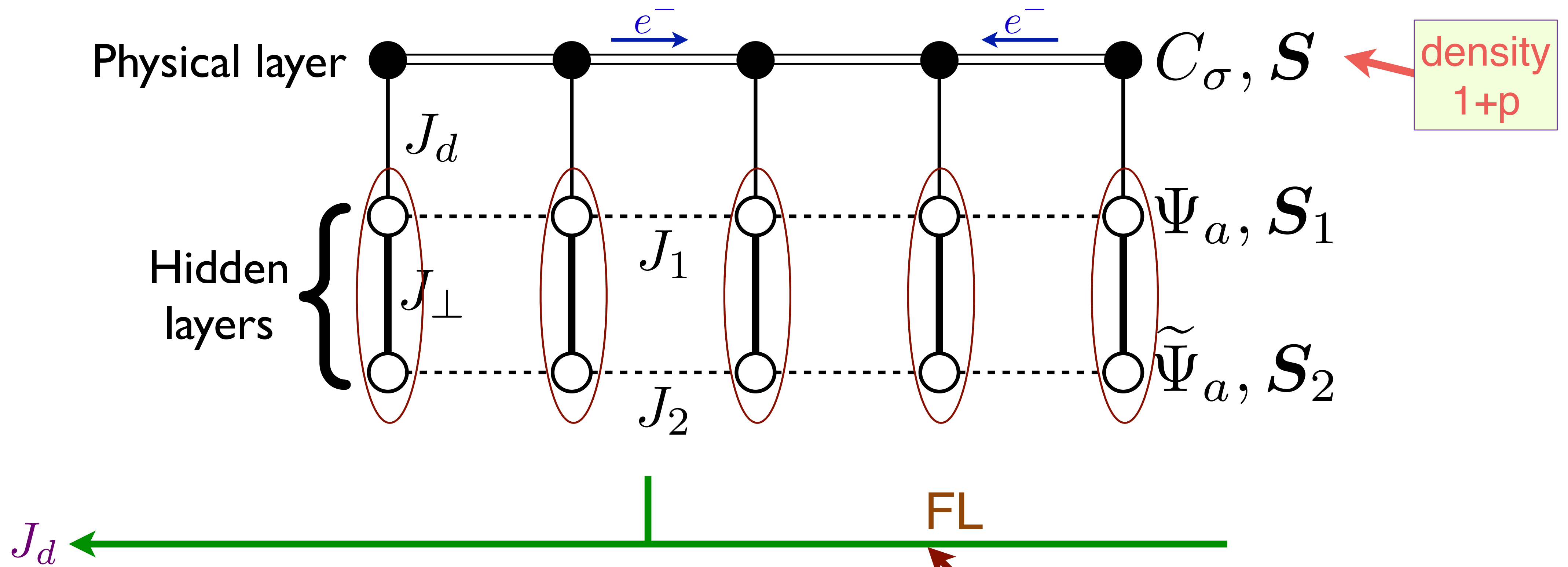


Ya-Hui Zhang

Large Fermi surface of size $1 + p$

$$|\Phi\rangle = \left| \text{Rung singlets of } \Psi, \tilde{\Psi} \right\rangle \otimes \left| \text{Slater determinant of } C \right\rangle$$

Metal-metal transitions in a **one-band** model



Ya-Hui Zhang

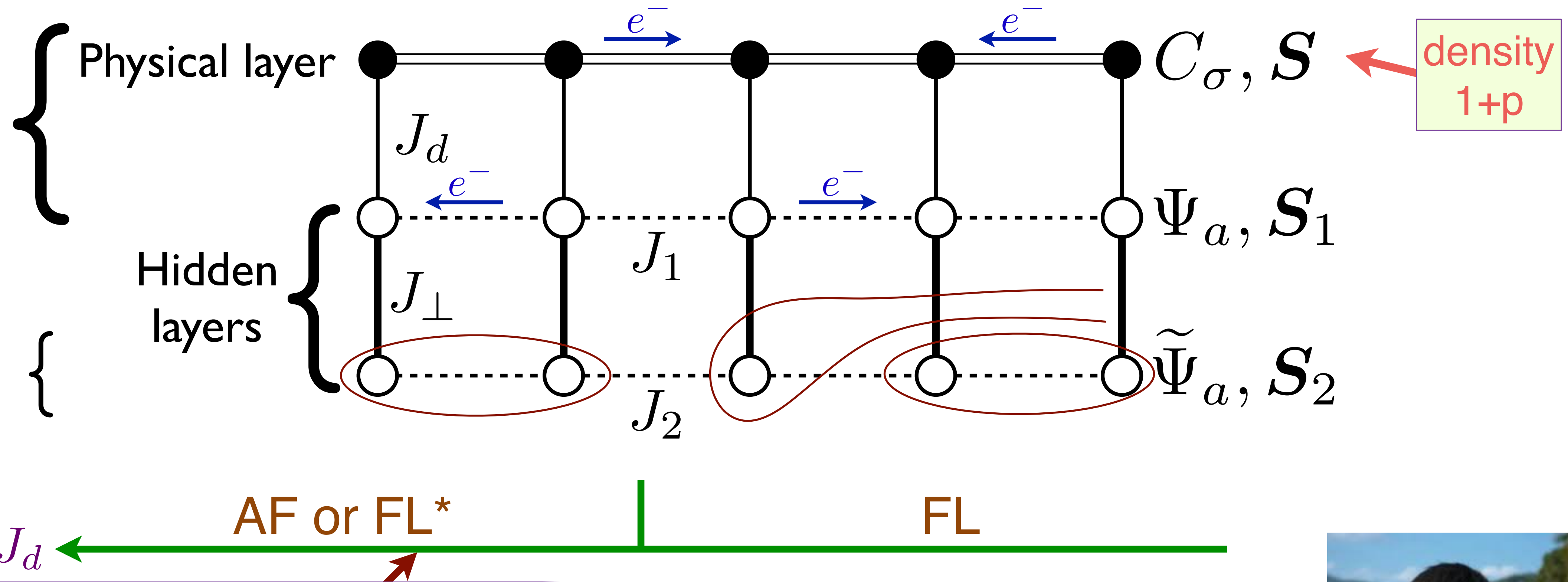
Luttinger
Theorem
obeyed

Large Fermi surface of size $1 + p$

$|\Phi\rangle = \left| \text{Rung singlets of } \Psi, \tilde{\Psi} \right\rangle \otimes \left| \text{Slater determinant of } C \right\rangle$

Metal-metal transitions in a **one-band** model

Metal.
Density
 $2 + p \cong p$



Small Fermi surface of size p

$$|\Phi\rangle = \left[\text{Projection onto rung singlets of } \Psi, \tilde{\Psi} \right] \otimes |\text{Slater determinant of } (C, \Psi)\rangle \otimes |\text{Spin liquid of } \tilde{\Psi}\rangle$$

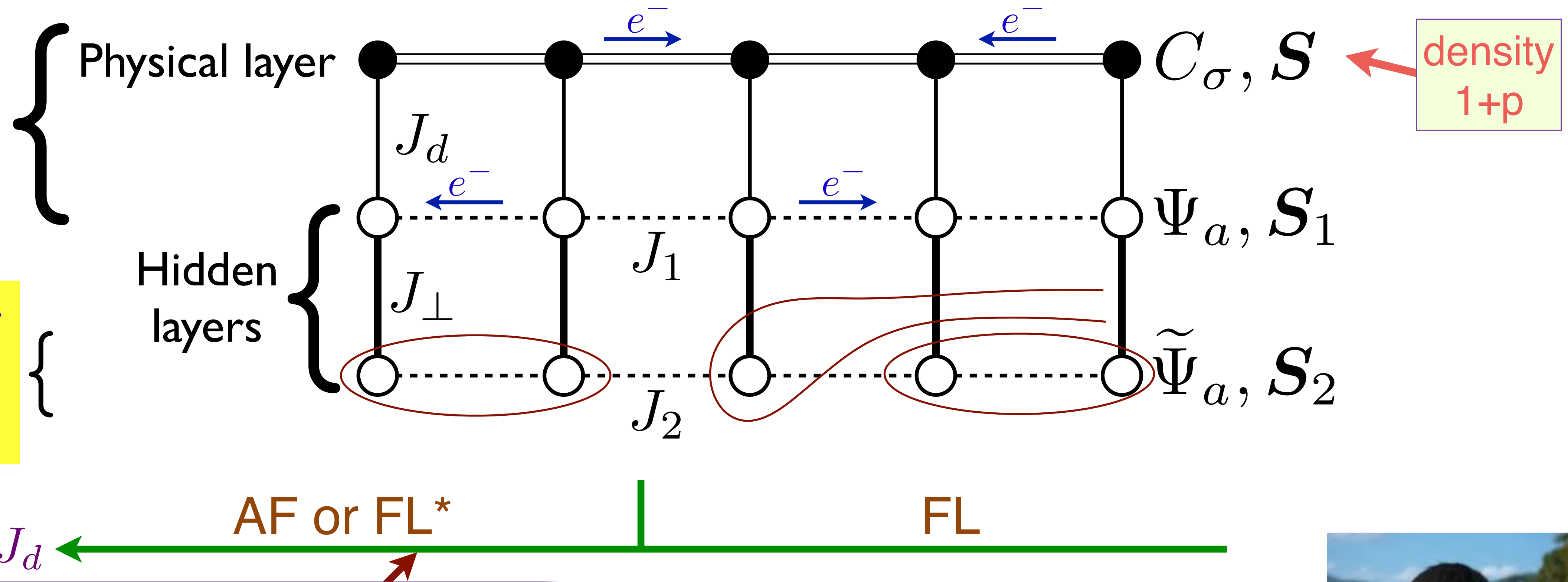


Ya-Hui Zhang

Metal-metal transitions in a **one-band** model

Metal.
Density
 $2 + p \cong p$

Mott insulator
Spin liquid
or AF order



Small Fermi surface of size p

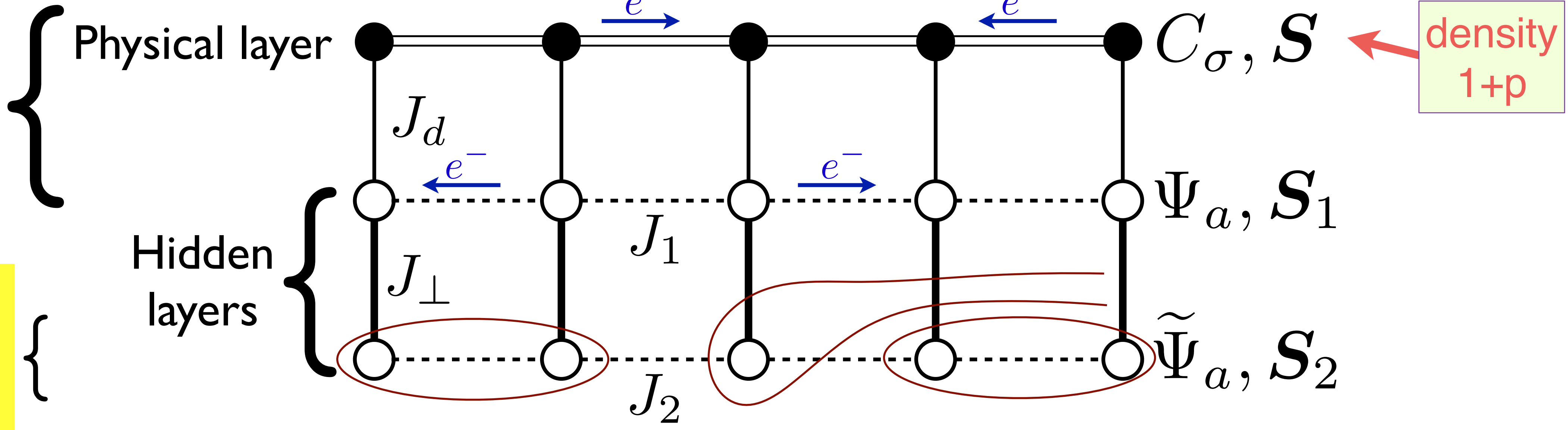
$|\Phi\rangle = \left[\text{Projection onto rung singlets of } \Psi, \tilde{\Psi} \right]$
 \otimes Slater determinant of (C, Ψ)
 \otimes Spin liquid of $\tilde{\Psi}$



Ya-Hui Zhang

Metal-metal transitions in a **one-band** model

Metal.
Density
 $2 + p \cong p$



Mott insulator
Spin liquid
or AF order



Small Fermi surface of size p

$|\Phi\rangle = \left[\text{Projection onto rung singlets of } \Psi, \tilde{\Psi} \right] \otimes |\text{Slater determinant of } (C, \Psi)\rangle \otimes |\text{Spin liquid of } \tilde{\Psi}\rangle$

Luttinger Theorem violated;
OK, because of topological order of $\tilde{\Psi}$

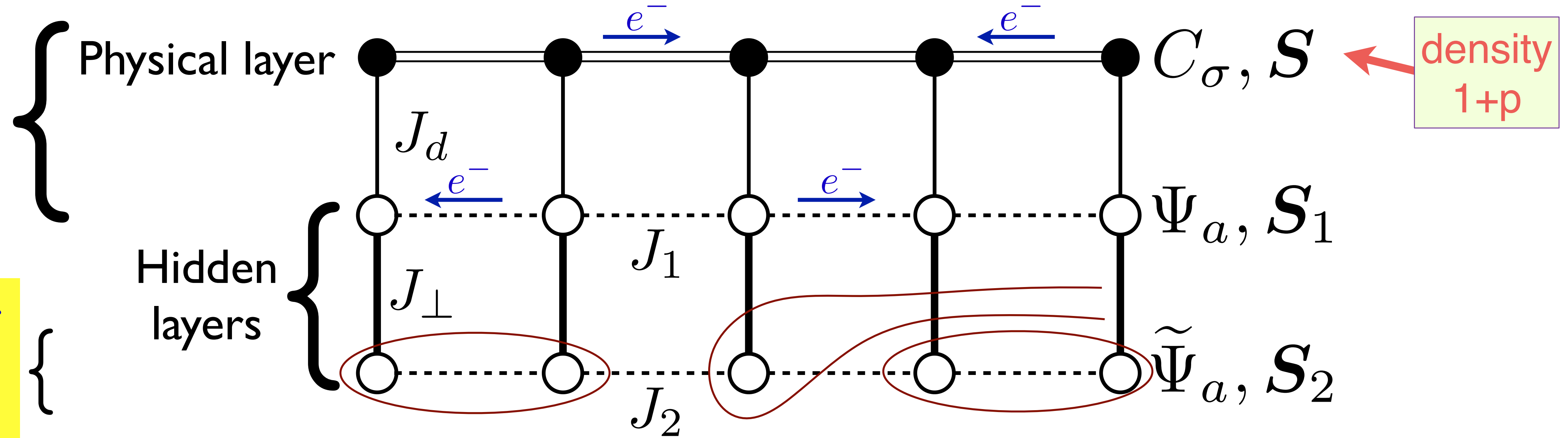


Ya-Hui Zhang

Metal-metal transitions in a **one-band** model

Metal.
Density
 $2 + p \cong p$

Mott insulator
Spin liquid
or AF order



J_d ← AF or FL* | FL

Small Fermi surface of size p

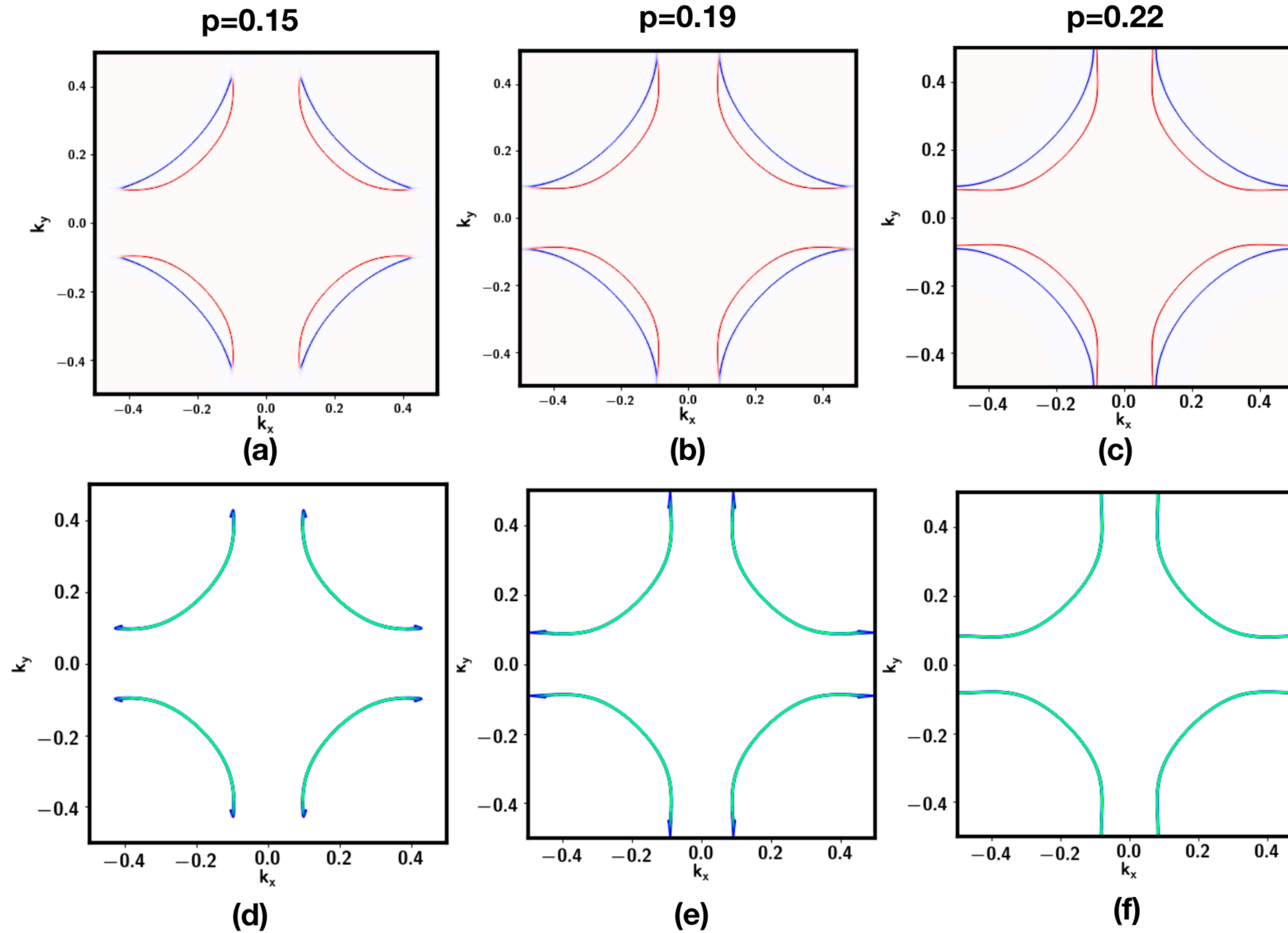
$$|\Phi\rangle = \left[\text{Projection onto rung singlets of } \Psi, \tilde{\Psi} \right] \otimes |\text{Slater determinant of } (C, \Psi)\rangle \otimes |\text{Spin liquid of } \tilde{\Psi}\rangle$$

Similar to a selective Mott transition in hidden layer 1: Ψ fermions are insulating in FL phase, and metallic in FL* phase.



Ya-Hui Zhang

Metal-metal transitions in a **one-band** model



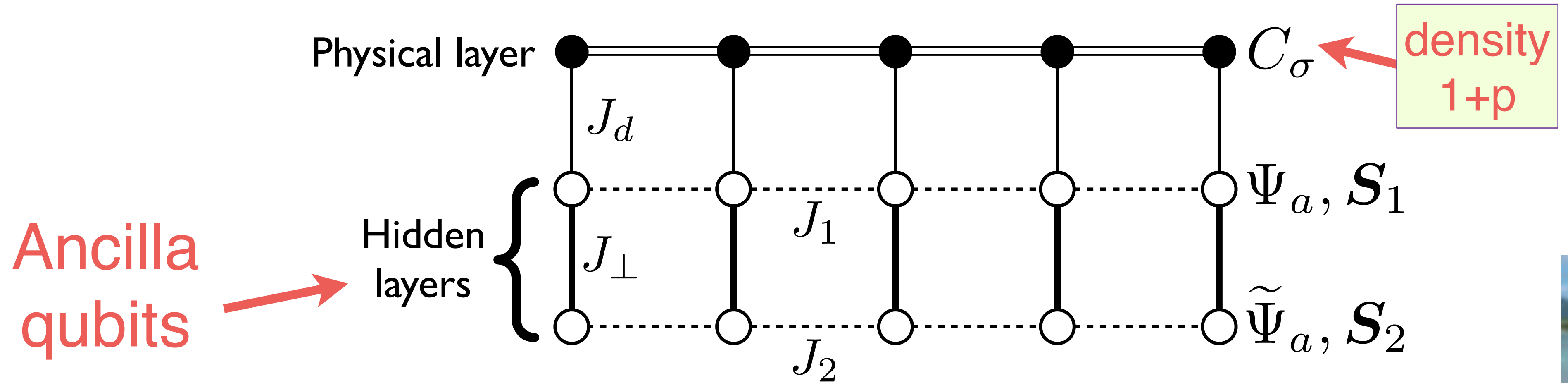
“Fermi arc”
spectral functions
in the FL* phase



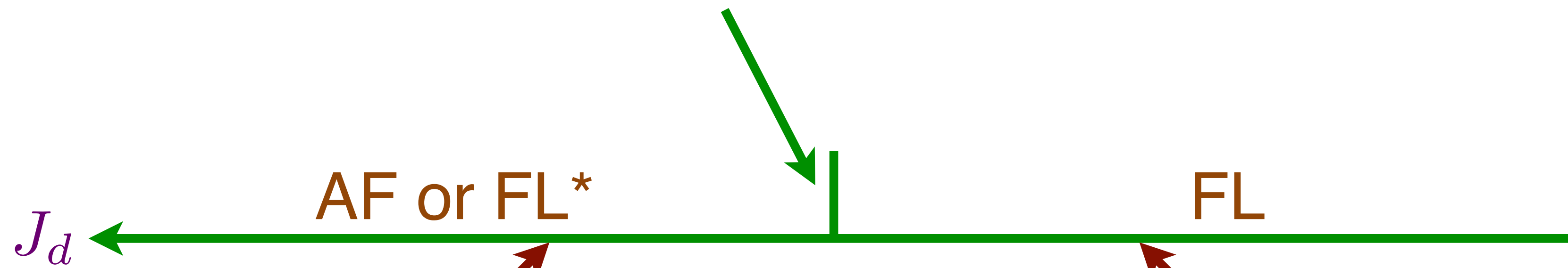
Ya-Hui Zhang

Zero frequency spectral density of electrons (red) and ghosts (blue)

Metal-metal transitions in a **one-band** model



Yahui Zhang



Small Fermi surface of size p

$$|\Phi\rangle = \left[\text{Projection onto rung singlets of } \Psi, \tilde{\Psi} \right] \otimes |\text{Slater determinant of } (C, \Psi)\rangle \otimes |\text{Slater determinant of } \tilde{\Psi}\rangle$$

Large Fermi surface of size $1+p$

$$|\Phi\rangle = |\text{Rung singlets of } \Psi, \tilde{\Psi}\rangle \otimes |\text{Slater determinant of } C\rangle$$

Metal-metal transitions in a **one-band** model

Write fermion operators as 2×2 matrices

$$\Psi = \begin{pmatrix} \Psi_{\uparrow} & -\Psi_{\downarrow}^{\dagger} \\ \Psi_{\downarrow} & \Psi_{\uparrow}^{\dagger} \end{pmatrix}, \quad \tilde{\Psi} = \begin{pmatrix} \tilde{\Psi}_{\uparrow} & -\tilde{\Psi}_{\downarrow}^{\dagger} \\ \tilde{\Psi}_{\downarrow} & \tilde{\Psi}_{\uparrow}^{\dagger} \end{pmatrix}$$

Single occupancy constraints of Ψ , $\tilde{\Psi}$ leads to $SU(2)_1 \times SU(2)_2$ gauge symmetry:

$$\begin{aligned} SU(2)_1 : & \quad \Psi \rightarrow \Psi U_1, & \tilde{\Psi} & \rightarrow \tilde{\Psi} \\ SU(2)_2 : & \quad \Psi \rightarrow \Psi, & \tilde{\Psi} & \rightarrow \tilde{\Psi} U_2 \end{aligned}$$

P.A. Lee, N. Nagaosa, and X.-G. Wen, RMP **78**, 17 (2006)

Local singlet formation ('antiferromagnetism') $\mathcal{S}_1 + \mathcal{S}_2 \approx 0$ leads to $SU(2)_S$ gauge symmetry:

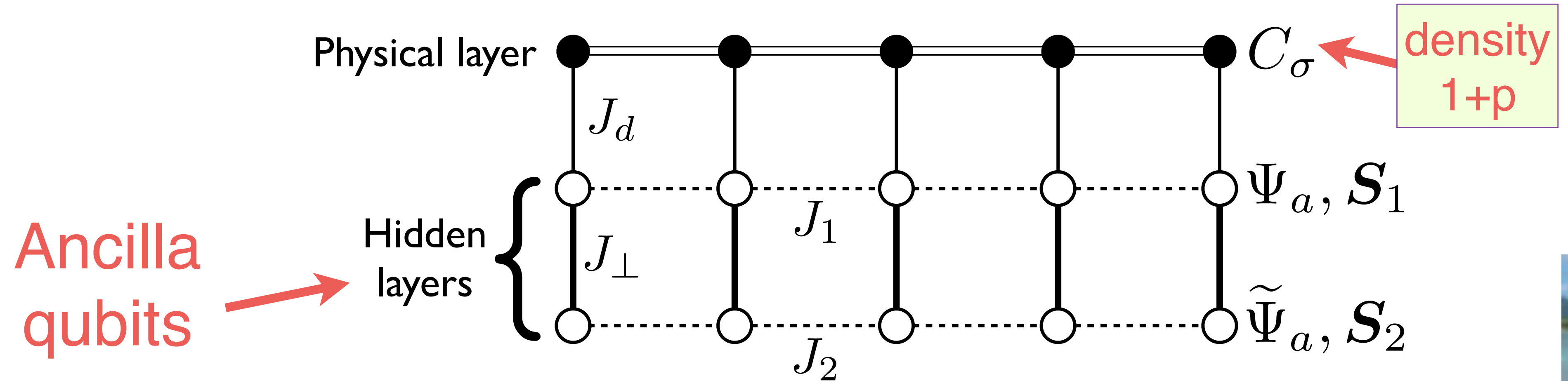
$$SU(2)_S : \quad \Psi \rightarrow U_S \Psi, \quad \tilde{\Psi} \rightarrow U_S \tilde{\Psi}$$

S. Sachdev, M.A. Metlitski, Yang Qi, and Cenke Xu, PRB **80**, 155129 (2009)

S. Sachdev, H. D. Scammell, M. S. Scheurer, and G. Tarnopolsky, PRB **99**, 054516 (2019)

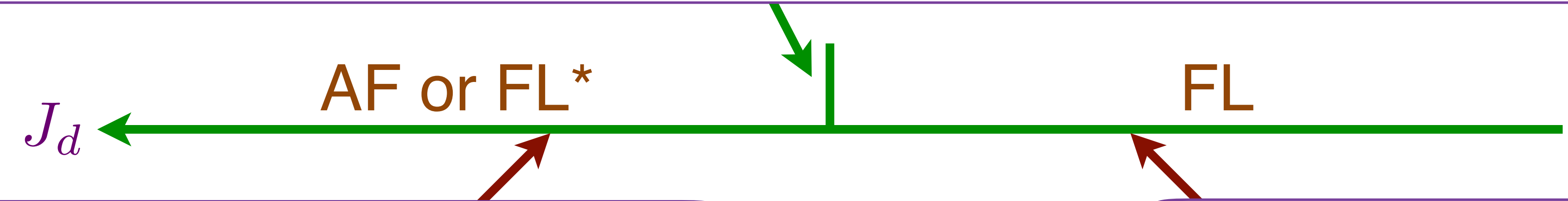
Ya-Hui Zhang, S. Sachdev, PRR **2**, 023172 (2020); arXiv:2006.01140.

Metal-metal transitions in a **one-band** model



Yahui Zhang

$(U(1)_S \times U(1)_1)/Z_2$ or $(SU(2)_S \times U(1)_1)/Z_2$ gauge theory of a Ψ ghost Fermi surface and a ‘hybridization-Higgs’ boson $\sim C_\sigma^\dagger \Psi_a$ which condenses on the ‘Small Fermi surface’ side.



Small Fermi surface of size p

$|\Phi\rangle = \left[\text{Projection onto rung singlets of } \Psi, \tilde{\Psi} \right]$
 $\otimes |\text{Slater determinant of } (C, \Psi)\rangle$
 $\otimes |\text{Slater determinant of } \tilde{\Psi}\rangle$

Large Fermi surface of size $1 + p$

$|\Phi\rangle = |\text{Rung singlets of } \Psi, \tilde{\Psi}\rangle$
 $\otimes |\text{Slater determinant of } C\rangle$

Ancilla qubit theory of metal-metal quantum phase transitions

- FL* as the pseudogap metal with carrier density p . Variants of the theory can have broken symmetries (*e.g.* antiferromagnetism) without fractionalization in the pseudogap metal.

Ancilla qubit theory of metal-metal quantum phase transitions

- FL* as the pseudogap metal with carrier density p . Variants of the theory can have broken symmetries (*e.g.* antiferromagnetism) without fractionalization in the pseudogap metal.
- Ghost fermions, carrying neither spin nor charge, emerge as additional low energy excitations near the critical point to the FL phase. While the ancilla qubits are gauged away as ‘fake’ in the UV theory, the ghost fermions are physical excitations in the IR theory, which can be detected by thermal probes.

Ancilla qubit theory of metal-metal quantum phase transitions

- FL* as the pseudogap metal with carrier density p . Variants of the theory can have broken symmetries (*e.g.* antiferromagnetism) without fractionalization in the pseudogap metal.
- Ghost fermions, carrying neither spin nor charge, emerge as additional low energy excitations near the critical point to the FL phase. While the ancilla qubits are gauged away as ‘fake’ in the UV theory, the ghost fermions are physical excitations in the IR theory, which can be detected by thermal probes.
- The ghost fermions are coupled to 2 gauge fields: the first arising from the no double occupancy constraint, and the second from transforming to a rotating reference frame in spin space. These gauge fields lead respectively to repulsive and attractive interactions between the ghost fermions.

1. Metal-metal transition in the Kondo Lattice

2. Metal-metal transition in a one-band model

A. FL model of the pseudogap*

B. Ancilla qubits and ghost Fermi surfaces

3. Random J model (insulator)

RG analysis and exact exponent

4. Random t - J model (metals)

Numerics, RG analysis and exact exponents

Physical Review X
10, 021033 (2020)



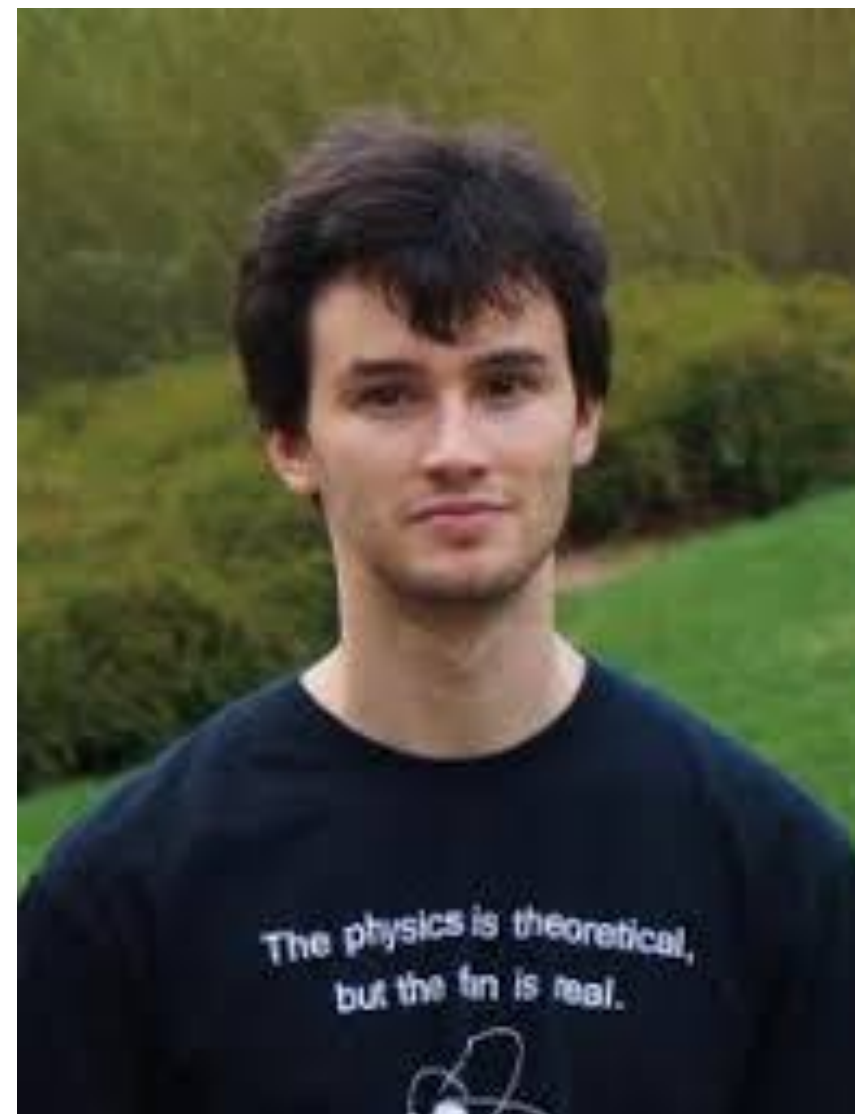
Darshan Joshi



Henry Shackleton



Chenyuan Li



Grigory Tarnopolsky



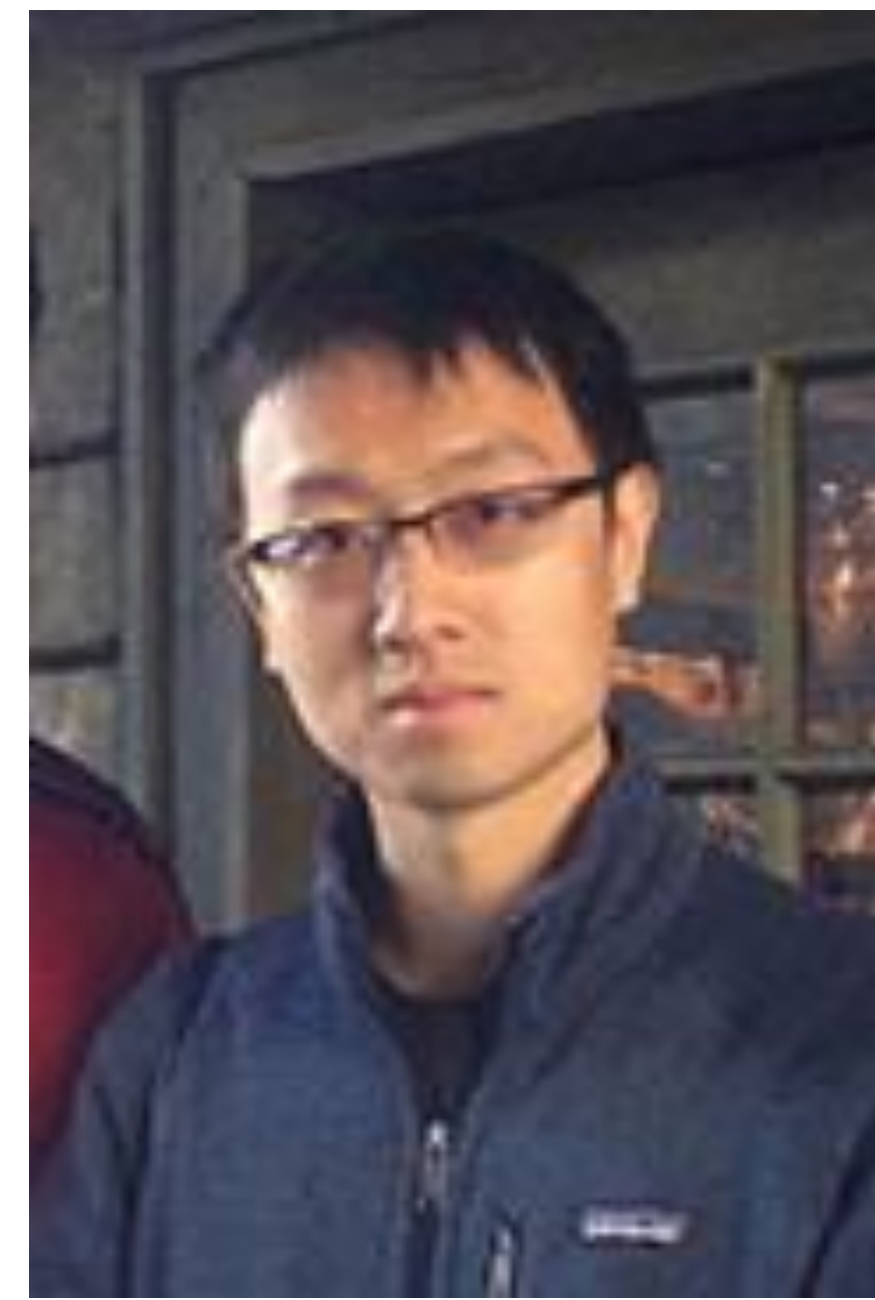
Alexander Wietek



Antoine Georges



Annals of Physics,
418, 168202 (2020)



Haoyu Guo

Yingfeu Gu



Maria Tikhanovskaya

M. Tikhanovskaya, Haoyu Guo, Grigory Tarnopolsky, S. Sachdev, to appear

Random t - J model

$$H = -\frac{1}{\sqrt{N}} \sum_{i,j=1}^N t_{ij} c_{i\alpha}^\dagger c_{j\alpha} + \frac{1}{\sqrt{N}} \sum_{i<j=1}^N J_{ij} \vec{S}_i \cdot \vec{S}_j$$

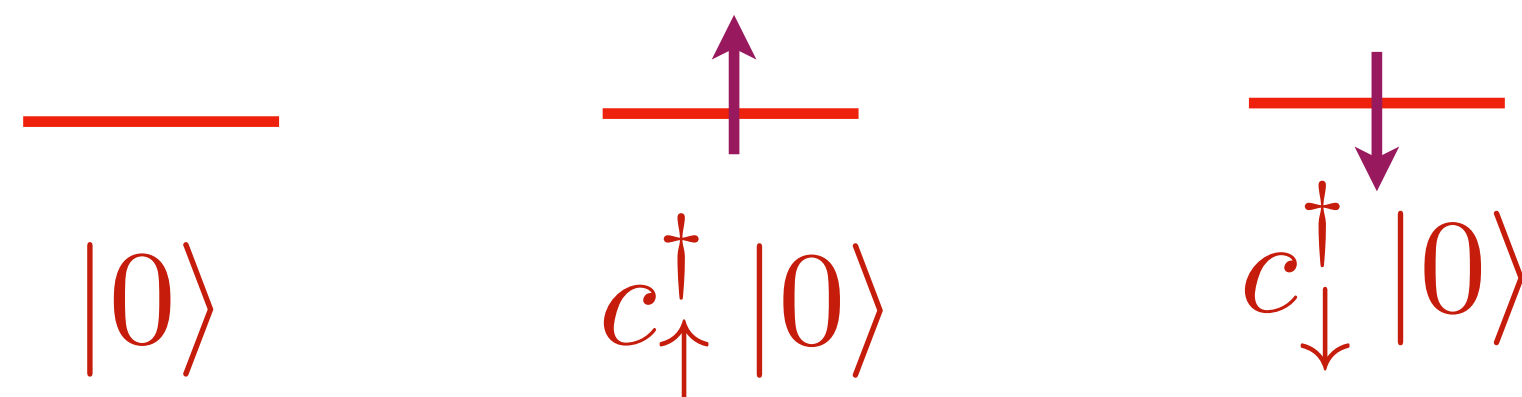
We consider the hole-doped case, with no double occupancy.

$$\alpha = \uparrow, \downarrow, \quad \{c_{i\alpha}, c_{j\beta}^\dagger\} = \delta_{ij} \delta_{\alpha\beta}, \quad \{c_{i\alpha}, c_{j\beta}\} = 0$$

$$\vec{S}_i = \frac{1}{2} c_{i\alpha}^\dagger \vec{\sigma}_{\alpha\beta} c_{i\beta}, \quad \sum_{\alpha} c_{i\alpha}^\dagger c_{i\alpha} \leq 1, \quad \frac{1}{N} \sum_{i\alpha} c_{i\alpha}^\dagger c_{i\alpha} = 1 - p$$

$$J_{ij} \text{ random, } \overline{J_{ij}} = 0, \quad \overline{J_{ij}^2} = J^2$$

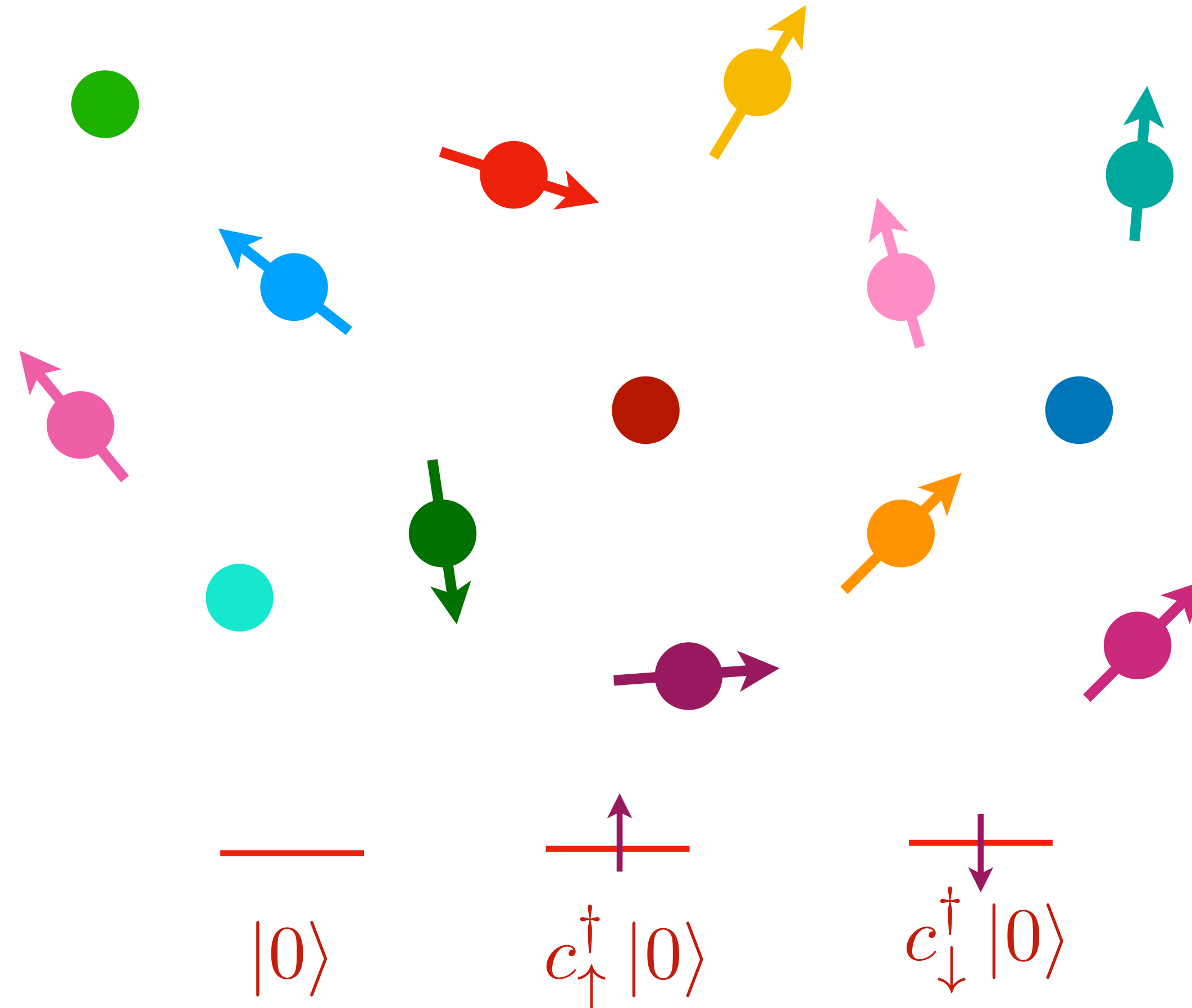
$$t_{ij} \text{ random, } \overline{t_{ij}} = 0, \quad \overline{t_{ij}^2} = t^2$$



Random t - J model

$$H = -\frac{1}{\sqrt{N}} \sum_{i,j=1}^N t_{ij} c_{i\alpha}^\dagger c_{j\alpha} + \frac{1}{\sqrt{N}} \sum_{i<j=1}^N J_{ij} \vec{S}_i \cdot \vec{S}_j$$

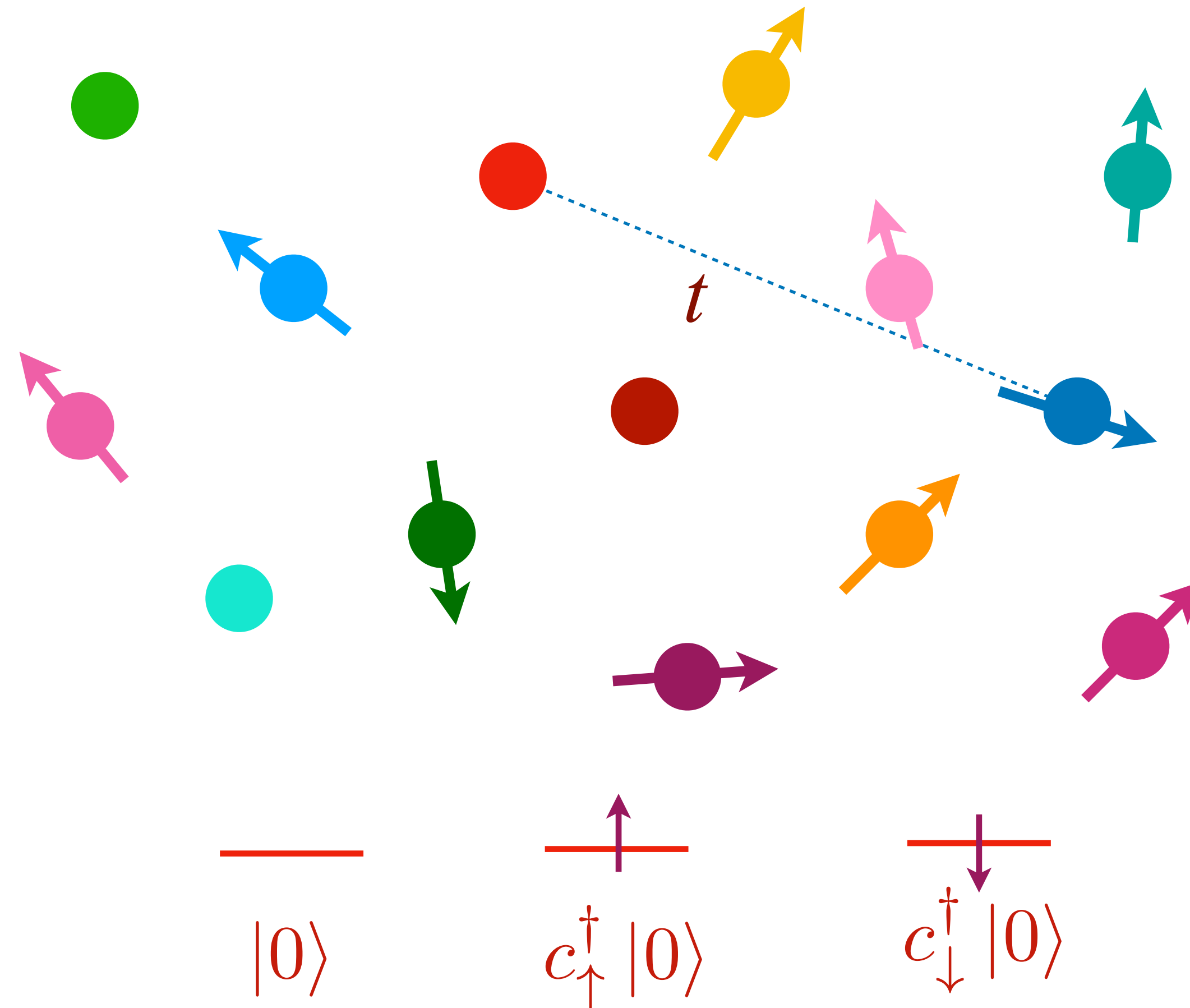
We consider the hole-doped case, with no double occupancy.



Random t - J model

$$H = -\frac{1}{\sqrt{N}} \sum_{i,j=1}^N t_{ij} c_{i\alpha}^\dagger c_{j\alpha} + \frac{1}{\sqrt{N}} \sum_{i<j=1}^N J_{ij} \vec{S}_i \cdot \vec{S}_j$$

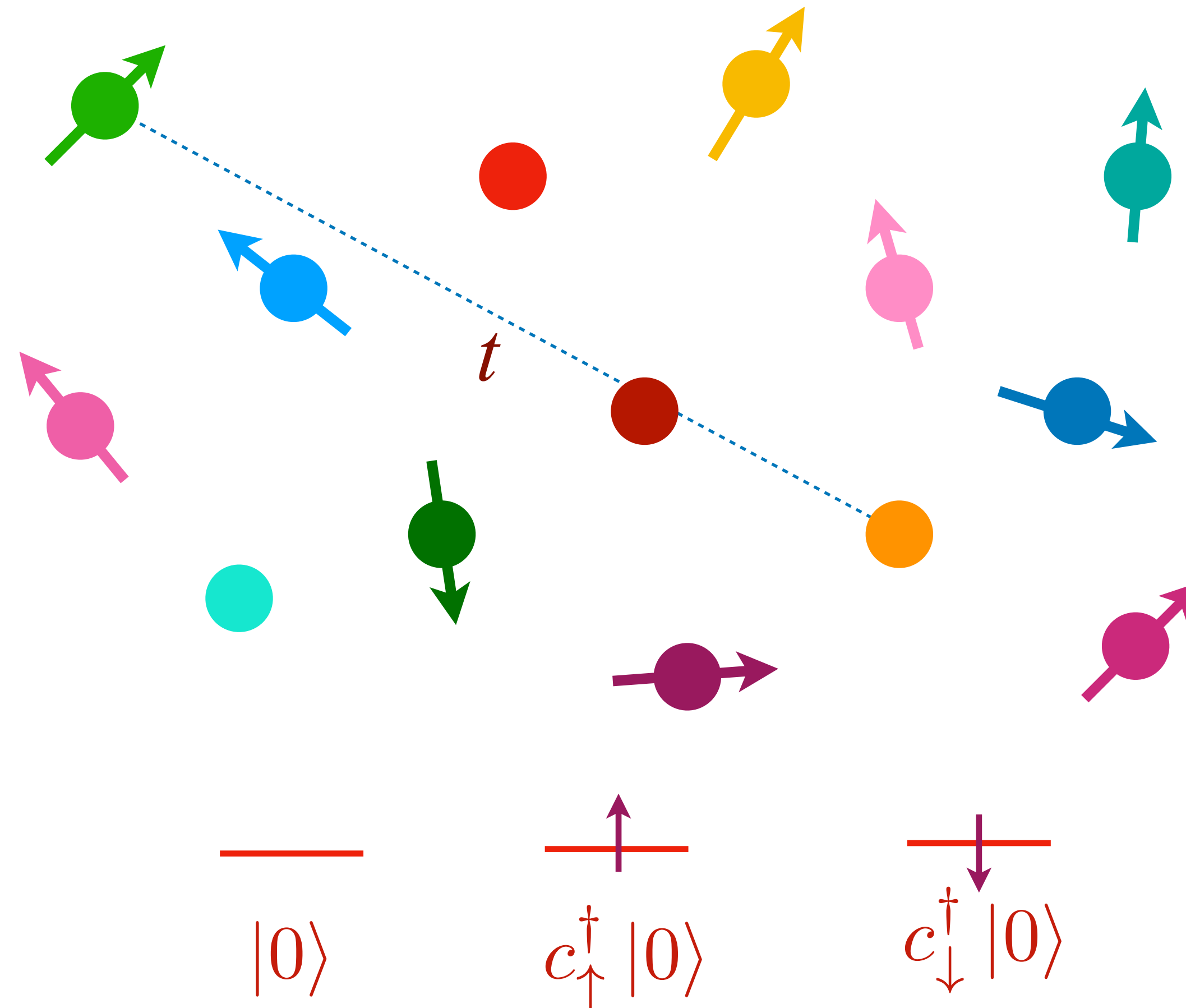
We consider the hole-doped case, with no double occupancy.



Random t - J model

$$H = -\frac{1}{\sqrt{N}} \sum_{i,j=1}^N t_{ij} c_{i\alpha}^\dagger c_{j\alpha} + \frac{1}{\sqrt{N}} \sum_{i<j=1}^N J_{ij} \vec{S}_i \cdot \vec{S}_j$$

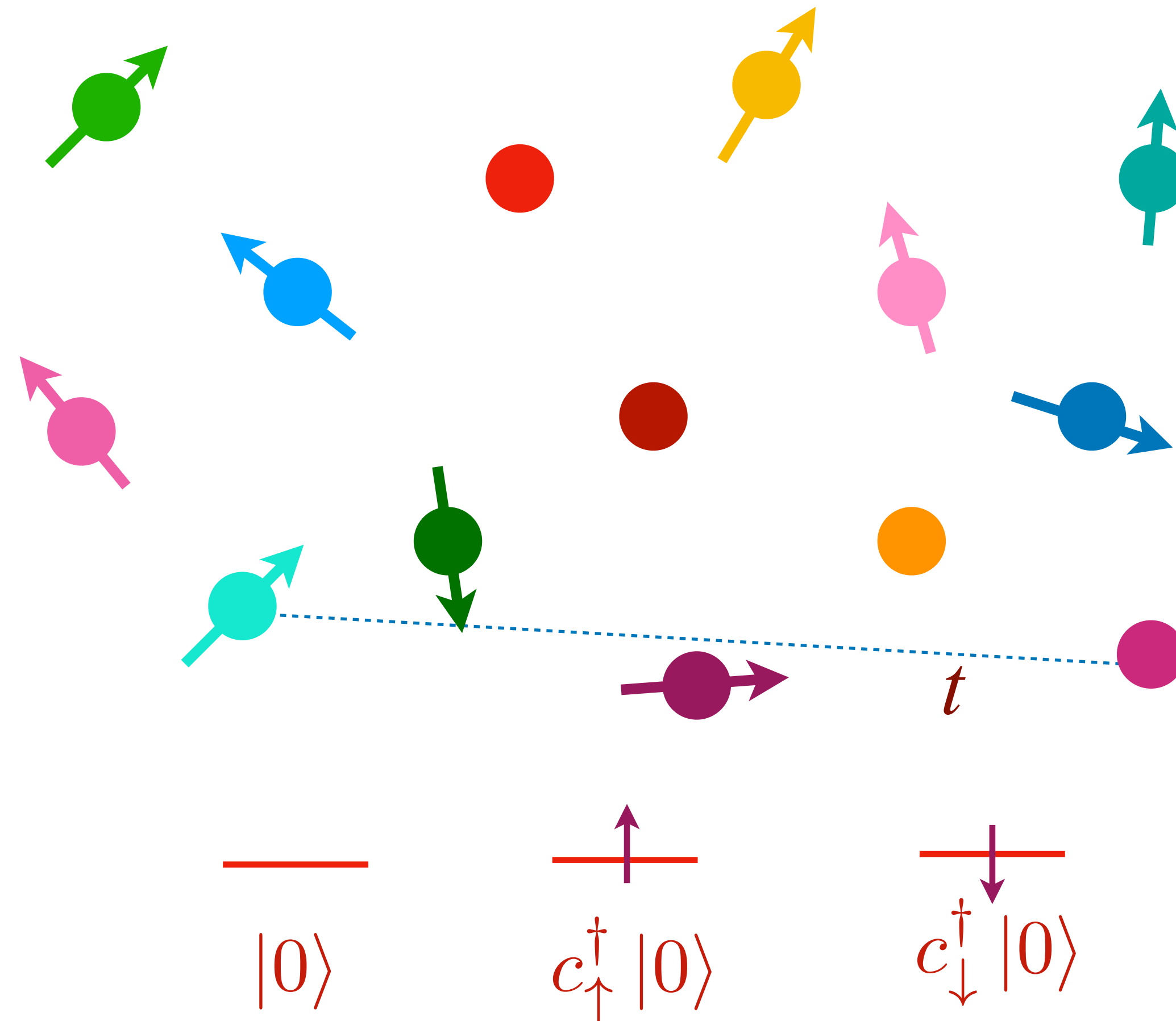
We consider the hole-doped case, with no double occupancy.



Random t - J model

$$H = -\frac{1}{\sqrt{N}} \sum_{i,j=1}^N t_{ij} c_{i\alpha}^\dagger c_{j\alpha} + \frac{1}{\sqrt{N}} \sum_{i<j=1}^N J_{ij} \vec{S}_i \cdot \vec{S}_j$$

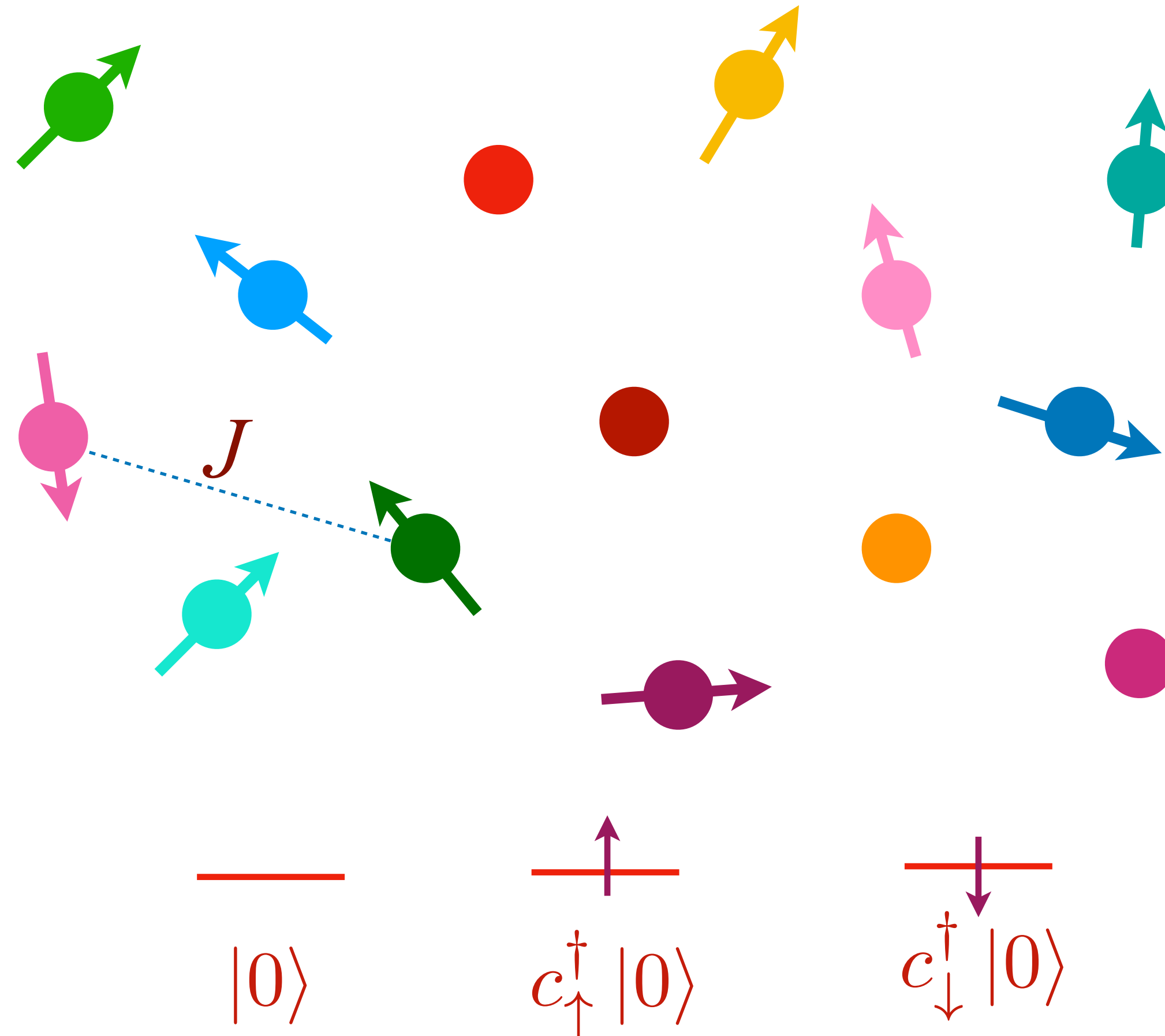
We consider the hole-doped case, with no double occupancy.



Random t - J model

$$H = -\frac{1}{\sqrt{N}} \sum_{i,j=1}^N t_{ij} c_{i\alpha}^\dagger c_{j\alpha} + \frac{1}{\sqrt{N}} \sum_{i<j=1}^N J_{ij} \vec{S}_i \cdot \vec{S}_j$$

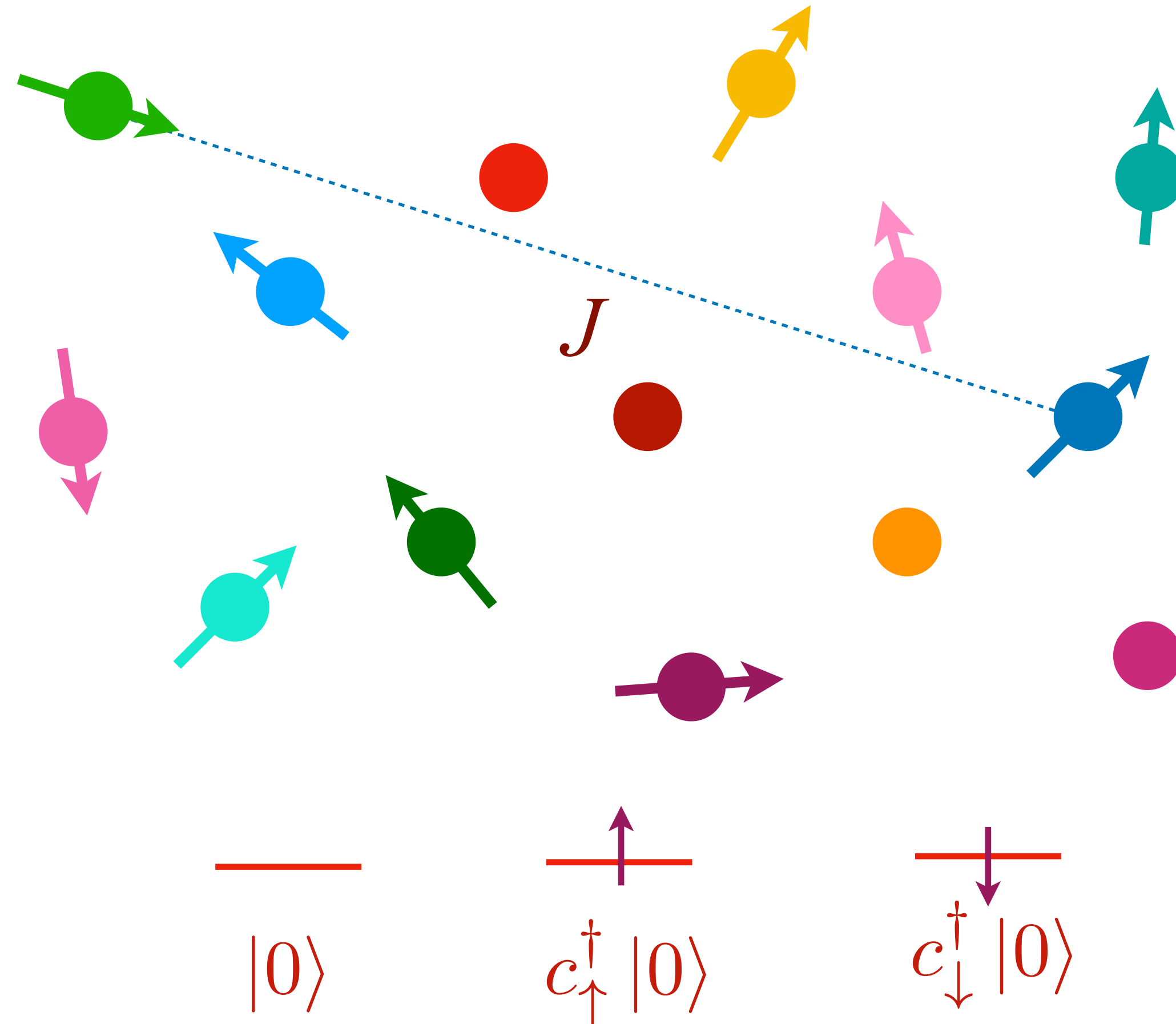
We consider the hole-doped case, with no double occupancy.



Random t - J model

$$H = -\frac{1}{\sqrt{N}} \sum_{i,j=1}^N t_{ij} c_{i\alpha}^\dagger c_{j\alpha} + \frac{1}{\sqrt{N}} \sum_{i<j=1}^N J_{ij} \vec{S}_i \cdot \vec{S}_j$$

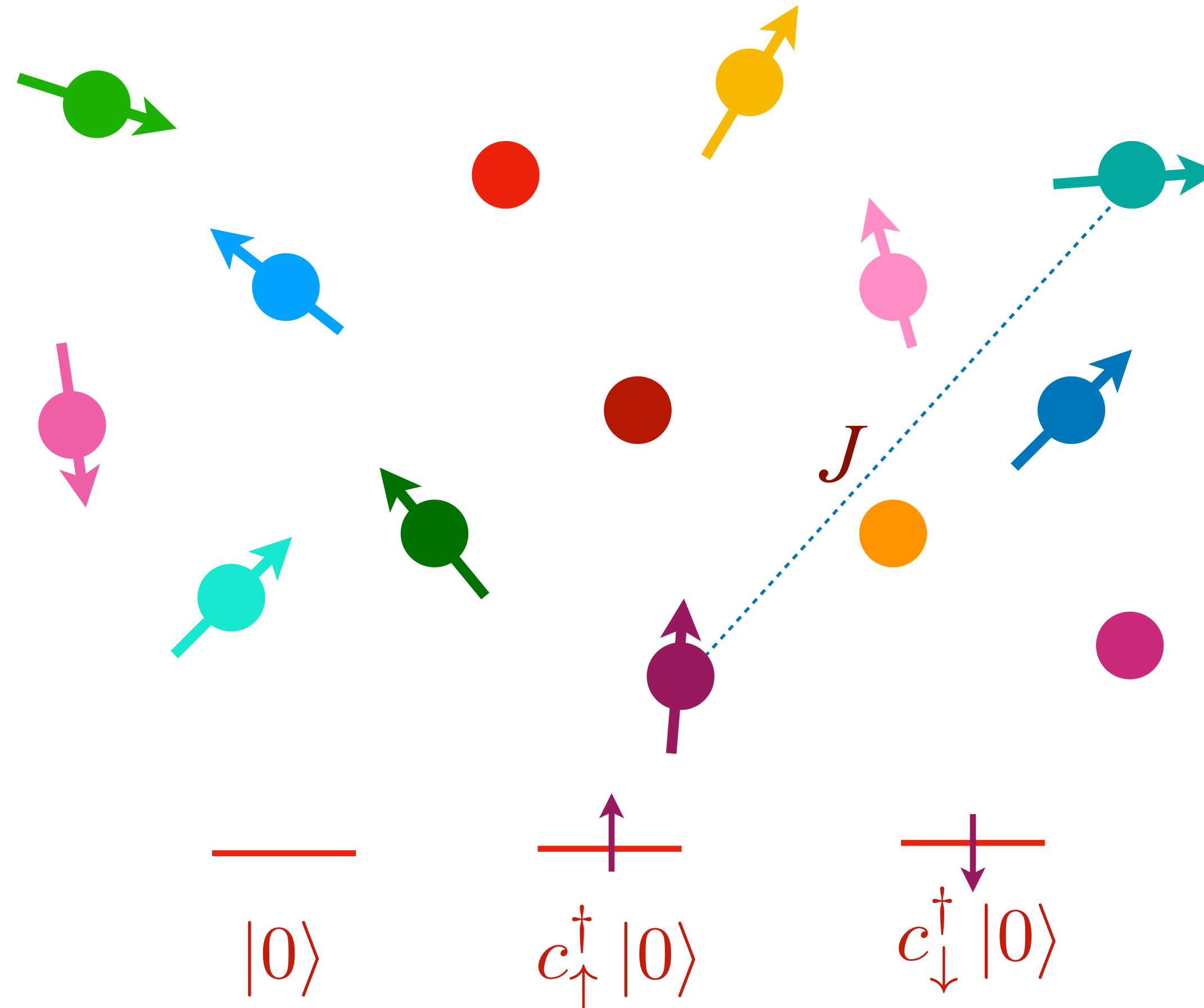
We consider the hole-doped case, with no double occupancy.



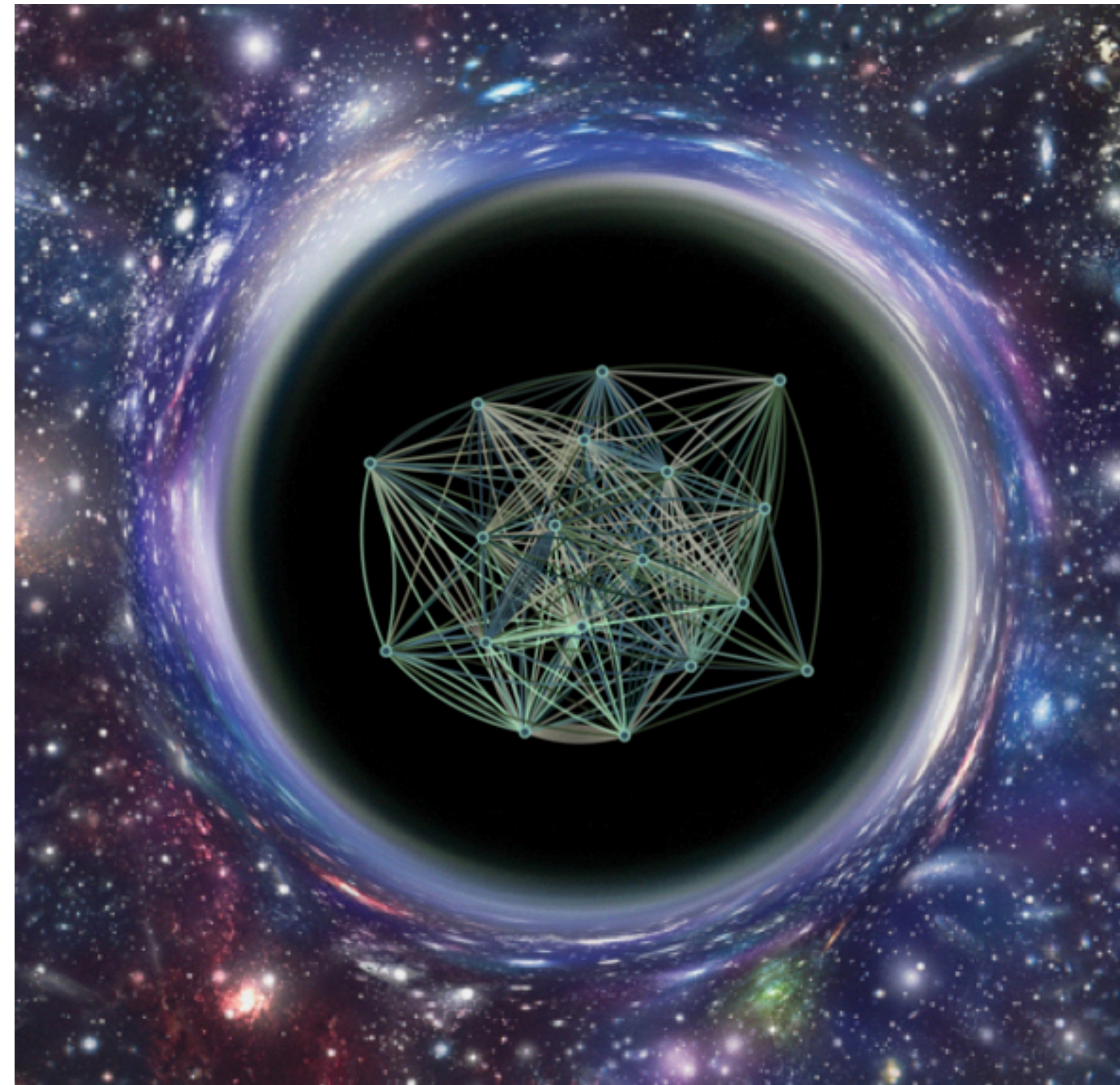
Random t - J model

$$H = -\frac{1}{\sqrt{N}} \sum_{i,j=1}^N t_{ij} c_{i\alpha}^\dagger c_{j\alpha} + \frac{1}{\sqrt{N}} \sum_{i<j=1}^N J_{ij} \vec{S}_i \cdot \vec{S}_j$$

We consider the hole-doped case, with no double occupancy.



- The t - J model with random and all-to-all hopping and exchange displays a phase diagram which captures many of the key characteristics of the cuprate phase diagram.
- It has an optimal doping metal-metal deconfined transition with SYK criticality.



Metal-metal quantum phase transitions

The ancilla qubit approach for non-random t - J models, and the random t - J model, have in common

- A metal-metal quantum phase transition with a change in carrier density from p to $1 + p$.
- Fractionalization of the electron in the critical regime
- Unexpectedly large low T entropy near the critical point (from ghost fermions, or the SYK black hole entropy).